INFORMATION TO USERS

This manuscript has been reproduced from the microfilm master. UMI films the text directly from the original or copy submitted. Thus, some thesis and dissertation copies are in typewriter face, while others may be from any type of computer printer.

The quality of this reproduction is dependent upon the quality of the copy submitted. Broken or indistinct print, colored or poor quality illustrations and photographs, print bleedthrough, substandard margins, and improper alignment can adversely affect reproduction.

In the unlikely event that the author did not send UMI a complete manuscript and there are missing pages, these will be noted. Also, if unauthorized copyright material had to be removed, a note will indicate the deletion.

Oversize materials (e.g., maps, drawings, charts) are reproduced by sectioning the original, beginning at the upper left-hand corner and continuing from left to right in equal sections with small overlaps. Each original is also photographed in one exposure and is included in reduced form at the back of the book.

Photographs included in the original manuscript have been reproduced xerographically in this copy. Higher quality 6" x 9" black and white photographic prints are available for any photographs or illustrations appearing in this copy for an additional charge. Contact UMI directly to order.

UMI

A Bell & Howell Information Company
300 North Zeeb Road, Ann Arbor MI 48106-1346 USA
313/761-4700 800/521-0600

Cytoskeletal architecture, organelle transport, and impulse conduction in hexactinellid sponge syncytia

by

Sally Penelope Leys
B.Sc., University of British Columbia, 1990

A Dissertation Submitted in Partial Fulfillment of the Requirements for the Degree of

DOCTOR OF PHILOSOPHY

in the Department of Biology

We accept this dissertation as conforming to the required standard

Dr. G.O. Mackie, Supervisor (Department of Biology)

Dr. R.D. Burke, Departmental Member (Department of Biology)

Dr. P. von Aderkas, Departmental Member (Department of Biology)

Dr. T.W. Pearson, Outside Member (Department of Biochemistry)

Dr. H.M. Reiswig, External Examiner (Redpath Museum, McGill University)

Supervisor: Dr. George O. Mackie

ABSTRACT

Hexactinellid sponges differ substantially from other sponges in having syncytial tissues and the ability to propagate signals rapidly, causing the arrest of the feeding current. To confirm existing light and electron microscopic evidence of the syncytial nature of hexactinellid tissue, live tissue models were developed from *Rhabdocalyptus dawsoni* and *Aphrocallistes vastus*. A native acellular tissue extract (ATE) was made from the sponges to which dissociated tissue adhered and spread in a species specific fashion. Video microscopy shows that dissociated tissue from *R. dawsoni* adheres to the ATE and aggregates by fusion of pieces to form a giant, multinucleated syncytium. Fusion, corroborated by dye exchange, is characterized by the bidirectional transport of organelles, including nuclei, and bulk cytoplasm at an average rate of 2.1 $\mu m \cdot s^{-1}$. Stress fibres line the periphery of adherent preparations, and giant actin-dense filopodia appear to anchor tissue to the substrate. Bundles of microtubules (MTs) bridge newly fused aggregates while extensive tracts of MT bundles are oriented in all directions in larger aggregates. Aggregates can become several centimetres in diameter and can cover a 5 cm^2 petri dish within 6-12 hours. Inhibition of organelle motility by colcemid and nocodazole but not by cytochalasin B suggests that transport occurs along MT bundles. A protein immunoreactive with cytoplasmic dynein was identified in whole cell lysate from *A. vastus*, and it is

suspected the same motor protein exists in *R. dawsoni* and other hexactinellids. No evidence was found for kinesin, although its presence cannot be ruled out. Ultrastructural evidence suggests that a membranous network may be involved in linking bulk cytoplasm to bundles of microtubules in streams, in a manner similar to the mechanism by which bulk cytoplasm is linked to microfilaments in characean algae. Transport of bulk cytoplasm and movement of individual organelles can also be seen in regenerating fragments of the whole sponge suggesting that cytoplasmic streaming may be involved in tissue morphogenesis. The fact that latex beads that are phagocytosed are also transported in streams indicates that hexactinellid sponges employ symplastic nutrient transport, like plants, rather than apoplastic nutrient transport, like animals. Because fusion and cytoplasmic streaming are features of both *Rhabdocalyptus* and *Aphrocallistes*, representatives of lysaccine and dictyonal hexactinellids respectively, it is probable that these phenomena are characteristic of the subphylum Symplasma.

Propagated arrests of the feeding current were recorded from *Rhabdocalyptus* in response to an increase in sediment in the sea water. Development of a new preparation in which aggregates are grafted on to parts of the adult body wall that demonstrate normal pumping physiology, allowed recording of action potentials which propagate through the sponge at 0.18 $cm \cdot s^{-1}$, simultaneously with the arrest of the feeding current. This is the first recording of a propagated electrical event from a sponge. Impulse conduction in these sponges can be explained by the finding that hexactinellid tissues are syncytial.

These results strongly suggest that hexactinellid sponges should be distinguished from other sponges at a high taxonomic level, and pose new questions for the evolution of intracellular transport mechanisms and excitability in the metazoa.

Examiners:

Dr. G.O. Mackie, Supervisor (Department of Biology)

Dr. R.D. Burke, Departmental Member (Department of Biology)

Dr. P. von Aderkas, Departmental Member (Department of Biology)

Dr. T.W. Pearson, Outside Member (Department of Biochemistry)

Dr. H.M. Reiswig, External Examiner (Redpath Museum, McGill University)

TABLE OF CONTENTS

LIST OF TABLES

LIST OF FIGURES

LIST OF ABBREVIATIONS

ABP	Actin binding protein
AF	Aggregation factor
AMP-PMP	Adenyl imidodiphosphate
ASW	Artificial sea water
ATE	Acellular tissue extract
CAM	Calcein acytoxymethyl ester
CBAM	Calcein Blue acytoxymethyl ester
CCD	Charged coupled device (video camera)
CDPK	Calcium-dependent protein kinase
CFSW	Calcium free sea water
CMFSW	Calcium and magnesium free sea water
Con A	Concanavalin A
DDW	Distilled deionized water
$DiOC_6(3)$	3,3'-dihexyloxacarbocyanine iodide
DMSO	Dimethylsulfoxide
ECM	Extracellular matrix
EGTA	Ethyleneglycol-bis-(ß-aminoethyl ether)N,N'-tetraacetic acid.
ER	Endoplasmic reticulum
FITC	Fluorescein isothiocyanate
HEPES	(N-[2-Hydroxyethyl]piperazine-N'-[2-ethanesulfonic acid])
HMM	High molecular mass
MAP	Microtubule-associated protein
MFs	Microfilaments
MTOC	Microtubule organizing centre
MTs	Microtubules
NEM	N-ethylmaleimide
OsO_4	Osmium tetroxide
PBS	Phosphate buffered saline
PEG	Polyethylene glycol
PEM	PIPES, EGTA, $MgCl_2$
PIPES	Piperazine-*N,N'*-bis[2-ethane sulfonic acid]
PMSF	Phenylmethylsulfonyl fluoride
SDS-PAGE	Sodium dodecyl sulfate poly acrylamide gel electrophoresis
SEM	Scanning electron microscopy
TEM	Transmission electron microscopy
TRIS	Tris(hydroxymethyl)aminomethane
VEC-DIC	Video enhanced contrast differential interference microscopy

FRONTISPIECE

Photograph of diver (S. Leys) and *Rhabdocalyptus dawsoni* taken at 35 m depth in Rainy Bay, Barkley Sound, Vancouver Island.

FRONTISPIECE

Aphrocallistes vastus photographed at 37 m depth at McCurdy Point in Saanich Inlet, Vancouver Island.

ACKNOWLEDGEMENTS

George deserves the credit for identifying this interesting project from observations he and Stuart Arkett had made in the early 1980s. He has always supported my plans, letting me choose where, and how far, to take the work, and he has generously allowed me to travel to numerous conferences, and institutions to gain new insights on the project, and to hone my techniques. He has been an enthusiastic and supportive mentor.

I thank Terry Pearson and Robert Burke, both members of my committee, for allowing me to use their labs to obtain the few biochemical results that I was able to extort from the hexactinellids, and for fruitful discussions on aspects of motor proteins and motile systems. Jim Cosgrove was most generous with his time. He was always willing to dive, collect and photograph the sponges, and he produced two excellent videos of the underwater work I have done. I warmly thank Louise Page, who has been a mentor and friend throughout my research. She has read numerous drafts of various papers, and advised on electron microscopy techniques and on proposals I have submitted for fellowships. Dorothy Paul has been supportive and helpful during times of conceptual planning, especially with respect to ideas about the electrophysiology of *Rhabdocalyptus*.

I thank the Director, staff and my fellow graduate students at the Bamfield Marine Station where much of this work was done. Nikita Grigoriev, in particular, deserves many thanks for time spent in projects which may not have yet

been fruitful. Mark Cooper, at the University of Washington, was most generous with his time and expertise with confocal microscopy, and I warmly thank David Walker at St. Pauls Hospital in Vancouver who taught me deep etch electron microscopy. I thank Lijuan Sun, Rob Beecroft, Mungo Marsden, Rossi Marx, Yogi Carolsfeld, Zen Faulkes, and Chris von Schalburg, for advice in many areas. I especially appreciate my good friend Laura Verhegge, who helped very early on with morale boosting while I explored various aspects of ecology and physiology, and eventually cell biology at the Bamfield Marine Station.

And finally, I cannot express enough thanks to Nelson Lauzon, for coming on well over 100 dives to the same gloomy deep sites to photograph or collect the same brown animals, without complaint. He has taken all the underwater photographs I have used in the course of this study, and has provided advice and support on numerous fronts. I am forever grateful.

GENERAL INTRODUCTION

Hexactinellids are the least studied of sponges because they inhabit deep waters. The silicious skeleton of these "glass sponges" has left a fossil record as far back as the Cambrian/PreCambrian boundary, making them possibly the earliest metazoans on the earth. Today they inhabit all the oceans of the world, but are only accessible by dredge or submersible except at four known sites, where the upper limit of populations just reaches depths accessible by SCUBA.

These sponges are highly unusual in that approximately 75 percent of the tissue mass is syncytial as opposed to cellular. In the past this marked difference in tissue structure from other Porifera was not emphasized because the accuracy of early reports on their histology, which were based on poorly preserved dredged specimens, required verification by modern techniques. During the last two decades, however, a number of studies have explored the ecology, histology, and physiology of hexactinellids. It has been shown that hexactinellids are extremely long-lived animals whose cytoplasm consists of a giant, multinucleated tissue, the trabecular syncytium, which is connected via open and plugged cytoplasmic bridges to cells such as archaeocytes, choanoblasts, thesocytes, and spherulous cells. Because all of the sponge is cytoplasmically interconnected, electrical signals can propagate through the animal turning off the feeding current.

The difficulty of collecting hexactinellids in good condition has hindered further examination of these remarkable characteristics. Although electron microscopy has been conducted on some eight species, confirming the multinucleated

microscopy has been conducted on some eight species, confirming the multinucleated syncytial tissue organization of hexactinellids, live tissue has not hitherto been examined. Furthermore, the soft tissues are so fragile that direct recordings of propagated action potentials have never previously been obtained.

There are a number of hexactinellid species in coastal waters of British Columbia, Canada, two of which can be most easily reached by SCUBA. I have exploited the local availability of hexactinellids to explore aspects of their ecology, physiology, and cell biology. The primary focus of my work over the last five years has been to develop and use live tissue models to examine the organization of hexactinellid tissue, the largest syncytium known to exist in the metazoa.

A. Historical background

Since the earliest histological descriptions of sponges from this group in the late 19th century, hexactinellid tissues have been thought to be largely syncytial (Schulze, 1880, 1887, 1899; Ijima, 1901, 1904). Both Schulze and Ijima described the major tissue component as a system of fine branching, multinucleate trabeculae which held the flagellated chambers in place and merged with a so-called connecting membrane (the *membrana reuniens* of Schulze) at the flagellated chambers (Fig 1A). The choanocytes were said to be nucleated and to lie on a reticular membrane (the *membrana reticularis* of Schulze) which connected the choanocytes at their base (Fig 1B,C). The thinness of the trabeculae and the reticular membrane was attributed to

Figure 1. Features of the soft tissues of *Euplectella marshalli*. Redrawn from Ijima (1904). (A) The space between apopyles - the entrances to the flagellated chamber - seen from the excurrent side (approx. 1000X magnification). (B) The incurrent lacunar space between four flagellated chambers (approx. 1500X magnification). The region of the reticular membrane marked with parentheses is shown in tangential section in C. (C) The chamber wall (reticular membrane) containing what were thought to be nuclei, but which are probably collar bodies and flagella (approx. 3500 X magnification). Abbreviations: mm, marginal membrane; ap, apopyle; cm, connecting membrane; t, trabeculae; a, archaeocyte; mr, membrana reticularis; c, choanocytes; n, nucleus; f, flagella.

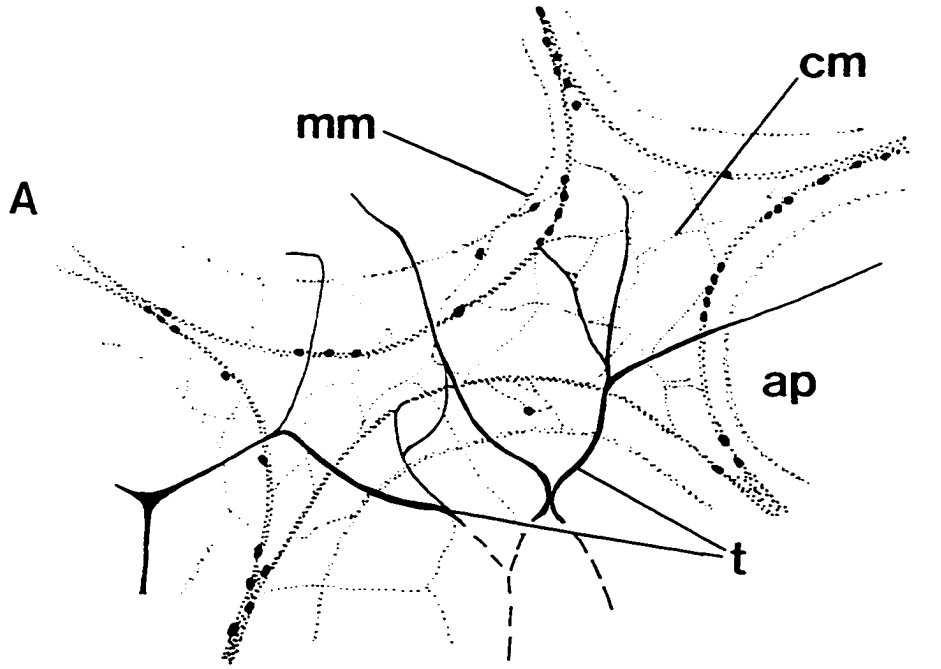
A
cm
mm
ap
t

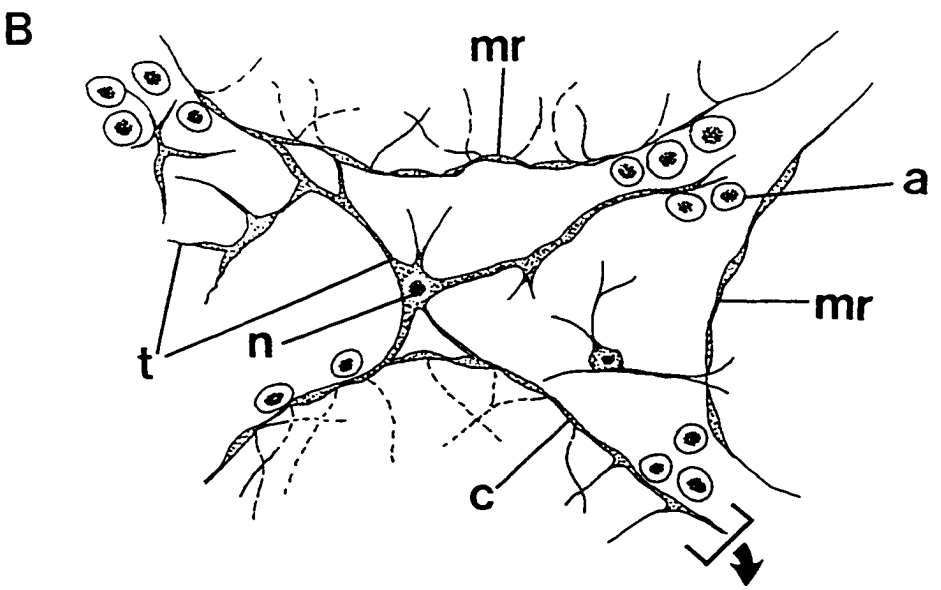
B
mr
a
mr
t
n
c

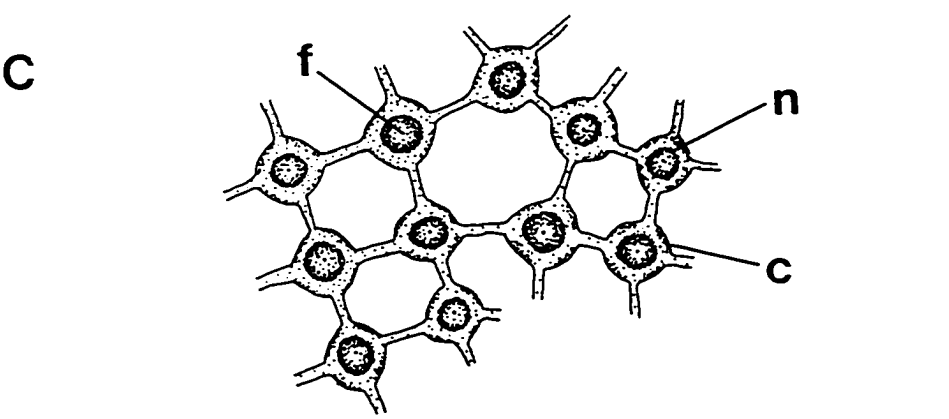
C
f
n
c

the minimal development or complete lack of a mesohyl. Both Schulze and Ijima agreed that although there were several cells which stained distinctly, the majority of the tissue constituted a giant multinucleated syncytium.

Bidder (1929) recognized the importance of the histological differences of hexactinellids by separating them from the Calcarea and Demospongiae, creating two phyla, the Nuda (Hexactinellida) and the Gelatinosa (Calcarea and Demospongiae), names which reflected the lack of a well developed mesohyl in hexactinellids compared with other sponges. By this classification scheme Bidder also implied that this characteristic was evidence that sponges evolved from different choanoflagellate ancestors, justifying separation at the phylum level. More recently Reid (1963) reshuffled the two groups to the subphylum level to reflect the probable common origin of sponges based on similarities in descriptions of larvae (Ijima, 1904; Okada, 1928).

These proposals were largely ignored until the histology of hexactinellids could be verified with modern techniques. In the 1970s SCUBA was used to collect specimens found in relatively shallow waters off the coast of British Columbia and initial attempts were made to fix the tissue for electron microscopy. Studying *Aphrocallistes vastus* and *Heterochone calyx*, Reiswig (1979a) discovered that normal fixation protocols for electron microscopy (protocols which work well for fixing demosponges) do not work well with hexactinellid tissue. Mackie and Singla (1983) had better success, after much trial and error, by using a one-step cocktail fixative. Both investigations concluded that the major part of the sponge consists of a

multinucleated syncytium termed the trabecular syncytium. The term choanosyncytium was inappropriately applied to what is now known to be a cellular portion of the sponge. They also found that choanocytes, the flagellated cells responsible for creating a feeding current in sponges, lacked nuclei, and hence termed them collar bodies, several of which emanated from a single nucleated cell which they called a choanoblast. A unique intracellular osmiophilic junction was found to plug most cytoplasmic bridges which connected archaeocytes (a totipotent cell common to all sponges), cells with inclusions such as thesocytes and spherulous cells, and choanoblasts to the multinucleated tissue (see fig 8 in Chp. II) (Mackie, 1981). As membranous material could be seen passing through pores which measured some 7 nm in diameter in the plugs, it was suggested that the plugs could selectively allow the passage of materials between cytoplasmic compartments, not unlike transport via plasmodesmata in higher plants, pit plugs in certain red algae, and even gap junctions in animal tissues. Use of the same or a similar cocktail fixative with other hexactinellids produced similar results, showing multinucleated syncytial tissues attached to nucleated cells by open or plugged cytoplasmic bridges (Reiswig, 1991; Reiswig and Mehl, 1991; Boury-Esnault and Vacelet, 1994).

One of the most interesting discoveries was that at least one hexactinellid (*Rhabdocalyptus dawsoni*) can propagate behaviorally meaningful signals (Mackie, 1979; Lawn et al., 1981). When mechanically or electrically stimulated the entire sponge responds by stopping its feeding current, which suggests that it can coordinate the shutdown of flagellar beating. This is the only sponge in which propagation of

electrical signals has been demonstrated. Electrical current can propagate either by synaptic transmission via neurons (nervous conduction), or by the movement of ions through gap junctions coupling cells (neuroid conduction). Despite many histological investigations there is no evidence for the existence of nerves in any member of the Porifera. Early studies focused on the possibility that elongated myocytes (muscle-like cells), which appeared "nerve-like" in morphology, could be responsible for the slow contractions of oscula or ostia in some demosponges (Pavans de Ceccatty, 1959, 1962). Loewenstein (1967) reported the only experiment demonstrating electrical coupling between two dissociated sponge cells, but this experiment has never been replicated, and no evidence for gap junctions or any similar connecting junction has been found in calcareous sponges or demosponges (Garrone et al., 1980), except for the perforate plugged junction of hexactinellids (Pavans de Ceccatty and Mackie, 1982; Mackie and Singla, 1983b). Although the mechanism of the contractions referred to above has still not been established, because the rates of contraction are far slower than any known rates of nervous or non-nervous conduction, and because action potentials have never been recorded in sponges, it is generally considered that the contractions are mostly likely caused by mechanical processes rather than by chemical diffusion or electrical impulses (Pavans de Ceccatty, 1989).

The discovery that hexactinellids can propagate signals strongly supported histological evidence that their tissues were syncytial. A new proposal put forward by Reiswig and Mackie (1983) placed hexactinellids in the subphylum Symplasma, and all other sponges in the subphylum Cellularia, to reflect this profound structural

difference. Although the essence of their new proposal reiterated that of Bidder, it has still to be adopted by the authors of text books today who continue, some 15 years later, to place the Calcarea, Demospongiae, and Hexactinellida in three equidistant classes. Although classifications understandably change very slowly, in this case reluctance to adopt the current proposal appears to be compounded by distrust of information derived only from preserved specimens, especially when common fixation protocols for electron microscopy are ineffective with hexactinellid tissue. The issue is further complicated by the fact that the definition of syncytia has changed somewhat since the time of Schulze and Ijima's observations, and syncytia are no longer considered in great detail by cell biologists. Since no other metazoan possesses such extensive syncytial tissues, it is, perhaps, difficult to imagine the extent to which hexactinellid tissue truly differs from a cellular grade of organization.

B. The nature of syncytial organisms

Before tissues could be viewed by electron microscopy the boundaries between cellular and syncytial tissues were less clear. Although most tissues were thought to be cellular, in some instances cells appeared to be tenuously connected by protoplasmic bridges. In other cases however, such as developing embryos in arthropods, cells were clearly multinucleate by way of incomplete cytokinesis. In addition, botanists had found many algae, such as *Caulerpa,* which clearly possessed multinucleate cells.

Figure 2. Different forms of cells and symplasmic states from the animal body. Redrawn from Studnička (1934). (A) Cell. (B) "Cyton", a cell with prolongations, such as a neuron (x). (C) "Holocyte", a cell with exoplasm belong to it, such as cartilage cell with a broad exoplasmic capsule (ex). (D) Reticular "syndesmium", cells with cell connections (on the left) passing over into a reticular "plasmodium", or a continuous protoplasmic mass with several cell nuclei (on the right). (E) "Syndesmium" composed of cells joined by cell connections. (F) "Syncytium", a well delimited mass of protoplasm with numerous cell nuclei.

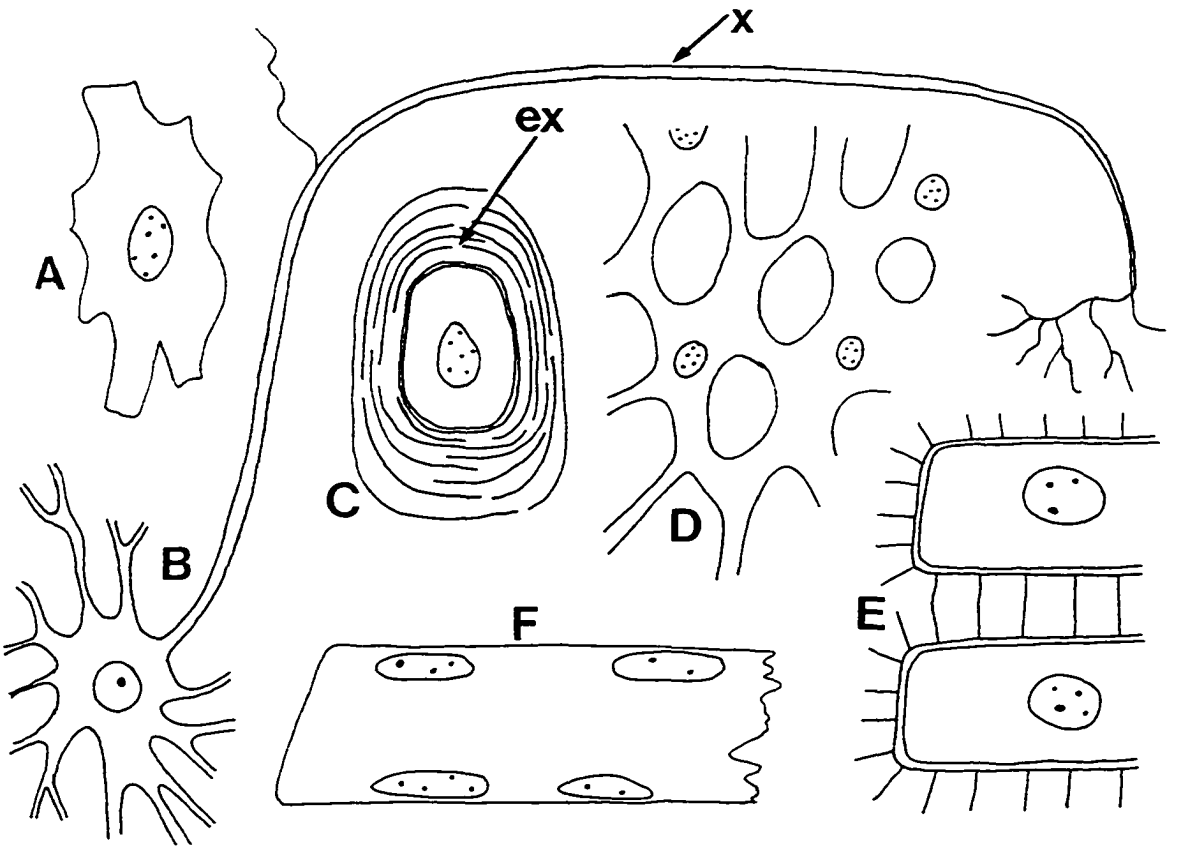
X
ex
A
B
C
D
E
F

Several attempts to standardize terminology were made. Sachs (1892) felt that a nucleus presiding over an area of cytoplasm was the functional unit, whether in a uninucleate or multinucleate cell, and described these regions as 'energids'. Others suggested distinguishing between 'protoplasts' as individual cells or unions of cells, and symplasts as multinucleate tissues where none of the nuclei has individual territory (Rubashkin and Besuglaja, 1932). Studnička (1934) proposed terminology which attempted to synthesize these viewpoints, using "symplasma" for cells which had cytoplasmic continuity as a result of incomplete cytokinesis but which otherwise remained independent, "syncytia" for multinucleated structures whose cytoplasm was not organized around centrioles (such as muscle cells), and "plasmodia" for multinucleated tissue which had been formed by fusion of separate cells or by division of nuclei in a growing cell (Fig 2).

Today the term syncytium is generally used to describe multinucleated giant cells. Tissues that are considered to be syncytial because they lack membrane barriers between adjacent nuclei are found, for example, in a number of algae in each of the Charophyta, Chlorophyta, Rhodophyta, and Chrysophyta, in the slime mold *Physarum*, in the epithelia in some cnidarians, in skeletogenic tissues of echinoids, in giant neurons in squid, in vertebrate striated muscle cells, in some embryonic tissues such as in *Drosophila*, and in developing sperm cells in many organisms. Although cells connected via gap junctions in animals, or plasmodesmata in plants, could also reasonably be called syncytial since they are connected protoplasmically, they are considered by both plant and animal biologists to be cells because they function

independently. In general syncytial tissues are suggested to serve as pathways for communication and transport, or for synchronous development as in germ cells or embryonic tissues, all of which are possible functions of syncytial tissue in hexactinellid sponges. Mackie and Singla (1983) have provided an in-depth review of the occurrence and proposed functions of syncytial tissues in plants and animals.

C. The present project

i) *Hexactinellid ecology*

I began this work by looking at the general ecology and physiology of *Rhabdocalyptus dawsoni*, studying growth rates, rates and mechanisms of regeneration, and patterns of pumping. Knowledge of hexactinellid ecology at the time showed that these sponges grew at an imperceptibly slow rate (Dayton, 1979) generating curiosity as to the true ages of hexactinellids. Two studies were initiated independently in the 1980s to measure growth rates of *Rhabdocalyptus* in B.C. waters, one by submersible (Tunnicliffe, unpublished) and the other by numerous volunteer divers (Marliave, 1992). Both had a sample size of only 6 individuals and found that the sponges grew about 3cm/yr. I have now measured growth in 19 individuals over three years and find average rates of growth for 20 to 40 cm-long animals to be approximately 2 cm/yr (Leys, unpublished). Reiswig (1990) studied particle uptake by *Rhabdocalyptus* and *Aphrocallistes*. Despite difficulties in processing the water samples, he found that the former fed mostly on dissolved and particulate organic carbon, and the latter on

bacteria and to a lesser extent dissolved organic carbon. Discovery of a shallow water population of the hexactinellid *Oopsacas minuta* in a submarine cave in France has enabled *in situ* work on feeding in hexactinellids (Perez, 1996). In *Oopsacas* particle uptake occurs on all surfaces of the trabecular reticulum, but apparently not in the collar bodies. There was no evidence of uptake of particles smaller than 0.5 μm. Our work with *Rhabdocalyptus* (Wyeth et al., 1996) confirms those findings. In 1991 no more was known about reproduction in hexactinellids than had been shown by early work on histological sections of preserved material collected throughout the year (Ijima, 1901; Okada 1928). Hexactinellid larvae were seldom encountered in any hexactinellid, but were thought to be produced year-round. Indeed, *Oopsacas minuta* was found to be reproductive year-round (Boury-Esnault and Vacelet, 1994), and the larvae differ from both amphiblastula and parenchymella larvae in possessing a belt of multiflagellated cells, choanoflagellate chambers, and plugged junctions between tissues.

ii) *Regeneration and aggregation*

Sponges possess remarkable regenerative abilities which may be largely due to a totipotent cell, the archaeocyte. Archaeocytes can differentiate into germ cells during sexual reproduction, form the core of gemmules and reduction bodies which arise asexually in some sponges when conditions are harsh, become amoeboid to transport nutrients (Imsieke, 1994), and they can also develop into pinacocytes during wound healing (Brondstead, 1953; Harrison, 1972). In fact, when wounds are severe the

tissue forms archaeocyte-rich reduction bodies, from which the whole sponge can regenerate (Brondstead, 1953; Korotkova, 1963). Because of the role of archaeocytes in regeneration from reduction bodies, this process has been termed "somatic embryogenesis" (Korotkova, 1963).

The most extreme form of regeneration in sponges was first demonstrated by Wilson (1907), who showed that sponges will reaggregate in a species specific manner after dissociation through fine mesh. Since then numerous studies have focused on sponge cell aggregation, looking in particular at the mechanism of cell-cell adhesion during aggregation. Dissociated sponge cells adhere and crawl on substrates and, moving in a random fashion, the cells encounter and adhere to other cells thereby forming aggregates (Gaino et al., 1985b). The mechanism of adhesion is by way of cell surface proteoglycans called aggregation factors (Moscona, 1968). Although cells initially adhere to the substrate (e.g. Gaino et al., 1985a), in time they generally form multilayered adhered cell cultures (Shimizu and Yoshizato, 1993). Several hours after dissociation aggregates normally form balls of cells, opaque to the light microscope, some of which continue over time to generate a new sponge. It has been shown that aggregates of purified archaeocytes are able to form a new sponge (Buscema et al., 1980).

The role of archaeocytes in both regeneration and aggregation in syncytial sponges is unknown. During preliminary experiments I found that rates of regeneration of 5 cm^2 cores removed from the body wall of *Rhabdocalyptus* both in the field and in laboratory aquaria were rapid (0.08cm^2/day) when compared to rates

of growth of the whole sponge, and these rates agreed well with those calculated for the same animal in a previous study in Saanich Inlet (Boyd, 1981). In addition, I found that a new dermal membrane formed overnight after wounding although archaeocytes did not appear to be clustered at the wound edge. A previous study of the process of aggregation in *Rhabdocalyptus* showed that aggregates form a giant cell, which encompasses archaeocytes, spherulous cells, and other cellular components of the whole sponge (Pavans de Ceccatty, 1982). In those experiments, only freshly collected animals produced aggregates, and no aggregates lived longer than two weeks. During further experiments with aggregation, however, an interesting observation was made. In some of the aggregates the cytoplasm could be seen moving, but the opaqueness of the aggregates prevented further observation of this phenomenon (Arkett, personal communication).

My examination of aggregation began from this point. As previous researchers, I found that only freshly collected sponges produced aggregates which formed opaque balls of tissue. In order to better view the cytoplasm of aggregates, I attempted to culture tissue by getting the aggregates to adhere and spread on substrata, rather than rounding into opaque spheres. This approach had not been taken in past investigations of hexactinellid tissue, most obviously because of the difficulty of retrieving living specimens, but also because of the difficulty of *in vitro* research. The adherent tissue cultures which form the basis for most of the work in this dissertation were developed using a substrate of tissue extract which causes binding of the dissociated tissue in a similar manner to cell-cell adhesion during aggregation. This

work is described in Chapter I.

The most unusual feature of adhered tissue cultures, however, is that the cytoplasm constantly moves in vast, plainly visible streams. Even at low magnification the streams can be followed with the eye as they slowly, but ceaselessly, move along the substrate. Interestingly, although the cytoplasm was known to be syncytial, this vast, complex mechanism of intracellular transport was quite unexpected. Consequently I have focused a large part of my attention in this dissertation on attempting to determine the mechanism and possible functions of cytoplasmic streaming in hexactinellids.

D. Cytoplasmic streaming

All organisms possess systems for intracellular transport. Depending on the size and primary function of the cell or syncytium this can involve transport of individual organelles or rivers of cytoplasm. In the centimetre-long internodal cells of characean algae, for example, nutrients are stirred in 30-50μm wide swaths of cytoplasm, while in neurons, fast axoplasmic transport carries individual vesicles to the axon terminal. The term cytoplasmic streaming was coined during the early days of motility studies to refer to transport of bulk cytoplasm, whereas organelle transport is the modern term describing all intracellular transport. The rapid development of motility assays (Shimizu et al., 1993), and improved microscope techniques such as video enhanced contrast (Allen et al., 1981) and, more recently, optical tweezers (Simmons and Finer,

1993), have revealed that at the centre of all motile systems is the cytoskeleton and its associated proteins, which can include any of a number of mechanoenzymes. Although the boundaries between systems that were considered to be actomyosin-based, and those considered to be microtubule-based, are now known to be less clear, in order to methodically dissect the properties of cytoplasmic streaming in hexactinellids it is logical to divide the characteristics and examples of cytoplasmic transport mechanisms into actin-based and tubulin-based systems.

i) *Actin-based transport*

The best-known examples of actin-based intracellular transport systems are found in plants, algae, fungi, and protists (e.g. amoebae and slime molds). In many of these organisms the large size of the cells allowed movement of the cytoplasm to be observed at low magnifications more than two centuries ago. With the advantage of modern microscopy we now know that all plant cells have active cytoplasmic transport. However, much of the knowledge we have today about actomyosin based cytoplasmic transport (reviewed by Kuroda, 1990) has come from experiments on the large internodal cells of characean algae (species of *Chara* and *Nitella*).

Streaming in *Chara* and *Nitella* is one of the fastest transport systems known, with rates up to 80 $\mu m \cdot s^{-1}$ recorded. In both algae, cytoplasm is transported along giant bundles of actin microfilaments which circumscribe the centimetre-long cells. Although evidence from perfusion assays, immunofluorescence, and pharmacological studies have demonstrated that myosin is responsible for force generation along actin,

it has also been shown that myosin alone could not generate the uniform velocity profile of bulk transport. Early transmission electron microscopy (TEM) micrographs suggested that sheets of endoplasmic reticulum (ER) were present throughout the endoplasm (Bradley, 1973; Williamson, 1980), prompting the formulation of a hydrodynamic model in which the cytoplasm is connected to myosin via a membranous or fibrous network (Nothnagel and Webb, 1982). The role of the ER in bulk transport in characean algae is now also supported by immunofluorescence microscopy and freeze etch electron microscopy (Grölig et al., 1988; Kachar and Reese, 1988).

Many authors have shown that greater than 10^{-5} M Ca^{2+} irreversibly inhibits streaming, while 10^{-6} M Ca^{2+} reversibly inhibits streaming, in both algae and higher plants (Tominaga et al., 1983; Takagi and Nagai, 1986; Kohno and Shimmen, 1988; Grölig et al., 1988). Moreover, actin microfilaments depolymerize at $>10^{-5}$ M Ca^{2+} *in vitro* (Alberts et al., 1989). In smooth muscle and non-muscle cells calcium regulates myosin via the calcium-calmodulin complex. The complex activates myosin-light-chain kinase, which phosphorylates the light chains of myosin (Alberts et al., 1989). A similar mechanism may exist in characean algae. In *Chara*, calmodulin is distributed throughout the endoplasm and on organelles bound to microfilament bundles, but not on the microfilaments themselves, and perfused cells contain no calmodulin (Jablonsky et al., 1990). Furthermore, a calcium-dependent but calmodulin-independent protein kinase (CDPK) has been found associated with filamentous actin in plant cells (Putnam-Evans et al., 1989), although no direct action

between CDPK and actin has been found in vitro. Tominaga et al. (1987) have proposed that a calcium-dependent, calmodulin-independent phosphorylation of myosin is associated with cessation of streaming, and that a calmodulin-dependent dephosphorylation is required for recovery of streaming.

In pollen tubes calcium stops streaming irreversibly both by inactivating myosin and by causing the fragmentation of actin microfilaments (Kohno and Shimmen, 1988). A gradient of calcium increasing toward the tips of pollen tubes is correlated with the presence of only short actin filaments at the tip (Lancelle et al., 1987; Nobling and Reiss, 1987), suggesting that calcium regulates the deposition of organelles for tip elongation (Kohno and Shimmen, 1988).

Factors other than calcium may assist in the regulation of actin-based streaming in plants. Microtubules in the subcortical layer aligned with actin bundles were found necessary for recovery from cytochalasin-induced cessation of streaming in both *Chara* and *Nitella* (Wasteneys and Williamson, 1991). Products of ATP hydrolysis, ADP and orthophosphate, inhibit streaming (Shimmen, 1988), as does sulfate (Shimmen et al., 1990). Few studies have examined the effect of pH on streaming, although it was reported that acidification of the cytoplasm accompanies cessation of streaming (Shimmen and Tazawa, 1985).

The mechanism of streaming in amoebae differs somewhat from that in characean algae. In amoebae, movement of the cytoplasm from the tail to the leading edge at rates up to 40 $\mu m \cdot s^{-1}$ (Taylor and Condeelis, 1979) is caused by hydrostatic pressure brought about by tail contraction (Jansen and Taylor, 1993). Monomeric

actin is distributed throughout the cell, while microfilaments are found sparsely in the cortex and at the rear of the cell (Bailey *et al.*, 1992). Actin binding proteins (ABPs) such as α-actinin and filamin cross-link microfilaments stiffening the cytoplasm, while activated actin severing proteins snip microfilaments, solating the cytoplasm. In both *Acanthamoeba* and *Dictyostelium* amoebae, myosin I, which is known to cause plasma membrane ruffling (Adams and Pollard, 1986), is found primarily at the leading edge, whereas myosin II, the conventional skeletal muscle myosin, is found on particles throughout the cytoplasm and at the tail (Yonemura and Pollard, 1992; Fukui et al, 1989). Calcium gradients lead to tail contraction and cytoplasmic streaming under decreasing gel strengths (Janson and Taylor, 1993).

In the multinucleate plasmodial slime mold *Physarum* cytoplasmic streaming occurs by a similar mechanism. This organism extends a sheet of protoplasm to the front and tube-like veins to the rear, in which cytoplasm shunts backwards and forwards regularly at rates up to 1.3 $mm \cdot s^{-1}$ (Komnick et al., 1973). Streaming is caused by waves of contraction of actin and myosin in the cortical cytoplasm. Such waves have been shown to correspond to calcium (Ridgeway and Durham, 1976; Ogihara, 1982) and ATP concentration (Ueda et al., 1990). Furthermore *Physarum* contains the actin severing protein fragmin which is thought to solate the cytoplasm upon local calcium increase (Hasegawa et al., 1980).

ii) *Tubulin-based transport*

Microtubules play a variety of roles in plant cells including laying down the

secondary walls in new tissue and in cell-plate formation. In the marine coenocytic alga *Caulerpa prolifera*, amyloplasts and some chloroplasts stream at rates up to 3-5$\mu m \cdot s^{-1}$ along microtubule bundles rather than microfilaments in the endoplasm (Menzel, 1987; Menzel and Elsner-Menzel, 1989). It is possible that a dynein- or kinesin-like motor drives the endoplasmic streaming. A protein recognized by anti-kinesin has been identified in *Nicotiana tabacum* (Tiezzi et al., 1992), although so far no such microtubule associated protein (MAP) has been found in *Caulerpa*.

Reticulomyxa, a multinucleate, freshwater foraminiferan, and *Allogromia*, a cellular, marine foraminiferan, both extend long, thin pseudopodia, known as reticulopodia, which are used in locomotion, burrowing into sediment, capturing food, and in aiding the dispersal of offspring (reviewed in Travis and Bowser, 1990). Bidirectional transport at rates up to 25 $\mu m \cdot s^{-1}$ occurs along microtubules (Travis and Allen, 1981); actin is important for adhesion and structural support (Bowser *et al.*, 1988). In addition, cortical flow of reticulopodial membranes has also been described. A dynein-like ATPase with a molecular weight of 440 kDa that is sensitive to UV-induced vanadate-dependent cleavage, and supports bidirectional movement along microtubules in vitro, has been isolated from *Reticulomyxa* (Euteneuer et al., 1988).

Both of these foraminiferans have been useful models for studies of microtubule-based motility in higher organisms because there appears to be little difference between the mechanism of microtubule-based transport in protists from axoplasmic transport in higher organisms. In axons, organelles are transported at up

to 5 $\mu m \cdot s^{-1}$ anterogradely, and at a slightly slower rate in a retrograde direction, along bundles of highly cross-linked microtubules (Allen et al., 1982; Hirokawa, 1982). Success in isolating the motor protein kinesin - a plus-end directed microtubule-based motor - from squid axoplasm, using the non-hydrolysable ATP analog, adenyl imidodiphosphate (AMP-PNP) (Vale et al., 1985a; Brady, 1985), has paved the way for the discovery of many different kinesin-like and dynein-like microtubule-associated proteins. Cytoplasmic dynein, usually a minus-end directed motor, appears to be responsible for retrograde transport in axons (Vale and Hotani, 1988). Localization of a kinesin binding protein, kinectin, on the ER in fibroblasts, astroglia, schwann cell bodies, and neurons provides tempting evidence that the ER is involved in axoplasmic transport (Toyoshima et al., 1992).

Dynein-like motors are also involved in the movement of chromatophore pigment granules, which show fast aggregation (20 $\mu m \cdot s^{-1}$) and slow dispersion (5 $\mu m \cdot s^{-1}$) along radial microtubule networks (Stearns, 1984). Calcium (10^{-6} M) is required for pigment aggregation, and again, the smooth endoplasmic reticulum, which extends outward along the microtubule array, is a candidate for intracellular calcium storage and release and control of pigment movement (Luby-Phelps and Porter, 1982). Microtubule-based transport has also been demonstrated in keratocytes, in intact epithelial cells of the renal proximal tubule of killifish, in fibroblasts, in epidermoid carcinoma cells (reviewed in Karnaky et al., 1992), and even in basal epithelial cells of freshwater sponges. In the last of these, transport of mitochondria and other organelles occurs at rates of 1.2-1.5 $\mu m \cdot s^{-1}$ along

microtubule tracks that radiate out from the nucleus (Weissenfels et al., 1990). Treatment with colcemid has demonstrated that the microtubules are also responsible for organizing the endoplasmic reticulum and Golgi with respect to the nucleus (Wachtmann and Stockem, 1992). Bulk transport of cytoplasm was not observed in these cells, which are approximately 100 μm in diameter.

In this general overview of the better-known intracellular transport systems it would appear that actin-based transport systems are restricted to plants, algae, fungi and protists, and microtubule-based transport to metazoans, with a few exceptions. However, recent evidence shows that organelles may also be transported along microfilaments in systems that in the past were considered to be strictly microtubule-based. Kuznetsov and others (1992) demonstrated ATP-dependent, unidirectional movement of organelles in extruded squid axoplasm along filaments that were not resolvable by video enhanced contrast differential interference contrast (VEC-DIC) microscopy but stained with Rhodamine phalloidin. Cytochalasin B fully inhibited movement while nocodazole, a drug which prevents microtubule assembly, had no effect on this movement. Neither the inhibitor of kinesin-driven motility, AMP-PNP, nor that of dynein-driven motility, sodium orthovanadate, had a significant effect on motility, implicating a myosin-like motor. However, the addition of 3μM calmodulin caused an 8.2-fold increase in movement of axoplasmic organelles on actin (Kuznetsov et al., 1993).

Injection of DNaseI, gelsolin, and synapsin I, all of which destabilize microfilaments, inhibits vesicle movements in axons (Goldberg et al., 1980; Brady et

al., 1984). What effect these molecules have on the stability of the microtubule organization in axons is not known. Nonetheless, the fact that actin isoforms have been found to be part of dynein-driven motors for vesicle transport along microtubules (Lees-Miller et al., 1992), and most recently the evidence that there are myosin motors on organelles in squid axoplasm (Bearer et al., 1993) both support the model of a less rigid transport system. While microtubules may be the predominant path for organelle transport in these systems, microfilaments may fulfil an equally important, albeit less conspicuous, role.

iii) *Streaming in hexactinellid sponges*

Considering the variety of intracellular transport systems found within protists and metazoans, it would be very interesting to know what kind of mechanism is used by hexactinellid sponges, an ancient group of animals, which current taxonomy places at the interface between protists and higher metazoans. A novel motile system involving bulk cytoplasmic transport could equally well be actin- or tubulin- based. The first step in identifying the mechanism is obviously to identify the cytoskeletal basis of streaming using pharmacological, immunofluorescence, and ultrastructural investigations. The role of particular molecular motors in force generation can normally be tested by pharmacological manipulation, and by the injection of antibodies, or by use of a reactivated permeabilized model, one of the best established techniques for defining the properties of molecular motors.

An equally interesting question to that of the mechanism is the function of

intracellular transport in hexactinellids. In foraminiferans streaming functions in food capture (partly by way of membrane transport), in burrowing, and in dispersal of offspring (Travis and Bowser, 1990). In algae, streaming seems primarily to provide a means of distributing nutrients. In axons, streaming is the means by which neurotransmitters reach the axon terminal. Whereas in cellular sponges nutrients are transported by motile amoebocytes (Kilian, 1952), there is no evidence that hexactinellids possess amoebocytes; archaeocytes have never been found with elongated processes, which are presumably required for motility. Furthermore, because the mesohyl seems too thin to be able support motile cells (Mackie and Singla, 1983), it is probable that cytoplasmic streaming serves to distribute nutrients in hexactinellids.

E. The use of live tissue models in hexactinellid cell biology

The ability to examine live syncytial tissues by light microscopy has opened up entirely new avenues of exploration in cell biology. It is now possible to look at the architecture of syncytial tissue and explore the basis of a novel motile system. Indeed there are many questions which it is tempting to investigate with live tissue models. What is the cytoskeletal organization of a syncytial organism? How does the syncytium form? Is there an organizing centre for morphogenesis of new tissue in syncytia? What is the relationship between archaeocytes and multinucleate tissue, and are these cells motile within the syncytia? Do syncytial tissues act as pathways for

electrical conduction? Is there a specific function that syncytial tissues serve in this group of sponges, or is it simply a developmental scheme? Do other sponges have syncytial tissues, or can they form syncytia, and if not, what might this say about the relationship of hexactinellids to other sponges?

From the nature of some of these questions one can see that the field of hexactinellid sponge cell biology is virtually untouched, and consequently the possibility of chancing upon novel discoveries is perhaps greater with these animals than with better-established models. However, the reader of this dissertation will discover that in several areas it has been impossible to elucidate more than the basic cell biology of this tissue, because time and again experimentally proven techniques (such as microinjection of substances or the development of a reactivated perfused cell model) have been ineffective with this sponge's tissue. In my opinion the most fruitful line of future research on these animals will come from molecular biology.

In the first chapter of this dissertation I describe the method of substrate preparation and sponge tissue culture, and discuss experiments designed to analyze the nature of the prepared substrate and the mechanism of adhesion by dissociated tissue.

In the second chapter I present evidence that tissue cultures from the rossellid hexactinellid sponge *Rhabdocalyptus dawsoni* fuse to form a giant multinucleated syncytium containing constantly moving streams of cytoplasm. I show that the cytoskeleton of these cultures starts off looking very much like that of any mammalian cell line, but that it grows, as pieces fuse, to form a single giant

scaffolding encompassing all of the tissue.

Cultured hexactinellid tissue does not appear to contain motile amoeboid cells. Instead the tissue is enveloped by an upper and lower plasma membrane, between which individual organelles and bulk cytoplasm are transported over vast distances along microtubule bundles in continuously flowing streams. In Chapter III I address the mechanism of intracellular transport in *Rhabdocalyptus*, looking at biochemical and physiological evidence for the role of motor proteins in transport and for linkage systems for bulk cytoplasmic transport.

In Chapter IV I extend these findings to a hexactinosan hexactinellid *Aphrocallistes vastus*, to demonstrate that fusion, cytoplasmic streaming, and the formation of a giant multinucleated syncytium are features of more than one family of hexactinellids. Since these two sponges are also representative of two distinct hexactinellid morphologies - lyssaccine (*Rhabdocalyptus*), which have separate spicules held in place by soft tissues, and dictyonine (*Aphrocallistes*), which have a fused, rigid skeleton - this suggests that streaming is likely to be characteristic of all hexactinellids.

Finally, in Chapter V, I show that hexactinellid tissues do propagate electrical impulses concurrent with the cessation of water flow through the sponge. Although attempts to record from adherent, spread aggregates, or from detached, spherical aggregates were unsuccessful, it was possible to record from aggregates which had been grafted back on to the sponge body wall. This is the first demonstration of propagated impulse conduction in the Porifera.

GENERAL METHODS

Specimen collection:

Specimens of *Rhabdocalyptus dawsoni* and *Aphrocallistes vastus* were collected by SCUBA from 30-40m depth at San Jose Islets in Barkley Sound, and at Willis Pt. in Saanich Inlet, British Columbia, and transferred without removal from sea water to flow-through seawater tanks at the Bamfield Marine Station, Vancouver Island, B.C., and recirculating seawater tanks at the University of Victoria. Specimens of *Haliclona* sp., *Ophlitaspongia pennata*, and *Halichondria* sp. were collected intertidally at Clover Point, Victoria, British Columbia, for use in adhesion assays and dye exchange experiments only.

Preparation of substrates:

The preparation of a natural substrate of an acellular tissue extract (ATE) dried onto coverslips or plastic petri dishes, to which dissociated tissue of *R. dawsoni* adheres, is described in detail in Chapter I. Alternatively, 50 μl (100 $\mu g \cdot ml^{-1}$) Concanavalin A (Con A) (*Canavalia ensiformis*, Sigma) was pipetted onto new, untreated, 22 x 22 coverslips (any brand) and allowed to air dry before being used as an adhesion substrate for dissociated tissue.

Preparation of aggregates:

Pieces of cleaned whole sponge tissue (1 cm^3) were squeezed through 100 μm Nitex mesh into a beaker to make 3.0-5.0 ml of dissociated tissue, and diluted to 200 ml with sea water. About 2 ml of the suspension was poured into 5 cm diameter plastic petri dishes containing several coated coverslips lying coated side up. The preparations were held at 11 ^{o}C either by floating the dishes on seawater or by placing them in an incubator. Alternatively, for video microscopy, the dissociated tissue was briefly pelleted by centrifugation at 1,000 x g for 15 s to remove spicule debris, and the top of the pellet was pipetted onto a coated coverslip in a dish of seawater.

Light, video enhanced contrast, and fluorescence microscopy:

Preparations were viewed with a Zeiss Universal compound microscope equipped with 10x, 16x, and 40x phase contrast and differential interference contrast (DIC) objective lenses and 25x, 40x, and 50x water immersion objective lenses, and with a cooling stage. For video microscopy images were captured with a Panasonic digital colour CCD video camera and processed in real time with an Omnex digital image processor (Imagen Inc., NY.). Photographs were taken from the screen of a Technitron television monitor using TMax 100 ASA black and white film. For immunofluorescence microscopy, preparations were viewed with a Leitz Aristoplan

lenses and Band Pass (BP) 340-380nm (DAPI/UV), BP 450-490 nm (FITC), and BP 515-560nm (Rhodamine) filters. Photographs were taken with a photoautomat on TMax 400 ASA black and white film or Ektachrome colour 400 ASA slide film. Some photographs of Rhodamine phalloidin-labelled preparations were taken with a manual 35 mm camera mounted on a Zeiss Universal microscope with epifluorescence.

Immunolabelling and vital staining:

Aggregates were transferred to calcium free sea water (CFSW) for 30 minutes prior to fixation to prevent depolymerization of the cytoskeleton due to excess calcium. In general the adherent tissue was robust enough to withstand transfer through air into fixatives or other media. For microfilament labelling, preparations were lysed at 2, 6, 12, and 24 hours after plating the tissue, in a PEM buffer consisting of 50 mM piperazine-N,N'-bis[2-ethane Sulfonic acid], 1 mM ethyleneglycol-bis-(ß-aminoethyl ether)N,N'-tetraacetic acid, 0.5 mM $MgCl_2$ at pH 6.9 with 10% dimethylsulfoxide and 0.1% Triton X-100 for 2 min and fixed in 2% paraformaldehyde in CFSW with 10 μM EGTA and 0.04% tannic acid for 10 minutes. It appeared that Rhodamine phalloidin did not penetrate preparations which were not lysed. Lysing the preparations removed the plasma membrane and some of the cytoplasm, but also caused microfilaments to remain anchored (see Stossel, 1993). For microtubule labelling preparations were fixed without lysing, in 2% paraformaldehyde in PEM

labelling preparations were fixed without lysing, in 2% paraformaldehyde in PEM buffer, at 30 minutes, 1, 6, and 12 hours after plating. Following one 30 minute wash in 0.05 M Tris buffer pH 7.0 with 0.1% TX-100, coverslips were incubated overnight in anti-tubulin antibodies or rhodamine-phalloidin (Molecular Probes Inc., Eugene, OR) 1:20 in phosphate buffered saline (PBS) to visualize actin microfilaments. The primary anti-tubulin antibodies used included (1) a polyclonal rabbit anti-tubulin antibody (Sigma, St. Louis, MO), (2) a monoclonal antibody against flagellar axoneme tubulin or isolated basal apparatus of *Polytomella* (Protista, Chlorophyceae) designated 5A6 (mouse host, IgG)(kindly provided by Dr. David Brown, University of Ottawa), (3) a monoclonal antibody against yeast tubulin clone YOL1/34 (rat host, IgG)(Sera Labs, Crawley Down, Sussex), (4) a monoclonal antibody against native chick brain alpha tubulin (mouse host, IgG)(Amersham, Arlington Heights, Ill.), and (5) a monoclonal antibody against *Drosophila* (insect) beta tubulin designated E7 (mouse host, IgG), developed by M. Klymkowski and obtained from the Developmental Studies Hybridoma Bank maintained by the Department of Pharmacology and Molecular Science, Johns Hopkins University School of Medicine, Baltimore, MD, and the Department of Biological Sciences, University of Iowa, Iowa City, IA. Secondary antibodies were as follows: (1) Rhodamine-conjugated goat anti-rabbit IgG (H and L), (Jackson Immunoresearch Laboratories, West Grove, PA); (2,4,5) either FITC- or Texas Red-conjugated goat anti-mouse IgG (H and L) (Calbiochem, La Jolla, CA); (3) FITC-conjugated goat anti-rat IgG (H and L) (Zymed, San Francisco, CA). After rinsing for 30 min, preparations were incubated

in their respective secondary antibody with 10% goat serum in TRIS buffer, pH 7.0, for 5 hours, rinsed thoroughly in PBS, pH 7.2, and mounted in PBS-glycerol with n-propyl gallate. To stain the nuclei, coverslips were incubated in 100 $\mu g \cdot ml^{-1}$ bisbenzamide, Hoechst #33342 (Sigma) for 5 min at 11 ^{o}C, and immediately observed with a 40X water immersion objective lens. To examine the microtubule network in severed streams, a stream was cut with a scalpel while the preparation was still in a dish of sea water on an inverted microscope. After the material downstream of the wound had completely drained away, the preparation was fixed and labelled for anti-tubulin immunofluorescence as above.

Electron microscopy:

For scanning electron microscopy (SEM) of adherent aggregated tissue from *Rhabdocalyptus*, coverslips with adherent tissue were transferred to CFSW for 30 min prior to fixation. Preparations were briefly lysed for 5-15 s, or fixed directly, in a fixative containing 2% glutaraldehyde, 1% OsO_4, 0.45 M sodium acetate buffer at pH 6.4, 10% sucrose and 5 μM EGTA final concentration, for 2 hours on ice. Coverslip preparations were dehydrated through a graded ethanol series, critical point dried in CO_2, mounted on stubs with silver conducting paint, coated with gold in an Edwards S150B sputter coater, and examined in a JEOL JSM-35 scanning electron microscope.

For transmission electron microscopy (TEM), whole mounts were prepared

Grids were critical point dried and viewed in a Hitachi H-7000 electron microscope. Unlysed preparations adhered to 5 cm diameter plastic petri dishes or plastic coverslips (Fisher Scientific) were acclimated to CFSW for 30 min and fixed as above for SEM. Unlysed preparations were treated with 4% hydrofluoric acid overnight to remove silica, dehydrated in ethanol and embedded in Epon. For cross sections the embedded material was taken off the coverslip or petri dish and reembedded in Epon. Thin sections were cut on a Reichert UM2 ultramicrotome and stained with uranyl acetate and lead citrate.

Chapter 1: SPONGE CELL CULTURE: A COMPARATIVE EVALUATION OF ADHESION TO A NATIVE TISSUE EXTRACT AND OTHER CULTURE SUBSTRATES.

INTRODUCTION

No continuous cell lines from marine invertebrates have been established to date, in part because little is understood of the nutritional requirements of these cells and because of complications caused by microbial contaminants in the sea water. None the less primary cell cultures have been developed with great success from a variety of marine invertebrates to study specific processes (e.g. starfish follicle cells - Mita et al., 1988; jellyfish neurons - Przysiezniak and Spencer, 1989; tunicate haemocytes - Rinkevich and Rabinowitz, 1993; cells from bivalve gills - Auzouz et al., 1993; abalone myocytes - Naganuma et al., 1994).

In the past, primary cell cultures of sponges have been invaluable for the study of histocompatibility responses and cell adhesion molecules (Wilson, 1907; Curtis, 1962; Humphreys, 1963; Moscona, 1968), but most recently interest in the vast number of novel biometabolites that sponges produce has rekindled the desire to develop continuous sponge cell cultures. Efforts in that direction have shown that long-term culture of sponge cells in suspension may be possible (Pomponi and Willoughby, 1994). Nonetheless, adherent and spread cell cultures are better suited for studies of cell types and cytological organization (e.g. Gaino et al., 1985a; Gaino et al., 1993), information that is still needed for this group of animals.

In particular, the use of primary cell cultures has been invaluable in studying the cytological organization of hexactinellid sponges. The inaccessibility of hexactinellid sponges, which inhabit deep water, as well as difficulties with fixation,

has meant that ultrastructural investigations of their tissues were only recently conducted (Reiswig, 1979a; Mackie and Singla, 1983; Boury-Esnault and de Vos, 1988; Reiswig, 1991; Reiswig and Mehl, 1991; Reiswig and Mehl, 1994; Boury-Esnault and Vacelet, 1994). These studies have supported earlier reports that claimed the tissue was syncytial rather than cellular (Ijima, 1901, 1904; Reiswig, 1979a). With the addition of electrophysiological evidence showing that the syncytial network is capable of propagating electrical impulses (Mackie, 1979; Lawn et al., 1981; Mackie et al., 1983), it was proposed that because of their vastly different tissue organization, hexactinellids be separated from other sponges at the subphylum level (Reiswig and Mackie, 1983). However, because many tissues once thought to be syncytial have subsequently been found to be cellular, an adherent tissue preparation was sought in which aspects of tissue morphology, and in particular the question of syncytiality could be studied in culture.

A central problem in culturing sponge cells for the purpose of studying cell morphology is the tendency for dissociated sponge cells to form opaque, multicellular aggregates. Some researchers have avoided this difficulty by using asexually produced propagules (gemmules) from fresh water sponges, which can be made to hatch and grow within a coverslip chamber (Weissenfels, 1980; 1992), or by explanting tissue from freshwater or marine sponges (Bond and Harris, 1988; Wachtmann and Stockem, 1992). Although hexactinellids lack gemmules, explants can be made (Wyeth et al., 1996). However, because these sponges have spicules up to several centimeters long, the preparations tend to be too thick for optimal viewing of the

tissue structure. An alternative is to provide dissociated cells with a highly adhesive substrate. Gaino et al. (1985a, 1985b, 1993) have shown that dissociated cells from calcareous sponges will adhere to mammalian extracellular matrix extracts and to synthetic substrates, although extended culture was not attempted. Cultures which do remain adherent generally form multicellular aggregates (Shimizu and Yoshizato, 1993), which eventually detach, again forming opaque spheres.

In order to obtain adherent tissue cultures from hexactinellids, an acellular tissue extract (ATE) was prepared from the hexactinellid sponge *Rhabdocalyptus dawsoni*. When dried onto glass coverslips or plastic petri dishes, the extract was found to promote both adhesion and spreading of dissociated *Rhabdocalyptus* tissue for periods up to two weeks. This chapter describes the preparation of the sponge acellular tissue extract and discusses characteristics of the adhesion it promotes in comparison with adhesion of sponge tissue to other natural and commercial substrates. Evidence of the syncytial nature of the adhered preparation is presented in Chapter II.

METHODS

1. Preparation of Substrates

a) Natural:

Blades of the red alga *Callyophyllis* sp., commonly found attached to the base of *R. dawsoni*, were used whole or the blade was crushed and the resulting extract was diluted in distilled water, pipetted onto coverslips and allowed to air dry. Fragments of clam or gastropod shell and pieces of rock from the habitat of *R. dawsoni* were used whole.

Dissociated sponge cell substrate, consisting of whole cells, portions of flagellated chambers and spicule debris was made from *R. dawsoni* by forcing 3-4 cleaned pieces of sponge, each approximately $1cm^3$, through 100μm Nitex mesh. The dissociated tissue was pipetted onto coverslips and allowed to dry overnight.

Acellular tissue extract (ATE), containing no whole cells or tissues was made from *R. dawsoni* and from the demosponges *Haliclona* sp., *Halichondria* sp., and *O. pennata*, using distilled water to lyse the cell membranes. The procedure involved briefly rinsing 3-4 pieces of sponge, again approximately $1cm^3$, in calcium- and magnesium-free sea water (CMFSW) to help dissociate cell-cell junctions, and then soaking the pieces four times for two hours each in 20 times the volume of distilled water at 4^oC. After the final soaking, the tissue was mechanically dissociated in one times the volume of distilled water, causing the release of a cloudy suspension, which was confirmed by light microscopy to be acellular. This suspension was diluted

approximately ten fold with cold distilled water, and stored at 4°C with 0.03% sodium azide. Fifty microlitres of the acellular tissue extract was pipetted onto coverslips and allowed to air dry overnight.

b) Commercial:

Concanavalin A (from *Canavalia ensiformis*, Sigma) was dissolved in phosphate buffered saline (PBS) and diluted in double distilled (DDW) water to make 100 $\mu g \cdot ml^{-1}$ and 20 $\mu g \cdot ml^{-1}$. Poly-l-lysine (Sigma) was diluted in DDW to 500$\mu g \cdot ml^{-1}$ and 10$\mu g \cdot ml^{-1}$. Type II collagen from chicken (Sigma) was used at a concentration of 2 $\mu g \cdot ml^{-1}$ in DDW to determine the behaviour of hexactinellid sponge tissue on a commercially available extracellular matrix tissue culture substrate. Fifty microlitres of each of the commercial substrates was pipetted onto glass coverslips and allowed to air dry overnight.

2. Preparation of primary tissue cultures

Sponges from collections made throughout the year varied greatly in their ability to produce well-adherent aggregates. Consequently all sponges were first tested for their ability to adhere to the ATE prior to starting an adhesion assay with different substrates.

Whole sponge tissue was cleaned of debris, and five pieces, approximately 1cm^3 each, were squeezed through 100μm Nitex mesh into a beaker to make 3.0-5.0 ml of dissociated tissue, and diluted to 200 ml with sea water. The dissociated tissue

was poured into petri dishes containing one or more coverslips coated with the ATE, and dishes were either floated on the surface of 10°C sea water or kept in an incubator at 10°C overnight. After 12-24 hours if the tissue had adhered, the coverslips could be removed and placed in dishes with clean sea water without dislodging the cultures from the coverslips.

3. Adhesion assays

a) Substrates: Approximately 2 ml of the dissociated sponge tissue were poured into each 1.8 cm plastic petri dish each containing one of the above substrates. Dishes were kept in a incubator at 10°C for 6-9 hours. After the allotted time, the coverslips, pieces of shell, rock, or algae, were removed, rinsed gently in a beaker of sea water and placed in a petri dish of clean sea water for observation, and any tendency of the sponge tissue to adhere to the substrates was noted.

b) Characteristics of the ATE: In order to shed light on the particular proteins of importance in the ATE, adhesion assays were carried out with ATE that had been subjected to the following treatments: 1. Centrifugation at 6000 x g; only the supernatant was dried on coverslips. 2. Dialysis through a 6000 MW membrane; only the fraction <6000 MW was dried on coverslips. 3. Treatment with Trypsin (0.2% and 2%) @ 4°C overnight followed by 30 min @ 37°C. 4. Treatment with Pronase E (0.2% and 2%) as in (3). 5. Treatment with collagenase (0.2% and 2%) as in (3). 6. Treatment with hyaluronidase (0.02% and 0.2%) as in (3). Finally ATE was made

using artificial sea water to determine if the adhesion factor was in the sea water. All adhesion assays with treated ATE were conducted with five sponges which had only been tested once previously for their ability to adhere to ATE. Tissue from each sponge was plated on all substrates. After 12 hours incubation at 10°C, coverslips were rinsed gently and placed in a dish of clean sea water for observation. A description of the tissue morphology on each substrate was made, whether tissue had adhered or not. In control experiments tissue was plated on uncoated coverslips, DW-coated coverslips, and coverslips with normal ATE.

c) Wounding: To determine the effect of continued wounding of sponges on tissue adhesion, pieces were cut from one sponge at 12 hour intervals and plated in three 1.8 cm petri dishes containing a coverslip coated with ATE, Con A (20-100 $\mu g \cdot ml^{-1}$), or type II collagen ($2\mu g \cdot ml^{-1}$). Control coverslips were coated with 2% PBS. After 12 hours at 10°C, coverslips were gently rinsed in clean sea water, and placed in a fresh dish of clean sea water for observation. Percent adhesion was calculated by estimating the amount of area of the coverslip covered by adherent tissue using a numerical scale of adhesion and tissue confluence. Adhesion of confluent tissue to the entire substrate coated area of the coverslip was interpreted as 50% adhesion. A rating of 100% indicated adhesion and spreading of the tissue beyond the coated area to cover the entire coverslip. The percent adhesion in the three dishes was averaged to give the mean percent adhesion. Because tissue from different sponges did not adhere equally well, adhesion experiments could only be conducted with those sponges that showed an ability to adhere during the first screening.

Consequently Figure 2 represents the results of adhesion by tissue from two individuals. This experiment was repeated with four more individuals from subsequent collections, and gave identical results.

4. Electron microscopy

Scanning and transmission electron microscopy of adherent tissue was as described in the general methods section.

Acellular tissue extract was prepared for TEM as follows. A white solid which formed upon addition of substrate to 10mM $CaCl_2$ or normal sea water (NSW) was fixed in 1% OsO_4, 6.25% glutaraldehyde and 10% sucrose in 0.2M s-collidine buffer (pH 7.4) on ice for 2 hours. The material was dehydrated in a graded ethanol series and embedded in Epon. Thin sections were cut on a Reichert UM2 ultramicrotome, stained with uranyl acetate and lead citrate, and viewed with a Hitachi 7000 electron microscope.

RESULTS

Because of the difficulties involved with collecting hexactinellid sponges, which generally inhabit depths of greater than 25m and have a patchy distribution, sponges were collected sporadically throughout the year. It was found that sponges which had been held in sea water aquaria for many weeks did not produce aggregates or adhere to any of the substrates; only freshly collected specimens were capable of producing aggregates. Furthermore, not all animals collected from one dive adhered equally well in culture. Tissue from some sponges adhered very well, tissue from others adhered only tenuously, and tissue from yet others did not adhere at all. Dissociated tissue from most animals collected during the winter months of November to April tended to form poor aggregates and to adhere poorly to all substrates. Generally, a greater number of the sponges collected during the summer months of May to October produced strongly adherent and well spread aggregates. These observations are summarized in Table 1.

1. Characteristics of adhesion

Dissociated sponge tissue plated on a coverslip without a substrate generally did not adhere but formed detached opaque aggregates of tissue (Fig. 3A). In some instances, these spherical aggregates made temporary attachments to the substrate, but always detached shortly thereafter. Of the natural substrates used, neither the

algal extract nor whole cell extract promoted adhesion of dissociated sponge tissue, nor did tissue show any particular association with the pieces of whole alga, shell, or rock (Table 2). In dishes with these substrates, the dissociated sponge tissue formed small (<1mm diameter) spherical aggregates in the petri dish. In contrast, *Rhabdocalyptus* tissue adhered to and spread on substrates coated with ATE from a conspecific. Although in initial experiments sponge tissue did not adhere to commercial tissue culture substrates, later experiments showed that *Rhabdocalyptus* tissue did in fact adhere to and spread to form confluent cultures on substrates coated with poly-l-lysine and Con A. The sponge tissue attached in the form of very small spheres, but did not spread or form confluent cultures, on type II collagen-coated substrates. The ATE and Con A-coated substrates promoted adhesion and spreading of the tissue on and away from the coated area, while tissue plated on poly-l-lysine-coated substrates generally did not spread further than the coated area. When dissociated *Rhabdocalyptus* tissue was plated on the ATE, the boundary of the dried extract was always evident from the morphology of adherent tissue (marked by the open arrows in Fig. 3B). This was not true for tissue plated on Con A or poly-l-lysine-coated substrates. Although the tissue attached to the area coated with ATE, small patches of tissue also adhered to adjacent, uncoated coverslip. At higher magnification some cell-like round objects could be seen that may be archaeocytes and other cellular components of the sponge when whole (Fig. 3C). However, the adherent tissue appeared fused and possessed giant lamellipodial and filopodial projections from its edges. Furthermore, vast streams of cytoplasm flowed

uninterrupted throughout the tissue mass at rates just greater than $2\mu m \cdot s^{-1}$ appearing blurred in Figure 3C. Thin sections through fixed adherent tissue cultures showed that nuclei were abundant in former streams, and were apparently randomly distributed throughout the adherent preparations. No membranes were found separating adjacent nuclei.

Dissociated cells from the demosponge *Haliclona* sp., adhered to ATE prepared from a conspecific, and spread to form a layer of cells which in some places was several cell layers thick and in others appeared to be a monolayer of cells (Fig. 3D). No streaming was found in these cultures although crawling of individual cells was readily observable.

Scanning electron microscopy of adherent tissue showed that dissociated cells from *Haliclona* sp. were approximately half the size of dissociated hexactinellid tissue pieces immediately after plating on ATE, and possessed filopodia but few lamellipodial projections (Fig. 4A). Dissociated tissue from *Rhabdocalyptus* adhered almost instantly upon plating, and spread a broad skirt-like lamellipodium (Fig. 4B). Such pieces contained between two and five nuclei when viewed by thin section transmission election microscopy. After 3 hours pieces of hexactinellid tissue had grown substantially (Fig. 4C), and 12-24 hours later, tissue masses had formed a confluent network coating the entire substrate (Fig. 4E). No cell boundaries could be seen; the surface of the entire aggregate was covered by a smooth, uninterrupted membrane, and large filopodia were abundant at the edges of tissue masses. In contrast 24 hour-old cultures from *Haliclona* sp. formed a monolayer of cells or

multicellular aggregates, in which individual cells could always be identified (Fig. 4D).

2. Wounding

Although dissociated tissue normally did not adhere to plain coverslips, repeated wounding of an individual sponge by removing tissue for dissociation, caused the tissue to adhere even to uncoated coverslips (Fig. 5). Wounding of the tissue seemed to improve responsiveness to higher concentrations of Con A more rapidly than to lower concentrations. After 3-4 periods of repeated wounding over 48 hours tissue from some animals readily adhered to control coverslips coated with either 2%PBS or DDW (Fig. 5). Thorough washing of the dissociated tissue prior to plating, by rinsing it with artificial sea water three times, each time pelleting the tissue and discarding the water, did not reduce adhesion to plain coverslips, or to coverslips coated with 2% PBS or DDW controls during the period of peak adhesion.

3. Characteristics of the tissue extract

The ATE formed a white, cloudy, buoyant solid when added to 10mM $CaCl_2$ or NSW (Fig. 6A). The ATE did not coagulate in calcium-free sea water with 50mM EGTA. Thin section transmission electron microscopy of the calcium-congealed material showed no collagen fibrils but rather profiles of membranous vesicles (Fig.

6B). Thin sections of tissue adhered to the ATE showed that the tissue formed a thin layer enclosed on top and bottom by a continuous membrane, and contained archaeocytes, enucleate vesicles, and other organelles (Fig. 6C). The ATE layer appeared as a thin electron-dense material (Fig. 4C inset).

Tissue adhered preferentially to the supernatant of extract centrifuged at 6000 x g, and to the fraction dialyzed through a 6000 MW dialysis membrane, compared to control coverslips with DDW. Enzymatic treatment of the ATE (Table 3) had little effect on tissue adhesion but substantially altered tissue spreading and the formation of cytoplasmic streams. Just as adhesion improved rapidly with wounding, it waned quickly 3-4 weeks after collecting the animals. At this time tissues of most sponges lost responsiveness first to plain uncoated substrates and then to coated substrates.

4. Species-specific adhesion

Dissociated tissue from newly collected specimens of *Haliclona* sp., *Halichondria* sp., *O. pennata*, and *R. dawsoni* plated on freshly prepared substrates, each showed a higher degree of adhesion and spreading on ATE from a conspecific (Fig. 7). *R. dawsoni*, *Halichondria* sp. and *Haliclona* sp. adhered most specifically to their own ATE, while *O. pennata* adhered best to its own extract but also to a lesser extent to the ATE from *Halichondria* sp.. All sponge extracts congealed in normal sea water, but to differing degrees. Sponge biomass affected the amount of congealable extract obtainable. Thin encrusting sponges, such as *Haliclona* sp. and *O. pennata*, were more

difficult to derive extract from than either large encrusting sponges, such as *Halichondria* sp., or large non-encrusting sponges such as *R. dawsoni*. When dried on coverslips, some extracts appeared transparent, and others, such as *Halichondria* sp. ATE, left a clearly visible opaque ring at the periphery.

Table 1. Percent of sponges which produced well-adherent aggregates from those collected throughout the year.

Table 1: Percent of sponges which produced well-adherent aggregates from those collected throughout the year.

Month	Number of sponges collected	Percentage of sponges which produced adhered cultures		
		A*	B	C
January	35	0	5.7	2.8
	10	10		
	14	0		
	15	33		
	12	0	8	
	11	10		
February	28	10	10	
March	25	12	12	8
April	3	0		
May	20	30		35
	15	0		
	15	27	47	20
	10	60	70	
June	10	50		
	10	10		
July	11	18		
August	12	58		
September	10	10		
	12	33		
October	3	33		
	3	33		
	10	100		
December	10	0	40	

*Time of plating. A: immediately after collection, B: 2-5 days after collection, C: 7-14 days after collection. Sponges were not plated more than once if used for other experiments .

Figure 3. Primary cultures of sponge tissue. A, Opaque, detached aggregates from *R. dawsoni* plated without extract coated substrate. Note that some spherical aggregates will form temporary attachments to the coverslip (arrowheads) Scale bar, 1mm. B, A low magnification micrograph of adherent and spread tissue from *R. dawsoni* adhered to ATE-coated coverslips. At this magnification the tissue gives the appearance of swirling tracks of cytoplasm. Tissue has adhered preferentially to the coated area (open arrows indicate where the extract ceases), but also adheres in patches to the uncoated parts of the coverslip. Scale bar, 1mm. C, An adherent culture of *R. dawsoni* shown at high magnification. A stream (st) of moving cytoplasm appears blurred in the micrograph. Spheres may be individual archaeocytes (arrowheads) or vesicles. Giant lamellipodia (l) and filopodia (f) anchor the entire tissue mass to the coverslip. Nomarski optics. D, Primary culture of tissue from the demosponge *Haliclona* sp.. Individual cells in which vesicles surround the nucleus can be identified where the culture is thin (arrowheads). In other areas, such as that indicated by the asterisk, the culture may be several cell layers thick. Scale bar, C and D, 20μm.

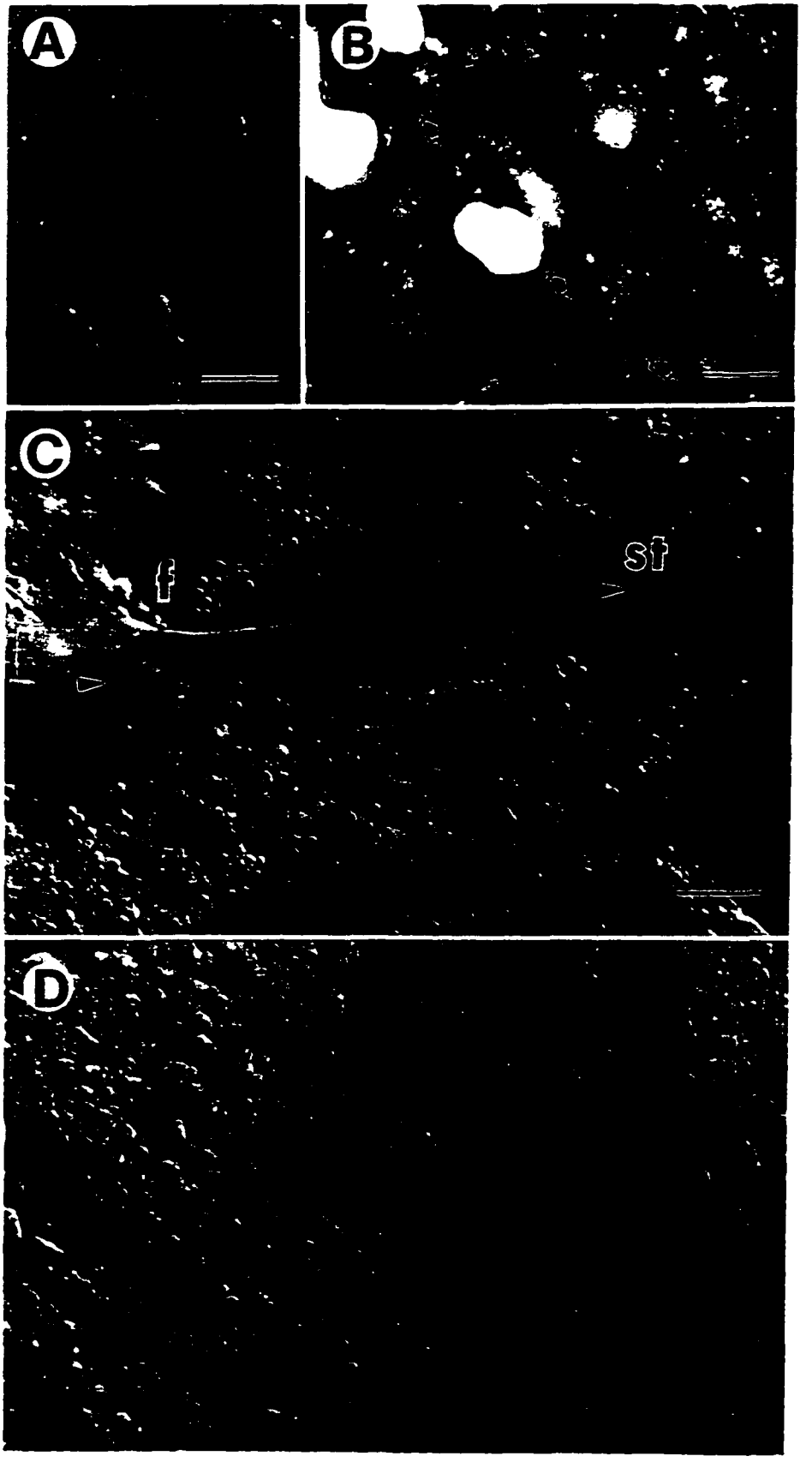
A
B
C
f
st
D

Table 2. Adhesion of *Rhabdocalyptus dawsoni* tissue to natural and commercial substrates.

Table 2: Adhesion of *Rhabdocalyptus dawsoni* tissue to natural and commercial substrates

Substrates tested	Adhesion
Algal extract	-
Whole cell sponge extract	-
Acellular sponge extract	++
Concanavalin A (20-100µg/mL)[c]	++
Poly-L-lysine (10-500µg/mL)[c]	++

(key: - no adhesion; ++ adhesion and spreading; [c] concentration dependent)

Figure 4. Adherent tissue from syncytial and cellular sponges viewed by scanning electron microscopy. A, Dissociated cells from *Haliclona* sp. immediately after plating are approximately half the size of dissociated tissue pieces from *R. dawsoni* (B). *Haliclona* cells generally extended long filopodia (arrowheads) while most tissue pieces from *R. dawsoni* spread a broad, skirt-like lamellipodium (Lm). Scale bars A, 5μm, B, 10μm. C, Three hours after plating tissue from *R. dawsoni*, pieces were considerably larger and had a smooth surface membrane. Bar: 10μm. D, Twelve hours after plating *Haliclona* sp. tissue, individual cells were clearly identifiable in the adherent tissue. Scale bar, 20μm. E, Twelve hours after plating tissue from *R. dawsoni*, cultures had spread to form a thin layer covered by a continuous membrane, only broken in places by desiccation caused by the preparation procedures. Former streams (st) of cytoplasm can be identified by their bulky appearance (arrow). Scale bar, 10μm.

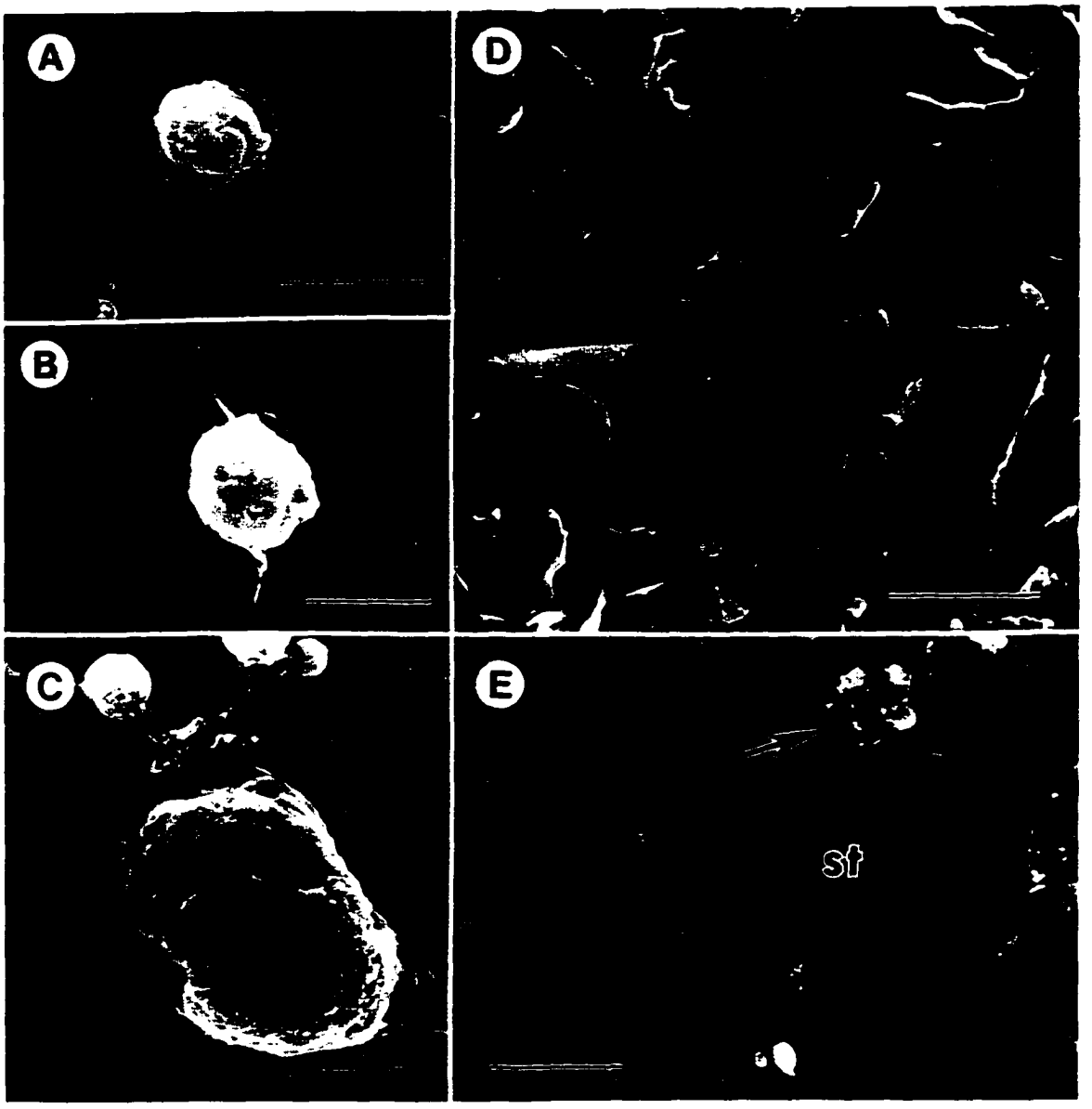
A
B
C
D
E
st

Figure 5. The effect of repeated wounding on adhesion by *Rhabdocalyptus* tissue. Percent adhesion was estimated as described in the text. Concanavalin A was very effective at causing both adhesion and spreading of sponge tissue in a concentration dependent manner. Tissue removed from the same individual every 12 hours eventually adhered even to control coverslips coated with 2% PBS. Circles, Con A 100μg/ml; squares, Con A 20μg/ml; upright triangles, *Rhabdocalyptus* ATE; inverted triangles, Type II Collagen 2μg/ml; diamonds, control 2% PBS.

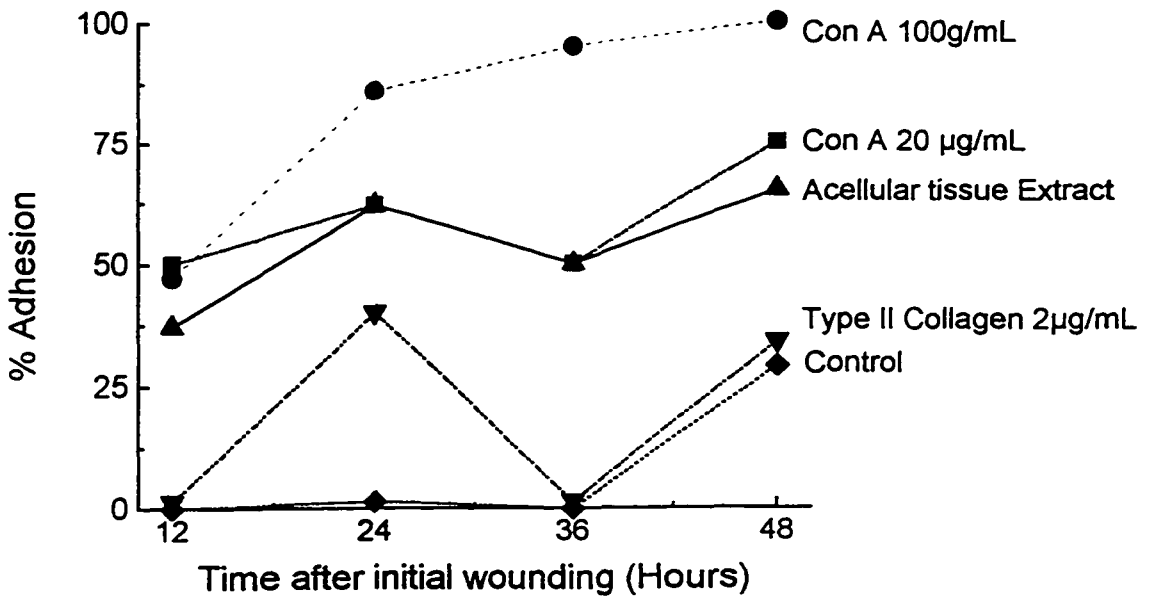
100
75
50
25
0
% Adhesion
12
24
36
48
Time after initial wounding (Hours)
Con A 100g/mL
Con A 20 µg/mL
Acellular tissue Extract
Type II Collagen 2µg/mL
Control

Figure 6. Acellular tissue extract from *Rhabdocalyptus dawsoni*. Light microscopy and transmission electron microscopy. A, The congealed, buoyant solid which forms when the acellular tissue extract, which is otherwise a transparent liquid, is pipetted into sea water. Scale bar, 2mm. B, A thin section through the calcium-congealed acellular tissue extract from (A) reveals profiles of membranes but no collagen. Scale bar, 0.5μm. C, A cross section of tissue from *R. dawsoni* adhered to the extract approximately 18h after plating shows a former stream of cytoplasm, which can be identified by the presence of microtubule bundles (mt). Open arrows indicate the substrate (magnified in inset). Archaeocytes (ar), nucleus (n), vesicle (v), mitochondria (m). Scale bar, 2μm; inset, 0.5μm.

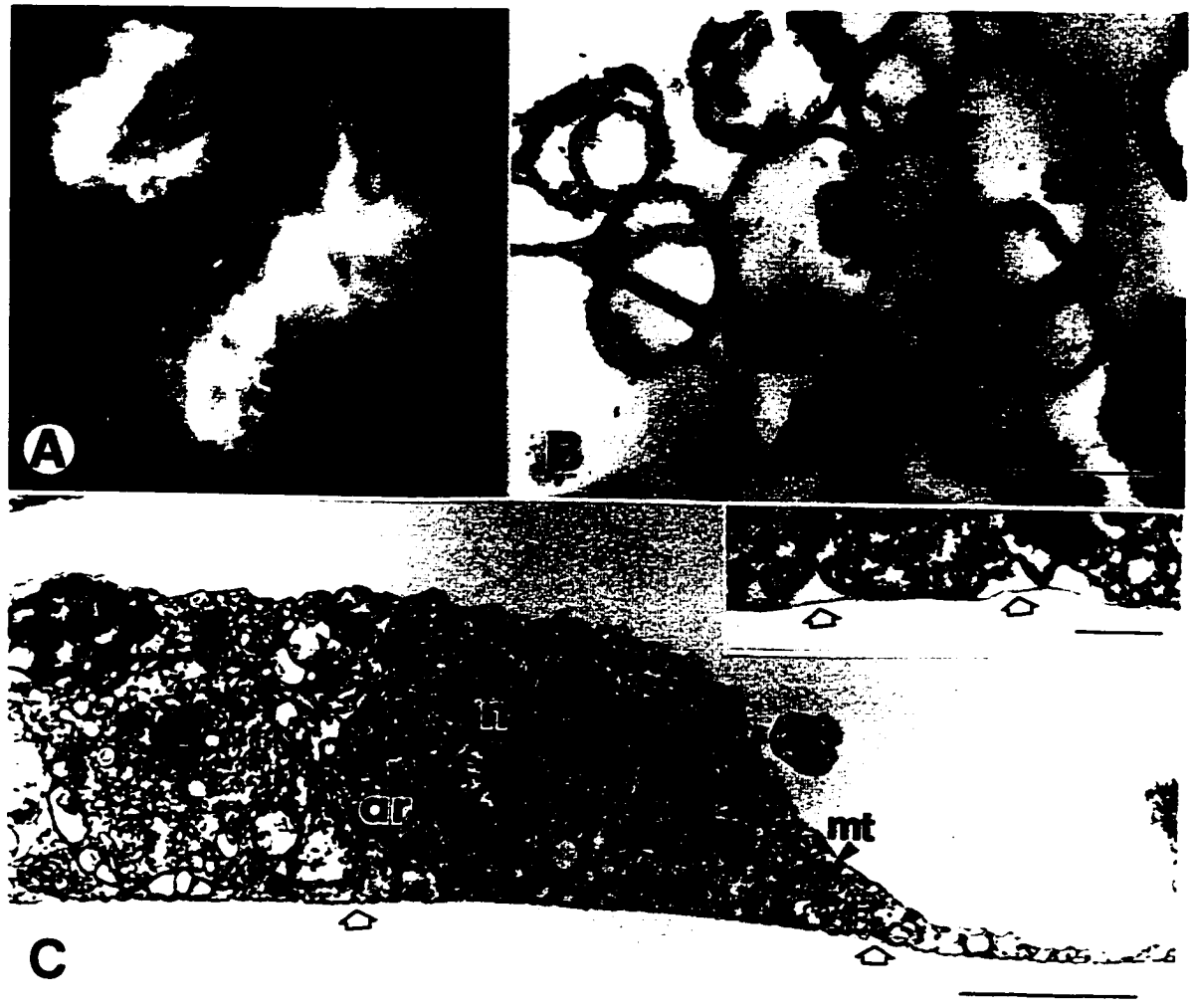
A
B
C
ll
dr
mt

Table 3. The effect of enzymatic treatment of the acellular tissue extract on adhesion and spreading by dissociated *Rhabdocalyptus* tissue.

Table 3: Effect of enzymatic treatment of the acellular tissue extract on adhesion and spreading by dissociated *Rhabdocalyptus* tissue (+/- = yes/no).

Enzyme treatment*	Adhesion (+/-)	Aggregate morphology	Streaming (+/-)	Spreading (+/-)	Confluence (+/-)
Trypsin					
2%	+	Large, round	-	-	-
0.2%	+	Small, round	+	-	-
Pronase E					
2%	+	Flat, adhered	-	-	-
0.2%	+	Small, round	-	+	-
Collagenase					
2%	+	Flat, adhered	-	+	-
0.2%	+	Flat, adhered	+	+	-
Hyaluronidase					
0.2%	+	Flat, adhered	+	+	+
0.02%	+	Flat, adhered	+	+	+
Control (overnight @ 4°C)	+	Flat, adhered	+	+	+
Control (30 min @ 37°C)	+	Flat, adhered	+	+	+

*overnight @ 4°C, 30 min @ 37°C

Figure 7. Preferential adhesion of sponges to acellular tissue extract from a conspecific. Fifty microlitres of each ATE extract were dried on 50mm-long coverslips. ATE left to right along top: *R. dawsoni* (R), *Haliclona* sp. (Hp), *O. pennata* (O), and *Halichondria* sp. (H). Dissociated tissue from each sponge was plated on one of the coverslips, top to bottom: (R) *R. dawsoni*, (Hp) *Haliclona* sp., (O) *O. pennata*, (H) *Halichondria*. The presence of white, almost particulate material, indicates adhesion of tissue. ATE from large, bulky sponges, such as *Halichondria*, left a clearly visible opaque ring marking the periphery of the dried extract.

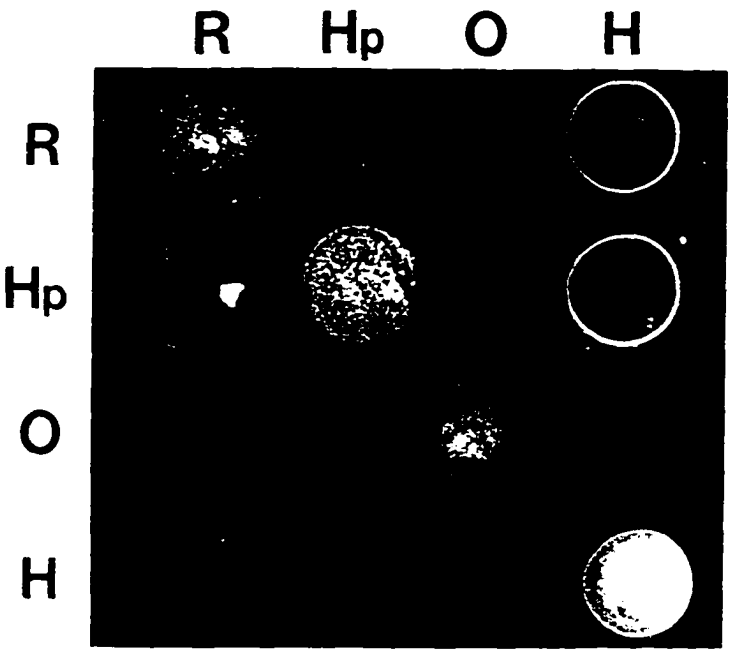
R
Hp
O
H
R
Hp
O
H

DISCUSSION

While dissociated sponge cells may adhere temporarily to uncoated substrates upon initial plating (e.g. Gaino et al., 1985a), I have demonstrated that an acellular tissue extract from a conspecific promotes prolonged adhesion and spreading of sponge cells. Adhesion and spreading of tissue from the demosponge *Haliclona* sp. on a substrate coated with ATE from a conspecific, produced cultures reminiscent of many mammalian cell cultures in which individual cells are recognizable. In contrast, hexactinellid tissue from *Rhabdocalyptus dawsoni* adhered and spread on the ATE in a manner that revealed its syncytial tissue organization. Hexactinellid tissue cultures possessed a smooth continuous membrane covering what appeared to be a single, multinucleate, giant cell, which may be many centimetres in diameter. A detailed description of adherent *Rhabdocalyptus* cultures is given in Chapter II.

1. Variability in aggregation and adhesion

The giant syncytial networks formed by adhered hexactinellid tissue are a fascinating preparation for study, but they are very awkward for analyzing adhesion in a quantitative assay for several reasons. Firstly, although *Rhabdocalyptus* is perhaps the most accessible of hexactinellids, it is nonetheless not very abundant and lives at such depths that animals are hard to collect in great numbers. Since only freshly collected animals produced adherent tissue cultures, often it was only possible to have fewer

than 10 individuals for an assay. Secondly, because tissue from different individuals varies greatly in responsiveness to coated substrates (see Table 1), it was often not possible to use all individuals collected during one dive, for an assay. Thirdly, although some sponges produced healthy aggregates during the winter months, tissue from most sponges adhered and aggregated poorly at this time. Field observations showed that during this period sponges are flaccid and in poor condition, often to such an extent that a number of the animals die (Leys, unpublished). Variability between individuals in adhesion of tissues in culture appears to be characteristic of other marine invertebrates (Przysiezniak, personal comm.). Considering the seasonal trends in adhesion ability observed here, this may reflect varying states of the health of individuals in the population, throughout the year. However, at all times of the year, some sponges nonetheless produced strongly adherent cultures on the ATE.

2. Wounding

Repeated wounding of the sponge tissue, by snipping off pieces for dissociation, was found to enhance the adhesion of dissociated tissue from that animal even to uncoated substrates. Even vigorous washing of dissociated tissue prior to plating did not prevent wounded tissue from attaching to uncoated substrates, suggesting that the adhesion factor is not soluble. There have been many reports of culture media being conditioned by wounded tissue (reviewed by Hay, 1981), but it is not known what factor is responsible for the activation of cells. Some evidence suggests that the

polysaccharide hyaluronan abounds in healing tissues where it is important for cell migration (Laurent and Fraser, 1992). The lack of effect on adhesion or spreading by treatment of the ATE with hyaluronidase may be a result of using too low a concentration of hyaluronidase, or might indicate that this polysaccaride is not important in adhesion and spreading in hexactinellids. Other enzymatic treatment did interfere with spreading but not adhesion, which suggests that there is a role for collagen and other ECM proteins in spreading in hexactinellids. However, the optimal incubation time and temperature of these enzymes with sponge extracellular matrix (ECM) proteins is unknown and hence their effectiveness in this assay cannot be assumed. Infrequently I have seen bundles of collagen between the tissue and the coverslip and within pockets of the tissue in thin sections of adherent preparations older than 24 hours. The actual mechanism by which adhesiveness to substrates increases with wounding is not clear and merits further investigation.

3. Acellular tissue extract

Previous attempts to examine adhesiveness of invertebrate cells to substrates have used a variety of matrix components (Day and Lenhoff, 1981; Gaino et al., 1993). In these studies, responsiveness to different substrates was determined by whether the cells adhered or not, the morphology of pseudopodia, and the extent of spreading. Based on the variation in sponge cell responsiveness to substrates in this study, it appears that cells may respond differently depending on the individual, on the

season, and on wounding. Furthermore, use of a native extract rather than mammalian and artificial matrix components is likely to promote a response closer to that *in vivo*.

Electron microscopy of the ATE prepared from *Rhabdocalyptus* showed membranes to be the predominant component prepared by this method, suggesting that the adhesion factor is a membrane-associated molecule rather than an extracellular matrix (ECM) component such as collagen, and that adhesion involves a cell-cell adhesion factor. Moreover, because a membranous solid formed when the ATE was added to a medium containing calcium but not in one without calcium, precipitation of material is calcium-dependent and it is possible that calcium-dependent cell adhesion proteins are present in the ATE. Tissue did not adhere to the ATE in CFSW (data not shown). In marine sponges, calcium-dependent and species-specific cell adhesion during aggregation may involve any or all of protein-protein, protein-carbohydrate, and carbohydrate-carbohydrate interactions (Müller, 1982; Coombe et al., 1987; Müller et al., 1988; Parish et al., 1991, Misevic and Burger, 1993). A fibronectin-like protein has been shown to be present in demosponges (Labat-Robert et al., 1981), but its role in cell adhesion is not well understood (Conrad *et al.*, 1982).

All the demosponges used in this experiment and *Rhabdocalyptus* showed a higher degree of adhesion to substrate from a conspecific, suggesting that adhesion to the ATE works in a similar manner to cell-cell aggregation. Family-specific adhesion by jellyfish cells to mesoglea has also been documented for hydrozoans, and

is thought to involve the carbohydrate groups of ECM-glycoproteins which are associated with collagen-like fibres (Schmid and Bally, 1988; Schmid et al., 1991). It will be interesting to confirm in further experiments whether other hexactinellid extracts promote family- or species-specific adhesion.

Attempts were not made to isolate the factor responsible for adhesion in the ATE because of the difficulty in carrying out adhesion assays with this sponge. However, considering that the so-called aggregation factor (AF) of demosponges is known to be soluble and can be isolated simply by washing a sponge in CMFSW, and that the AF does not require calcium for adhesion, it is unlikely the ATE contains aggregation factor. On the other hand, it is possible that the ATE contains the so-called aggregation receptor which requires extraction from cell membranes with trichloroacetic acid (Müller, 1982). Considering the role of carbohydrate-protein interactions in sponge cell aggregation, the presence of sugar groups on most cell membranes, and the role of lectins in primary aggregation (Müller, 1982), it is not surprising that Con A, a plant lectin which recognizes α-d-glucose and α-d-mannose groups, should promote adhesion of sponge tissues when used as a substrate.

This study has demonstrated that the preparation of an acellular tissue extract which promotes the adhesion and spreading of sponge tissue as primary cultures is uncomplicated. With further analysis and purification, similar extracts from other marine invertebrates might be useful in primary culture of marine invertebrate tissues, and may even help in developing continuous cell lines from these animals.

Chapter 2: CYTOSKELETAL ARCHITECTURE AND ORGANELLE TRANSPORT IN GIANT SYNCYTIA FORMED BY FUSION OF HEXACTINELLID SPONGE TISSUES.

(A version of this chapter was published in 1995 in the *Biological Bulletin* volume 188, pp 241-254.)

INTRODUCTION

The syncytial organization of hexactinellid sponge tissue has been in question since the histology of dredged specimens was first examined. Early sponge researchers reported that there were no discernable membrane boundaries between nuclei (Schulze, 1887; Ijima, 1901). Although two cell types, archaeocytes and thesocytes, could be distinguished, most of the sponge was thought to be syncytial. At the time, however, many animal tissues were considered to be syncytial, including the pinacoderm of demosponges (Hyman, 1940), but phase contrast and electron microscopy have since revealed their cellular nature. Thus, the idea that hexactinellids were syncytial animals received little serious attention from modern sponge workers until recently.

Reiswig (1979a) investigated hexactinellid histology using several populations accessible by SCUBA on the coast of British Columbia. Although his first attempts at electron microscopy with *Aphrocallistes vastus* and *Heterochone calyx* were thwarted by difficulties with ultrastructural preservation, Reiswig nonetheless found no evidence to contradict Schulze's and Ijima's conclusions. Perseverance with electron microscopy with *Rhabdocalyptus dawsoni* (see diagrams Fig. 8A) resulted in an improved fixation technique which provided ultrastructural evidence for two kinds of reticular, multinucleate tissues, the trabecular syncytium and the choanosyncytium, and for several types of cells (Mackie and Singla, 1983b) (Diagram; Fig. 8B). Most interestingly, the syncytial cytoplasm was found to be connected to cellular

components either by open cytoplasmic bridges or by a unique osmiophilic perforated plugged junction (Mackie, 1981). Sclerocytes were the only cell type not connected by plugs to the syncytium.

Concurrent electrophysiological studies with *Rhabdocalyptus* showed that following mechanical or electrical stimulation this sponge was capable of propagating signals at a rate of 0.26 $cm \cdot s^{-1}$ that stopped the flow of feeding currents throughout the whole animal, presumably by causing flagellar arrest (Lawn et al., 1981; Mackie et al., 1983). As no nerves could be found, the syncytial tissues were proposed as the pathways for conduction, though no recordings of propagated electrical signals could be obtained.

Plugged junctions have since been reported in six of the seven hexactinellids examined by transmission electron microscopy, the exception being *Dactylocalyx pumiceus* (Reiswig, 1991). In this animal, no such junctions were found, but their presence could not be completely ruled out. Because of the remarkable differences in cellular organization between hexactinellids and other sponges and the physiological evidence of signal conduction it was proposed that this group be separated from cellular sponges at the subphylum level (Reiswig and Mackie, 1983). Nonetheless, conclusive proof of syncytial organization from dye exchange experiments or from observations of cytoplasmic movements in living tissues has not been obtained, and recent investigations have raised doubts about the syncytial nature of hexactinellid larvae (Boury-Esnault and Vacelet, 1994).

When demosponges are dissociated by squeezing them through a fine mesh,

the cells have the ability to reaggregate forming a new individual (Wilson, 1907). The mechanisms underlying reaggregation have been extensively studied. The process is homeotypic, and therefore of interest in relation to self- and non-self discrimination in the earliest metazoa (Curtis, 1962; Moscona, 1968; McClay, 1971; Müller, 1982). Studies of newly dissociated demosponge cells shows that they exhibit rapid non-directional crawling along the substrate (Noble and Peterson, 1972; Gaino *et al.* 1985b). Initial contacts between cells may be made by membrane bridges (Evans and Bergquist, 1974), while the formation of secondary aggregates is by species-specific cell adhesion molecules (Müller, 1982). Whether aggregation is brought about by cell migration or artificially, e.g. by the rotary technique of Humphreys (1963), aggregates rapidly grow in size becoming opaque under the light microscope.

In the only previous study on hexactinellid aggregation (Pavans de Ceccatty, 1982) aggregates were found to form large spherical masses as in demosponges, and their contents could not be observed with light microscopy. In the present study, however, substrates containing sponge tissue extract or concanavalin A were used on which the tissues will adhere and spread out, permitting observation of the cytoskeleton in vitro. The findings reported here show that, in such preparations of *Rhabdocalyptus*, tissue aggregation leads to the formation of giant syncytia in which multidirectional streaming occurs over great distances in a manner unique among the Porifera.

Figure 8. *Rhabdocalyptus dawsoni*. Diagrams of the whole sponge and of its tissue components. (A) Drawing of the hexactinellid sponge *Rhabdocalyptus dawsoni* with its osculum partially cut open. (B) Diagram illustrating the tissues of whole sponges. Water flows into choanoflagellate chambers (FC) as shown by the curved arrows, and is pumped out directly up from the centre of the chamber. A portion of the flagellated chamber (black box) is shown enlarged on the right to illustrate detail of the membranes separating cellular and syncytial components of the tissues. (Trabecular syncytium (TS), collar body (CB), choanoblast (Chb), plugged junction (PJ), mesohyl (M), dermal membrane (DM), nucleus in the syncytium (N_S), nucleus of an archaeocyte (N_{ar}), spherulous cell (SC), archaeocyte (AR).)

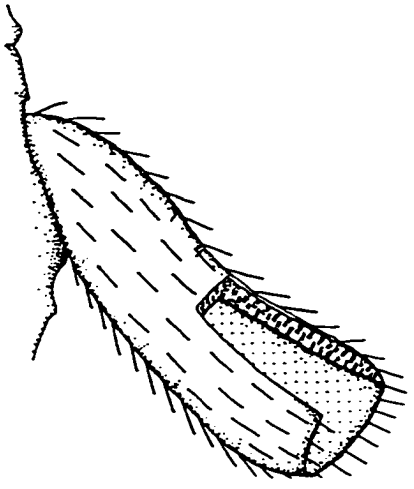

A

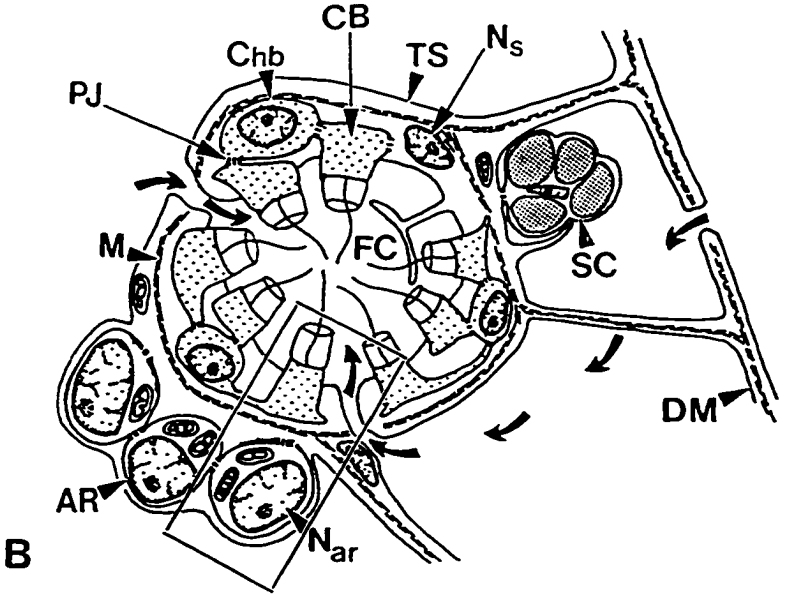

B

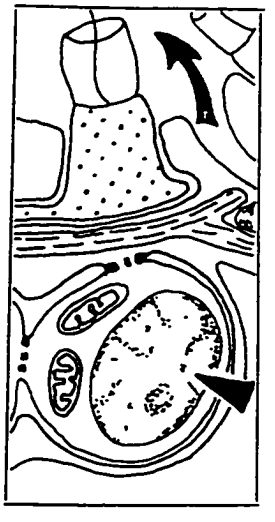

METHODS

Methods for the preparation of tissue cultures, video microscopy, immunolabelling and fluorescence microscopy, and electron microscopy, are described in the general methods section.

Pharmacological manipulations:

To demonstrate the effect of various cytoskeletal disruptors on streaming, drugs (cytochalasin B, colcemid, nocodazole, Taxol, EGTA) were added to 2 ml sea water in a plastic petri dish containing one preparation to give the final concentrations as noted in Table 4. To demonstrate reversibility of the effects of cytochalasin B and nocodazole, preparations were incubated in these drugs for 5 min and 2 min respectively, and transferred immediately to clean sea water every 15 min thereafter for 4.5 h. Preparations were kept at 11 ^{o}C for the duration of the experiment.

Dye exchange experiments:

To confirm that fusion of tissues and exchange of cytoplasm occurred during aggregation in syncytial sponges but not in cellular sponges, dissociated tissues of both sponges were loaded with fluorescent, membrane-impermeable dyes and allowed to aggregate. Dissociated tissue from both *Rhabdocalyptus* (R) and *Haliclona*

(H) was briefly centrifuged at 1,000 g for 15-30 s to remove spicule and other debris. Calcein acytoxymethyl ester (CAM) (515nm emission) and Calcein Blue acytoxymethyl ester (CBAM) (437nm emission) (Molecular Probes, Inc., Eugene, OR) were made up in dimethylsulfoxide (DMSO) to stock concentrations of 1 mM and 2 mM respectively. The dyes were added to the sponge tissue at a final concentration of 10 μM in microfuge tubes which were left at 10 ^{o}C for 15 min. The tissue was then rinsed three times by pelleting the tissue, drawing off the remaining sea water by pipette and resuspending the pellet in fresh seawater. After the final rinse equal volumes were plated in a 1.8 cm extract-coated plastic petri dish as follows: (R)-CAM with (R)-CBAM; (R)-CAM with (H)-CBAM; (H)-CAM with (H)-CBAM.

RESULTS

1. Fusion

Immediately after plating, the dissociated tissues consisted of unattached rounded masses of various sizes, some of which could be identified as parts of choanoflagellate chambers by their collars and flagella. All pieces adhered to the coverslip within seconds of plating and flattened and spread out between 5 s and 10 min after plating (Fig. 9). The larger (10 μm diameter) pieces developed a broad, skirt-like lamellipodium, or extended long filopodia, into which the cytoplasm streamed. These adherent tissue pieces, which were 3-4 μm thick, incorporated other smaller, rounded pieces of tissue, by drawing them in to a central location within the aggregate. Independent adherent pieces encountered each other by lamellipodia or filopodia. Fusion did not always occur immediately upon contact of lamellipodia. Lamellipodia even overlapped one another for 10-30 min before the exchange of organelles could be clearly detected (Fig. 9B, 54 min). A clear sign of fusion, however, was a shared lamellipodium at the point of touching, followed by exchange of organelles. Within minutes of fusion there was no evidence that the single piece of tissue had ever been other than single. Lamellipodial extension continued in all directions, and streams of cytoplasm started to become clearly visible circumnavigating the aggregate in both clockwise and anti-clockwise directions. Fusion continued with other tissue pieces which were encountered and eventually the

entire coated substrate was covered by a confluent tissue layer 1-8 μm thick. Lamellipodia of large and small adherent aggregates were always less than 0.5 μm thick.

2. Cytoplasmic streaming

As aggregates increased in size by incorporating neighbouring tissue masses, organelle movement became organized into wider and straighter streams, until eventually the entire coverslip was covered in tissue which consisted of dramatic rivers of flowing cytoplasm traversing the coverslip, sometimes running parallel in opposite directions (Fig. 10A), and even crossing each other without apparent interruption in volume or velocity of flow. Streams of cytoplasm flowed uninterrupted for distances up to several centimetres, limited only by the area of coated substrate available. Large streams continually changed direction and both gained and lost volume. Under DIC microscopy bulk cytoplasm in streams could be seen to contain vesicles of various sizes, and spicule debris. Similar objects were revealed by electron microscopy in cytoplasm fixed while streaming, along with numerous mitochondria, nuclei, Golgi bodies and some archaeocytes. Fluorescent staining with Hoechst #33342 showed nuclei in both the flowing and stationary cytoplasm (Fig. 10B). Individual nuclei could be followed in streams for distances up to several millimetres.

Organelles resolvable by video-enhanced contrast microscopy in thin areas of tissue moved at an average rate of $2.15 \pm 0.33\ \mu m \cdot s^{-1}$ ($n = 100$), while bulk streams

moved at an average rate of 1.72 ± 0.30 $\mu m \cdot s^{-1}$ (n = 100) (Fig. 10C). However, some organelles moved haltingly, sometimes reversing direction or apparently bumping into each other; these organelles seemed to buckle or bend as they reversed. Organelles moving in broad lamellipodia followed no one direction, and occasionally paused for some seconds. In some streams the bulk cytoplasm which had been flowing diminished in volume to isolated organelles, to be followed once again by bulk cytoplasm.

Cutting a stream with a scalpel caused cytoplasm to build up on the upstream side of the wound. Downstream of the wound cytoplasm continued to flow away until no movements of organelles could be detected but birefringent tracks could still be seen by phase contrast and DIC microscopy (Fig. 11A). Immunofluorescence of tubulin on the depleted side showed that microtubule bundles remained even though all streaming along them had ceased (Fig. 11B). Eventually the cytoplasm upstream of the wound began to turn back upon itself, initiating a new stream parallel to the original one but in the reverse direction. At the same time lamellipodial and filopodial processes were extended toward the downstream side until, after several minutes, contact was once again made, followed by fusion, and a few organelles, soon followed by the full stream, began to flow along the original track. These stages are summed up diagrammatically in Figure 11C.

With time, the tissue amassed in central locations and gradually withdrew from the substrate until an opaque sphere was formed. Such spheres could temporarily adhere once again if new substrate was offered.

3. The actin cytoskeleton

Only by briefly lysing preparations prior to fixation was it possible to obtain a clear picture of actin distribution in adhered tissue preparations. Attempts to label microfilaments with a polyclonal antibody to actin and with rhodamine phalloidin in whole preparations gave, at best, weak labelling of microfilament bundles, whose precise location could not be determined. However, lysing the tissue for 5 s - 2 min resulted in detachment of the superficial part of the tissue mass, exposing the layer adjacent to the substrate in which actin labelling produced clearer results.

Two hours after plating, aggregates were 30-100 μm in diameter and possessed blunt rods containing thick actin bundles which projected from the periphery (Fig. 12A). The edges of large lamellipodia labelled strongly with rhodamine-phalloidin, and stress fibres some 20 μm in length, transected the tissue. After 6 h these masses had joined and no membranes demarcating cell boundaries could be seen within the tissue mass by phase contrast microscopy. Rhodamine phalloidin-labelled microfilament bundles up to several hundred micrometers long were observed to run around the edges of adhered aggregates (Fig. 12B). A network of fine filaments was apparent beneath the stress fibres throughout the syncytium. One-day-old adherent aggregates showed no change in general morphology or in actin distribution, although the distances over which bundles of microfilaments could be followed now exceeded 500 μm. After 24 h much of the tissue had been drawn into central, opaque areas. The edges of such dense tissue masses possessed blunt rod-like extensions reaching

some 18.0 ± 4.5 μm (n=20) from the edge of the lamellipodium forming a "hairbrush effect" (Fig. 12C). These extensions labelled very strongly for actin (Fig. 12D). The organization of actin in aggregates older than 48 h did not change significantly as most tissue was centralized at that time, anchored firmly by massive projections from the edges. Scanning electron microscopy of the giant rods in intact and lysed preparations revealed thick actin bundles forming their core (Figs. 12 E and F).

4. The microtubule cytoskeleton

Preservation of microtubules required the use of a special fixation method (see General Methods) after which it was possible to visualize microtubule bundles by phase contrast and immunofluorescence microscopy. These bundles were still visible after cytochalasin B treatment, but not after treatment with nocodazole or colcemid. Of five anti-tubulin antibodies only two monoclonal antibodies, one prepared against beta tubulin in *Drosophila* and the other against chick brain alpha tubulin gave good immunofluorescence in whole mounts. Control experiments showed that all antibodies labelled microtubules in neurons and cilia of tunicate branchial basket and veliger larvae.

Immunofluorescence microscopy revealed a remarkable change in the microtubule network over the course of aggregation. At 30 min microtubules formed a fine meshwork in tissue pieces up to 80 μm in diameter; microtubules appeared delicate, some directly crossing and others winding around the tissue mass. Nuclei

appeared randomly scattered among the microtubules. After 6 h, the microtubules were already well organized into striking bundles many of which traversed an entire coverslip (Fig. 13A). Where many bundles of microtubules converged into one path they became rigidly straight (Fig. 13B). At the edge of preparations, the entire bundle gave way to a reticular network of lines (Fig. 13C). These often wound through giant lamellipodia before joining the main stream and traversing the coverslip again.

Double labelling of actin and tubulin proved unsatisfactory as the lysing procedure required for clear visualization of the microfilament network most often destroyed the continuity of microtubules. However, double labelling of nuclei and microtubules clearly demonstrated that nuclei were randomly distributed among microtubules (Fig. 15F).

The microtubules were difficult to fix for electron microscopy. The fixative used by Mackie and Singla (1983b) does not stabilize microtubules except in flagella. The fixative of Harris and Shaw (1984) (see fixation for electron microscopy in the chapter on general methods) gave excellent results for both general ultrastructure and microtubule preservation. In cross sections of the adherent tissue, microtubules were seen both in bundles and lying individually (Fig. 14A and inset). In thicker areas of the tissue, large bundles were seen at the surface of the preparation as well as through the depth of the tissue. Rarely in these areas did they occur singly, and rarely were they on the bottom of thick tissue masses. In horizontal section, microtubule bundles could be traced for many hundreds of micrometers (Fig. 14B).

Nuclei, mitochondria, coated vesicles, and tubulovesicular organelles were all found adjacent to microtubule bundles, as well as lying free in the cytosol. Tracts of microtubules ran beside, but not through, clusters of archaeocytes and spherulous cells. In whole mounts of aggregates adhered to tissue extract on formvar-coated gold EM grids, organelles of various sizes were also seen associated with linear structures with diameters of approximately 22 nm, presumably microtubules (Fig. 14C).

5. Inhibition experiments

Organelle movement was reversibly inhibited by both nocodazole and colcemid, but was unaffected by cytochalasin B (Table 4), although the latter caused the tissue to detach from the substrate. Neither Taxol nor 10 μM EGTA had any effect on rate of organelle transport.

6. Dye exchange

Attempts to inject the fluorescent dyes carboxyfluorescein or lucifer yellow through glass capillary microelectrodes were not successful because of difficulty in obtaining stable penetrations. The surface membrane of adhered aggregates either blocked the electrode, or did not reseal around the electrode after penetration. However, fluorescent dyes coupled to acytoxymethyl esters such as Calcein AM (CAM) and Calcein blue AM (CBAM) could be readily loaded into dissociated

tissue. Tissue loaded with CAM plated in the same culture dish with tissue loaded with CBAM produced fused aggregates in which streaming occurred. After 6-12 hours these aggregates were uniformly blue-green (Fig. 15 A,B,C). In control experiments in which dissociated tissue from the cellular sponge *Haliclona permolis* loaded with CBAM was plated with tissue from *Rhabdocalyptus* loaded with CAM, *Haliclona* cells rapidly formed large round aggregates, did not mix with *Rhabdocalyptus* tissue, and did not take up the green dye (Fig. 15D). *Haliclona* tissue, even if adhered, showed no sign of cytoplasmic streaming. When two samples of *Haliclona* tissue were loaded with CAM and CBAM respectively and plated together, there was no exchange of dye, although after 12 hours aggregates were mosaics of both colours (Fig. 15E).

Figure 9. Fusion by adherent aggregates from *Rhabdocalyptus*. Video microscopy. (A) Upon plating, pieces of tissue adhere and spread a skirt-like lamellipodium or long filopodia. After about 1 hour of spreading, such pieces encounter each other, as shown by the overlapping lamellipodia (B, arrow). Tissues fuse and exchange cytoplasm between 5 and 30 minutes after first contact (C). Fused tissue pieces continue to grow in diameter, incorporating some tissue pieces (asterisk in A and B) and fusing with others (D, arrow). Minutes after plating dissociated tissue: a: 33 min, b: 54 min, c: 102 min, d: 134 min; bar: 10 μm.

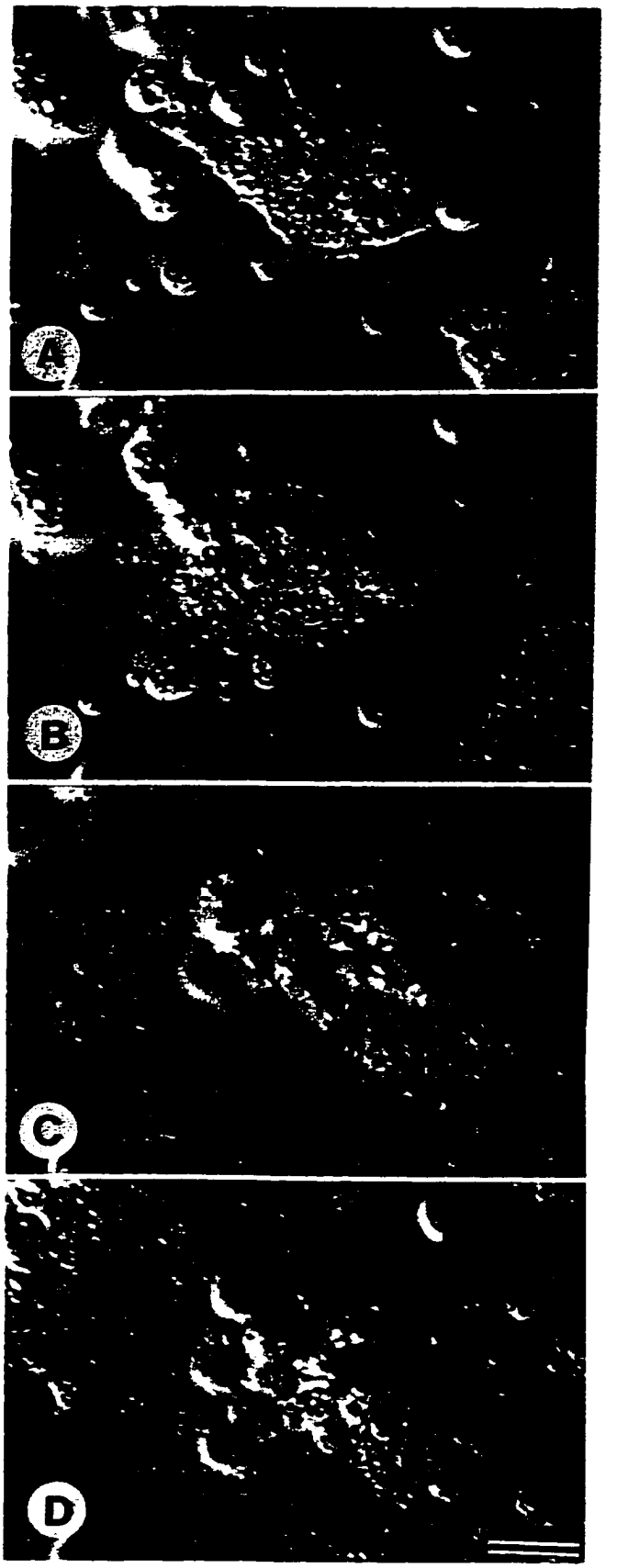
A
B
C
D

Figure 10. Organelle transport in day-old cultures from *Rhabdocalyptus*. Light and fluorescence microscopy. 24 hours after plating sponge tissue, a single tissue mass covers an entire petri dish. (A) Streams (arrowheads) are abundant and run in opposite directions, winding throughout the entire coverslip. A 5 s shutter exposure allowed moving objects to leave trails. Bar: 20 μm. (B) Hoechst-labelled nuclei are visible both in streaming (STR) and stationary cytoplasm. Nuclei move in streams at just over 2 $\mu m \cdot s^{-1}$. A 30 s shutter exposure causes all moving nuclei to leave a trail of light marking their path. Bar: 20 μm. (C) Images from a video monitor showing bulk transport of material in streams (asterisk) beside organelles which are being transported individually (arrow and arrowhead). Streams move continuously but at a slower rate than individual organelles. The organelle marked by an open arrow moves steadily, leaving the field of view in the third frame, while the organelle marked by an arrowhead moves haltingly eventually stopping. Frames shown are at 8 s intervals. Bar: 10 μm.

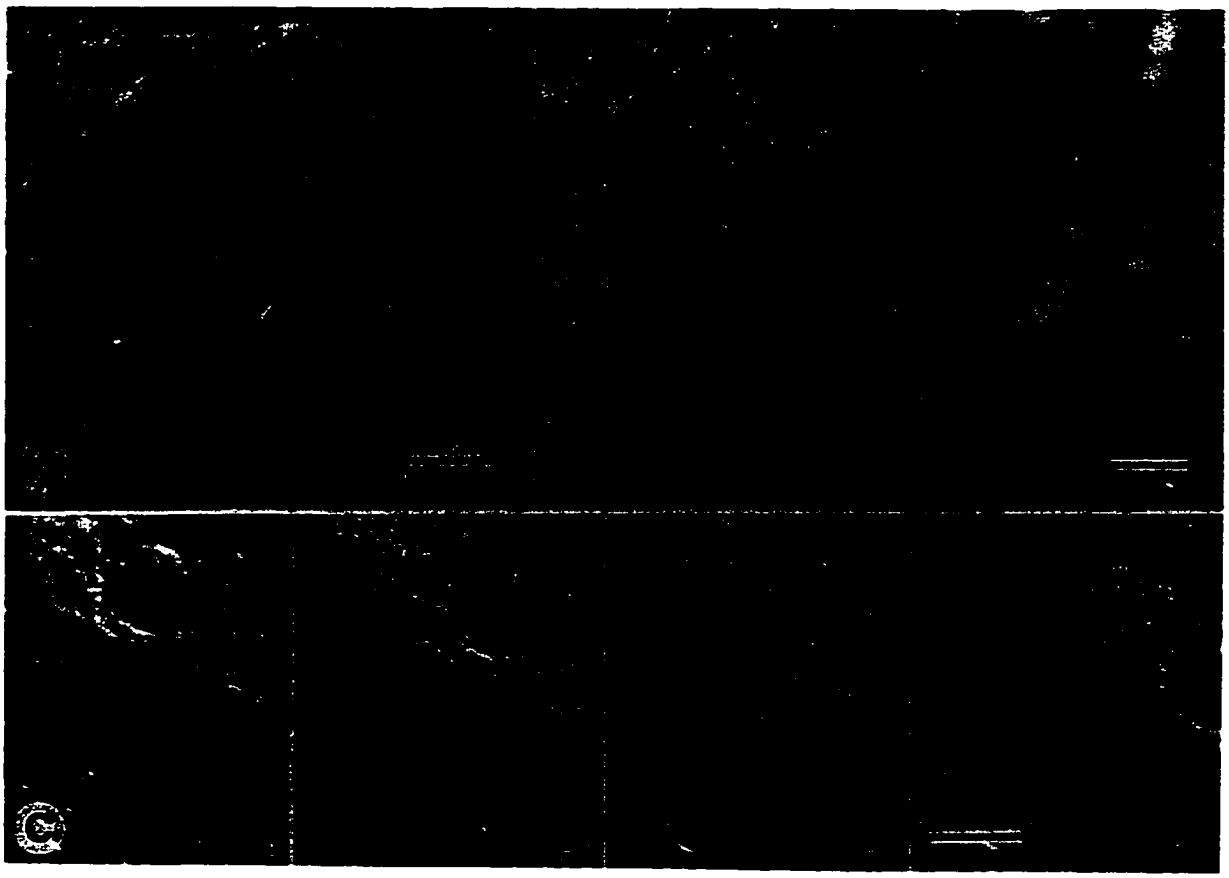

Figure 11. The effect of severing streams of cytoplasm in adherent tissue cultures from *Rhabdocalyptus*. (A) When cut, the cytoplasm downstream (DS) of the wound (arrowhead) continues to drain in the direction of the arrow, while that upstream (US), builds up. Bar: 30 μm. (B) Anti-tubulin labelling of microtubules in the wounded stream. Microtubules remain, even though all visible organelle movement has ceased downstream of the wound. Bar: 30 μm. (C) Diagram illustrating the sequence of events after wounding a stream. The cut cytoplasm (dashed line, (1)) builds up on the upstream side (2), eventually forging a new path in the reverse direction (3), as indicated by arrowheads. Filopodial and lamellipodial projections extend across the wound, making contact with the original tracks (4). Single organelles, rapidly followed by the bulk cytoplasm, begin to stream along the former path (4). Arrows indicate direction of flow.

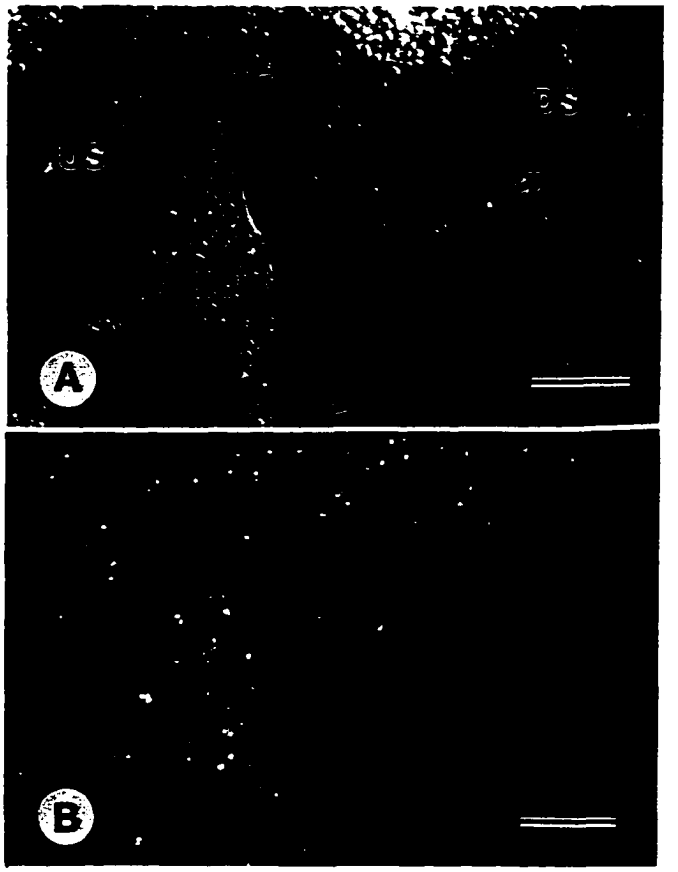

C

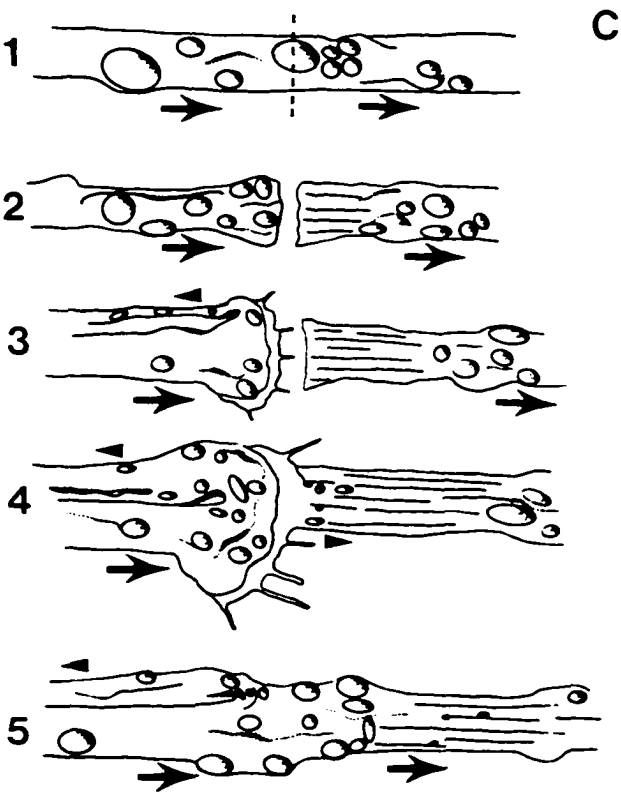

Figure 12. The actin cytoskeleton in adherent aggregates from *Rhabdocalyptus* after lysing. (A) Rhodamine-phalloidin labelling of aggregates 2 hours after plating reveals tissue masses 30-100 μm in diameter which possess well defined rods projecting from their periphery (arrowheads). Bar: 20 μm. (B) 6 hours after plating dissociated tissue, aggregates are already 0.5mm in length and can be much larger. A portion of a fused aggregate shows giant bundles of microfilaments delineate the border (filled arrows). A network of microfilament bundles traverses the basal layer adjacent to the substrate (arrowheads) and small, actin-dense rods lie within lamellipodia (open arrow). Bar: 20 μm. (C,D) Adherent aggregates older than 12 hours possess giant rods projecting from the periphery as a "hairbrush" (C: phase contrast; D: rhodamine-phalloidin labelling of unlysed tissue, bar: 10 μm). (E) SEM shows several giant rods extending from the lamellipodium (LM). (F) High magnification SEM of a lysed actin-dense rod. E,F Bar: 0.5 μm.

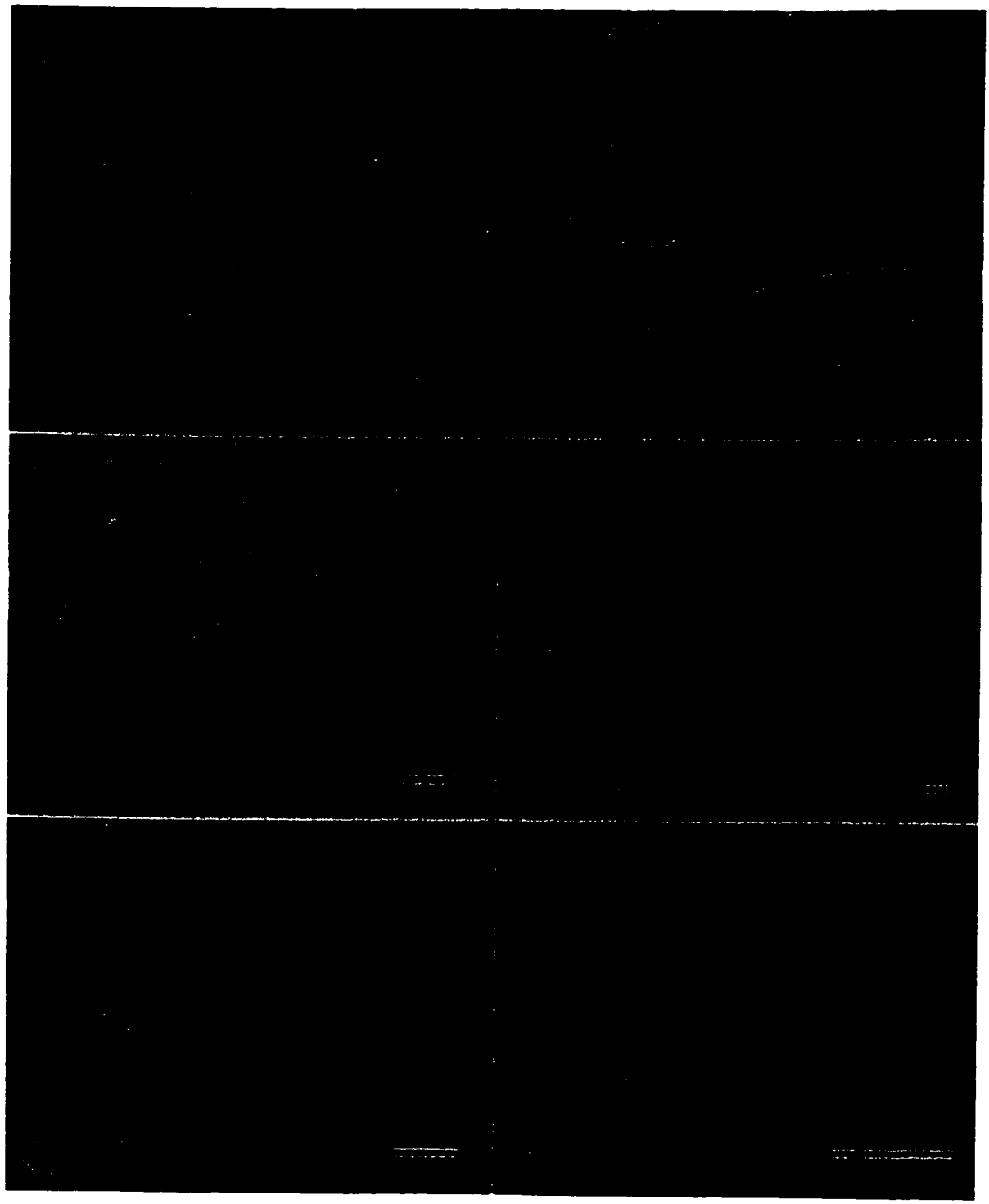

Figure 13. Immunofluorescence of the microtubule cytoskeleton in adherent aggregates from *Rhabdocalyptus*. (A) 6h after plating, microtubule bundles already stretch up to a centimetre across an entire coverslip. A-C Bar: 20 μm. (B) Microtubule bundles are rigidly straight (STR) in streams, while those leaving, or converging on a stream (arrowheads) are often curved. (C) At the edges of preparations, bundles give way to a fine meshwork of microtubules which reach into lamellipodia (arrowheads).

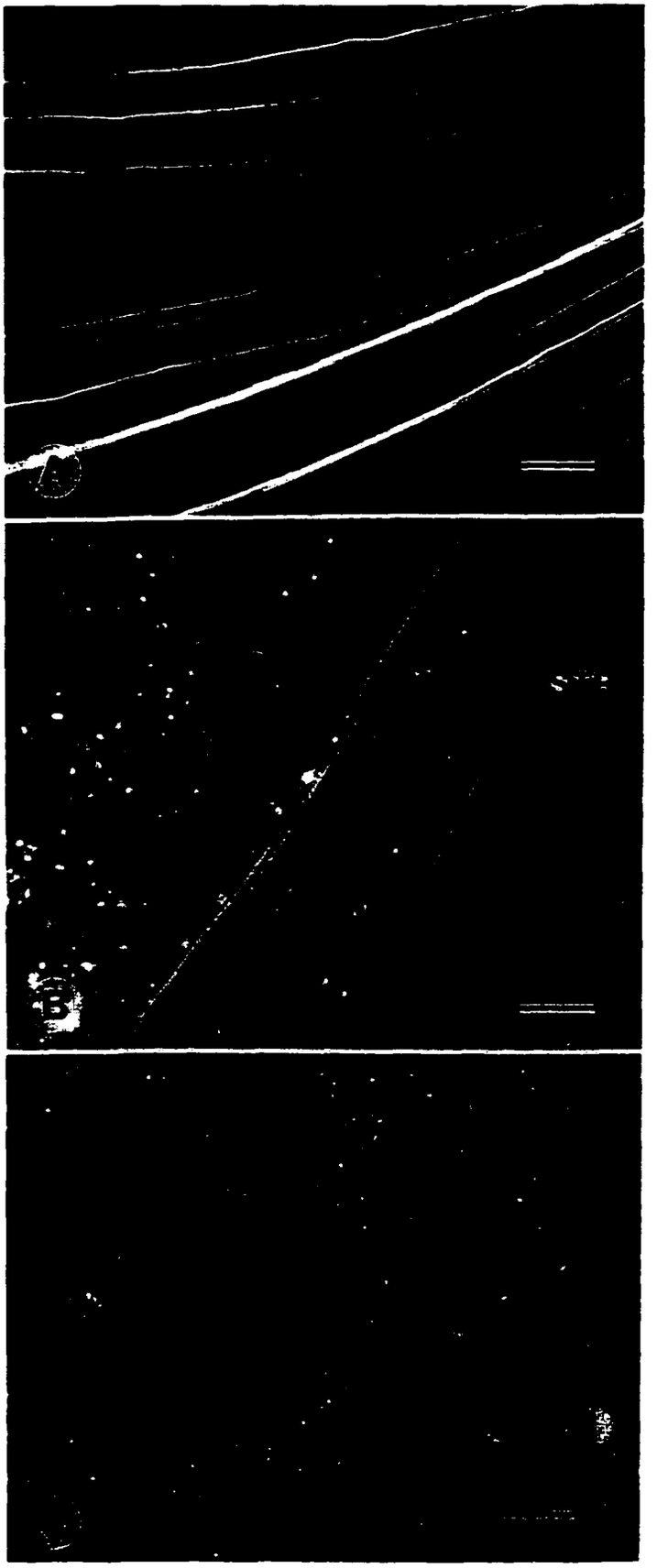
A
B

Figure 14. Transmission electron microscopy of microtubules in adherent aggregates from *Rhabdocalyptus*. (A) In cross section, cellular components (such as archaeocytes) lie in membranous pockets in the multinucleated cytoplasm which is itself surrounded above and below by a continuous membrane. In fixed tissue, streams were still identifiable as pathways of cytoplasm. Microtubule bundles were at the surface of former streams and throughout the tissue (arrows). Bar: 1 μm. Inset shows an enlargement of microtubules from within the box. Bar: 0.1 μm. (Nuclei, N; archaeocyte, AR; Golgi, G; mitochondria, M). (B) Horizontal section through a stream showing a bundle of microtubules (MT) with associated organelles. Bar: 0.5 μm. (C) A whole mount preparation showing an organelle associated with linear structures. Bar: 0.2 μm.

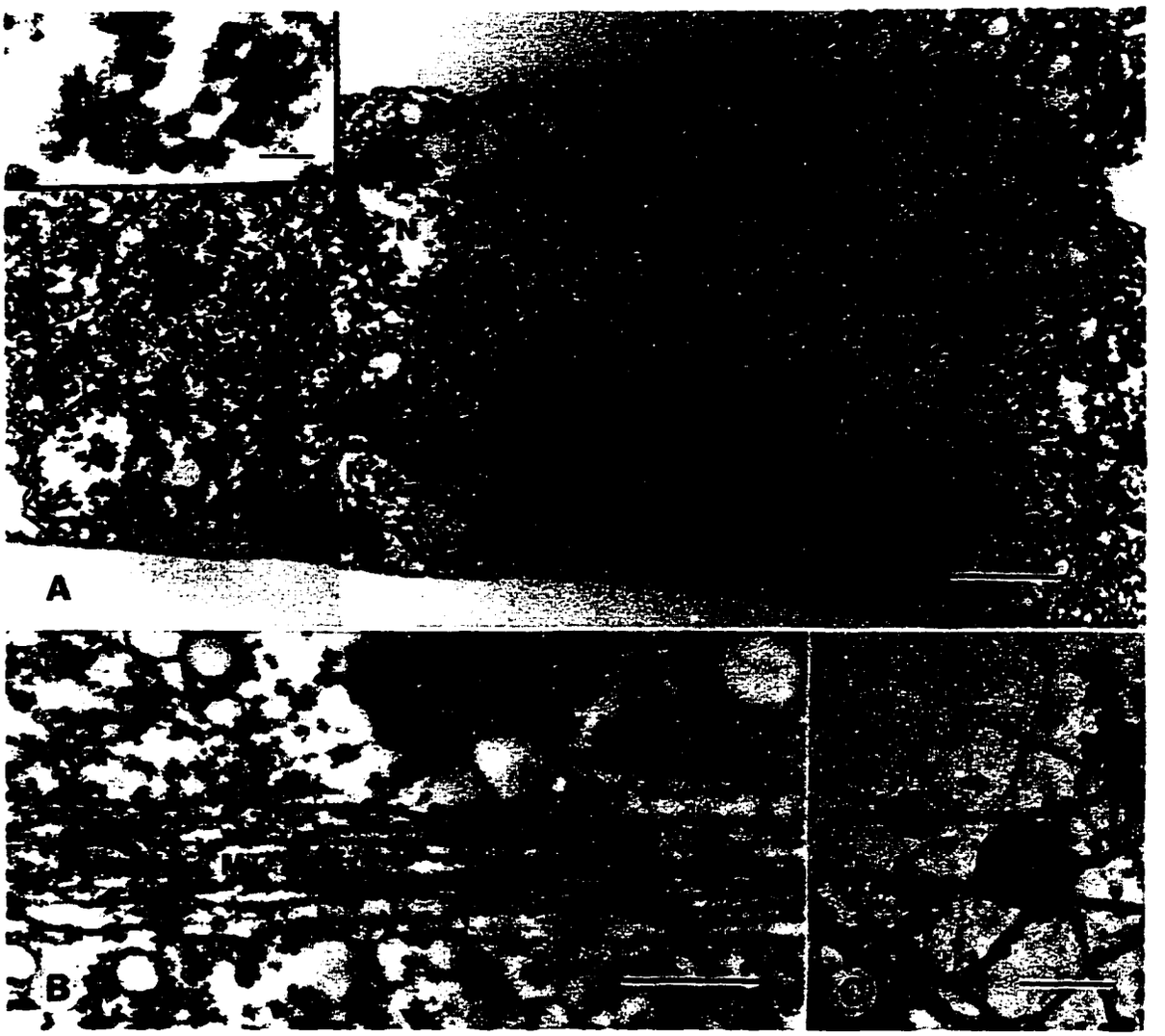
N
A
B

Table 4. The effects of cytoskeletal inhibitors on rates of streaming in *Rhabdocalyptus* preparations.

Table 4: The effect of cytoskeletal disruptors and stabilizers on organelle transport in *Rhabdocalyptus dawsoni*

Drug	Action	Effect on streaming
Cytochalasin B (10μg/ml)	Depolymerizes MFs	No effect
Colcemid (10μg/ml)	Inhibits MT polymerization	Stops streaming
Nocodazole (1μg/ml)	Inhibits MT polymerization	Stops streaming
Taxol (10μg/ml)	Stabilizes MTs	No effect
EGTA (10μM)	Chelates calcium	No effect

Microtubules: MTs; Microfilaments: MFs.

Figure 15. Demonstration of syncytial tissues in *Rhabdocalyptus* aggregates: dye spread during aggregation and distribution of nuclei and microtubules. *Rhabdocalyptus* tissue loaded separately with Calcein AM and Calcein blue AM and plated together fuses to allow blue dye throughout (A) and green dye throughout (B) so that a double exposure (C) shows a blend of the two colours. A-C Bar: 25 μm. (D) *Rhabdocalyptus* tissue loaded with Calcein AM (green) and plated with tissue from the cellular sponge *Haliclona* loaded with Calcein blue AM (blue) shows that neither dye was membrane permeable once loaded as neither sponge incorporated the other dye. Although both small and large round aggregates of *Rhabdocalyptus* have adhered to the larger *Haliclona* aggregate, no exchange of dye occurs. D,E Bar: 50 μm. (E) Tissue from *Haliclona* loaded separately with Calcein AM and Calcein blue AM and plated together did not exchange dye after 12 h, although aggregates often consisted of mosaics of both colours as shown by a double exposure. (F) Double labelling of microtubules (red) and nuclei (blue) in a day-old adhered aggregates of *Rhabdocalyptus dawsoni* demonstrates that the tissue is multinucleate. Bar: 25 μm.

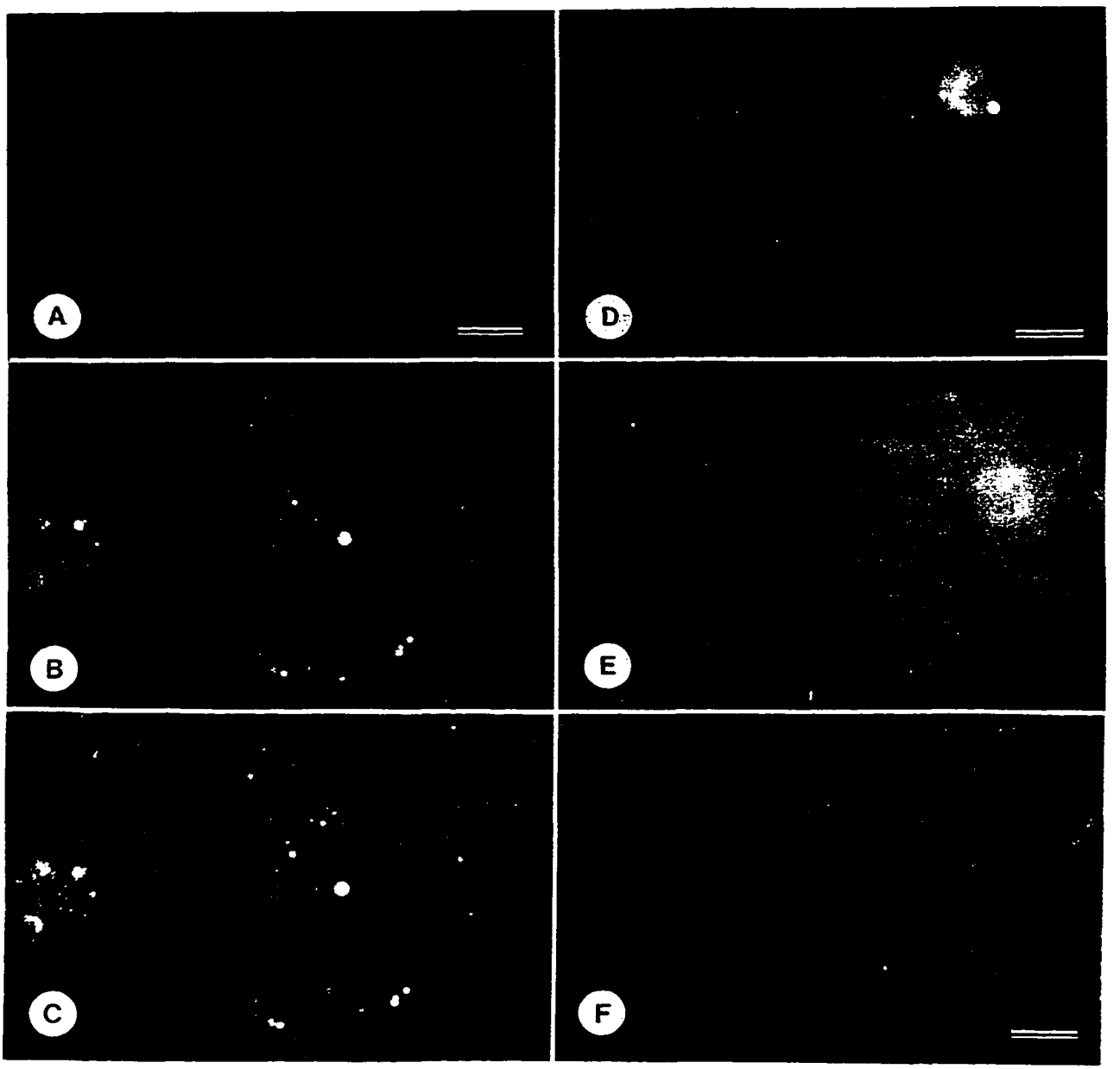
A
D
B
E
C
F

DISCUSSION

This remarkable adherent tissue preparation from hexactinellid sponges provides the first evidence of fusion during aggregation of dissociated hexactinellid sponge tissues and reveals an entirely novel form of cytoplasmic streaming in the Porifera. It further reveals a cytoskeletal framework which in terms of sheer size is certainly unique in sponge histology and, perhaps, in the entire metazoa. The syncytial condition of hexactinellid sponges appears to be significant in two ways. First, syncytialization would allow the transport of nutrients throughout the animal in the absence of mobile archaeocytes (Mackie and Singla, 1983b). The present findings suggest that cytoplasmic streams may be the transport routes. Second, the lack of membrane barriers within the syncytium presumably makes possible the propagation of impulses coordinating flagellar arrests (Lawn et al., 1981; Mackie et al., 1983). Cellular sponges, lacking nerves and gap junctions, have no such capability.

1. Formation of a syncytium

Membrane fusion is the means by which *Rhabdocalyptus* forms a syncytium during aggregation. Nonetheless, not all tissue components fuse. Small rounded pieces of tissue, which do not form lamellipodia, are drawn into the centre of larger aggregates which are fusion products. Whether syncytia can be formed by fusion of tissues from two species of hexactinellids has not yet been tested, although allografts

do not fuse (see Chapter V). The observation of dye spread following fusion in *Rhabdocalyptus* confirms the syncytial state of the tissues of this sponge, in contrast to *Haliclona*, where no dye spread was observed during aggregation. Failure of dye to spread within *Haliclona* might be due to inability of Calcein to pass through gap junctions, or to the absence of gap junctions or other aqueous intercellular pathways (see Mackie, 1984).

2. Streaming

Prior to the first fusion event, organelles appeared to move in adherent tissue pieces in the way described for other cells, including basal epithelial cells of freshwater sponges (Wachtmann and Stockem, 1992). Subsequent to fusion, however, streaming in *Rhabdocalyptus* aggregates takes on characteristics unlike any transport mechanism previously described. For example, streams do not maintain a constant volume, nor a single direction. Flow may reverse direction, albeit with a slight decrease in rate at the point of turning. And there is no limit to the length of streams. The closest parallel to this system is the streaming of bulk cytoplasm and individual organelles in reticulopodia of the protists *Allogromia* and *Reticulomyxa* (Travis and Allen, 1981; Koonce *et al.*, 1986), and there may be parallels with bulk cytoplasmic flow in characean algae, where a mechanism for coupling of bulk cytoplasm to microfilament bundles via the endoplasmic reticulum has been described (Kachar and Reese, 1988).

Rates of organelle transport in *Rhabdocalyptus* are within the range reported for fast axoplasmic transport (Allen *et al.*, 1982) and other systems involving microtubule-associated motors. The prominence of the network of microtubule bundles and the inhibition of streaming by colcemid and nocodazole, drugs which interfere with dynamic instability of microtubules, strongly implicate the microtubules as the transport pathway, making it likely that microtubule-associated motor proteins are involved. A recent account of cell shape changes in newly hatched freshwater sponges and sandwich cultures of marine sponges showed that in these sponges cells are capable of movement at rates of up to 15 $\mu m \cdot min^{-1}$ (Bond, 1992). Lamellipodial movements in *Rhabdocalyptus* aggregates appear to occur at approximately the same rate. However, the transport of nuclei and other organelles in streaming cytoplasm at seven to ten times that rate suggests that the two mechanisms of movement are different.

The effects of cutting cytoplasmic streams in *Rhabdocalyptus* are reminiscent of the effects of ligating axons (Weiss and Hiscoe, 1948). Streams, when cut, build up on the upstream side and drain on the downstream side. Furthermore, the lamellipodium that extends in search of the lost distal stump greatly resembles a nerve growth cone. Nonetheless, although streams may run in opposite directions beside or above one another, there is no evidence of bidirectional flow within the same stream or along the same microtubule as occurs in *Reticulomyxa* and possibly also in axons. Further work with a perfused, reactivated sponge preparation will help to determine the precise mechanism of transport.

3. Cytoskeletal architecture

One of the most exciting findings of this study is the vast cytoskeletal framework of the adherent aggregates. The lengths of both microfilament and microtubule bundles are of proportions unheard of in any other tissue. Figure 16 presents a three-dimensional summary diagram of the cytoskeletal architecture in a stream at the edge of an adherent preparation, showing the relationship between cytoplasmic organelles, microtubules, and microfilaments.

It is tempting to infer from the difficulty of fixing and labelling microtubules that, as in *Reticulomyxa* (Koonce *et al.*, 1986), tubulin in lower eukaryotes differs significantly from mammalian tubulin, or that bundling somehow interferes with antibody recognition. The composition of microtubules, the sites of microtubule nucleation, and microtubule polarity are topics which merit further study in this sponge.

Filopodia containing dense actin cores have been reported in aggregating cells from cellular sponges (Burlando *et al.*, 1984; Gaino *et al.*, 1985a) suggesting functional similarities. However, the stiff actin-filled extensions which form a "hairbrush" effect in older adherent aggregates are unique. These processes appear to be implicated in the adhesion of aggregates as some areas could be found where the tissue had detached, leaving the "hairbrush" attached.

Figure 16. An illustration summarizing the cytoskeletal architecture in a 24h adherent aggregate from *Rhabdocalyptus*. Microfilament bundles (MF) traverse the basal layer of aggregates. At the periphery microfilament bundles give rise to giant actin-dense rods (R), which extend through lamellipodia (LM) to anchor the preparation to the substrate. Inside a cutaway of the plasma membrane (PM), a stream is exposed showing bundles of microtubules (MT) with associated nuclei (N_s), mitochondria (M) and vesicles (V). Also adjacent to the microtubules are groups of archaeocytes (AR), with their own nuclei (N_{ar}), connected to each other and the rest of the cytoplasm by perforate plugged junctions (PJ).

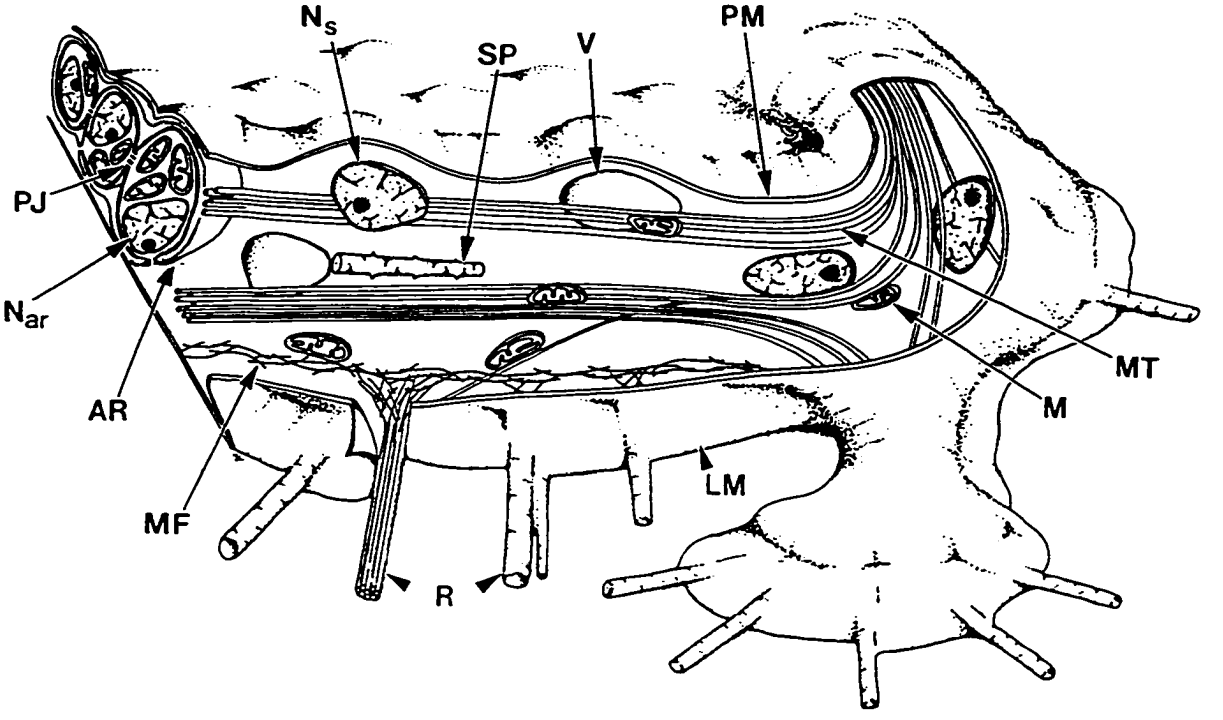
N_s
SP
V
PM
PJ
N_{ar}
AR
MF
R
LM
M
MT

4. Adherent aggregates as a model of whole sponges

The difficulty of visualizing cytoplasmic movements in intact sponges makes it hard to say if similar processes are going on to those seen in cultured aggregates, but it seems likely that streaming occurs in the intact sponge. This is borne out by observations of streaming in regenerating fragments of the whole animal (Leys and Mackie, 1994). Video microscopy of aggregates suggests that streaming, or the microtubule network involved in streaming, may play a role in organizing the tissues of intact sponges, for instance by influencing the distribution and clustering of archaeocytes, spherulous cells, choanoblasts and collar bodies. Archaeocytes do not appear to play the central role during aggregation in *Rhabdocalyptus* that they do in cellular sponges (Buscema et al., 1980). Because adults of this species can be up to 2 m in length, and assuming that the trabecular tissues are continuous throughout the animal, *Rhabdocalyptus* must represent one of the largest syncytial organisms within the metazoa.

The evidence presented in this chapter shows that adhered aggregates of *Rhabdocalyptus* possess an entirely unique cellular motile system, and a giant cytoskeleton. The observations strongly support the view that most of the cytoplasm in hexactinellids constitutes a multinucleate syncytium. It now seems clear that hexactinellids differ substantially from cellular sponges and should be differentiated from them at a high taxonomic level (Bergquist, 1978), as reflected in the two subphyla, Symplasma and Cellularia, proposed by Reiswig and Mackie (1983).

Chapter 3: THE MECHANISM OF ORGANELLE TRANSPORT IN HEXACTINELLID SPONGES

INTRODUCTION

Mechanisms of intracellular transport have been the focus of a great deal of attention since the development of video enhanced contrast (VEC) microscopy (Allen, *et al.*, 1981; Brady *et al.*, 1985). This widely used technique has made it possible to visualize and quantify organelle movement in much greater detail than was previously possible, both in cultured cells and whole small organisms. Use of VEC microscopy with both purified and native preparations from a number of model systems for actin- and tubulin-based intracellular transport has resulted in a picture of tremendous functional diversity. Motor proteins from essentially three superfamilies, kinesin, dynein, and myosin interact with cytoskeletal elements to generate motility.

(a) Kinesin. Since its initial purification from the squid giant axon (Brady, 1985; Vale *et al.*, 1985a), conventional kinesin has been isolated from bovine brain (Kuznetsov and Gelfand, 1986), sea urchin (Ingold *et al.*, 1988), *Drosophila* (Anastasi *et al.*, 1990), nematodes (Patel *et al.*, 1991), and fungi (Steinberg and Schliwa, 1995). Numerous kinesin-like proteins have been partially purified from *Xenopus* (Sawin *et al.*, 1992), protists (Kachar *et al.*, 1987), and yeast (Lillie and Brown, 1992) in addition to the above organisms, while a protein recognized by anti-kinesin has even been identified in plants (Tiezzi *et al.*, 1992). Characteristically kinesin drives plus-end directed motility along microtubules at rates of 0.1-0.9 $\mu m \cdot s^{-1}$ in purified preparations (Walker and Sheetz, 1993). This motor can hydrolyse any nucleotide triphosphate in

the presence of magnesium, but becomes firmly bound to tubulin in the presence of AMP-PNP, a non-hydrolysable ATP analog. Members of the kinesin superfamily can carry a diverse array of cargo, some acting in mitosis, others in axonal transport. That some kinesin-like proteins, such as the *Drosophila* ncd protein, can transport organelles to the minus end of microtubules, and others are even bipolar and can presumably crosslink microtubules (Kashina *et al.*, 1996), demonstrates the extreme functional diversity of the kinesin superfamily (Goldstein, 1991).

(b) Dynein. Most organisms in which kinesin has been identified also possess cytoplasmic dynein. Movement of vesicles along microtubules by means of dynein in contrast to kinesin depends on ATP hydrolysis alone and is faster than with kinesin, occurring at 1-2 $\mu m \cdot s^{-1}$ in purified systems (Walker and Sheetz, 1993), and even faster in native preparations (Euteneuer *et al*, 1988). Although usually a minus-end directed motor, cytoplasmic dynein is known to drive bidirectional motility along microtubules (Walker and Sheetz, 1993; Euteneuer *et al.*, 1989). Dynein powered motility can be inhibited by vanadate and micromolar concentrations of N-ethylmaleimide (NEM)(Vale and Hotani, 1988).

(c) Myosin. Actin-based intracellular transport is best known from streaming in characean algae and amoebae or slime molds, but has also been reported in squid axoplasm (Kuznetsov *et al.*, 1992), where it is speculated to form a mechanism of local pick-up and delivery of cargo to microtubules (Atkinson *et al.*, 1992). It is not yet known whether kinesin and cytoplasmic dynein can also bind to and move along actin microfilaments, or whether cargo is transferred to myosin I, a relative of myosin

II which forms bipolar filaments in muscle sarcomeres and generates contractions in the cortex of amoebae and slime molds. Unlike myosin-driven streaming in algae, however, non-muscle actin-based movement in animal cells tends to be saltatory, organelles run along invisible tracks, and movement is sensitive to high concentrations of NEM (Kuznetsov *et al.*, 1992).

A commonly used approach to determine mechanisms of intracellular transport is to use permeabilized cell models to examine the effects of various inhibitors or ATP analogs on transport systems (eg. Ueda and Götz von Olenhusen, 1978; Clark and Rosenbaum, 1982; Shimmen and Tazawa, 1982; Forman *et al.*, 1983; Swanson, 1993; Haimo and Thaler, 1994). Though permeabilised cell models are certainly useful, their disadvantage lies in the variety of effects substances can have on cytoplasm. Inhibitors such as vanadate, for example, can affect dynein motility, protein phosphatases, and perhaps also nucleotide hydrolysis (Stearns and Ochs, 1982; Haimo and Thaler, 1994). Direction of transport can vary depending on post-translational modification of some motor molecules, e.g. AMP kinase-dependent phosphorylation of dynein (Bray, 1992), and rate of translocation can be reduced by the viscosity of the cytoplasm, as occurs in bulk streams in the characean alga *Chara* (Nothnagel and Webb, 1982). Where the responses to experimental treatments do not fit within the physiological parameters of any one motor, models have been developed to describe the interaction of actin-based and microtubule-based systems and the role biomechanical properties of the cytoplasm play in motility (Nothnagel and Webb, 1982; Taylor and Fechheimer, 1982; Janson and Taylor, 1993; von Dassow

and Schubiger, 1994). Direct visualization of cytoskeletal interactions by electron microscopy (eg. Hirokawa *et al.*, 1991; Kachar and Reese, 1988) has often provided fundamental support for theoretical models.

The hexactinellid sponge *Rhabdocalyptus dawsoni* possesses an extensive and dynamic organelle transport system which is unique to this group of animals (Leys and Mackie, 1994; Leys, 1995). Immunofluorescence microscopy and pharmacological inhibition studies have demonstrated that microtubules form the pathways for transport of bulk cytoplasm and individual organelles over immense distances in cultured tissue preparations (Leys, 1995). Microtubule-based organelle transport has also been demonstrated in basal epithelial cells of fresh water sponges (Wachtmann *et al.*, 1990), and there is immunocytochemical evidence for both kinesin and cytoplasmic dynein in pinacocytes from these sponges (Kirfel and Stockem, 1995). However, the syncytial character of hexactinellid tissues allows transport over much greater distances than are possible in cellular sponges, and transport of bulk cytoplasm does not occur in cellular sponges, so a comparison between cellular and syncytial sponges cannot be accurately made. Because current taxonomy places hexactinellid sponges at the beginnings of metazoan evolution in a subphylum of the Porifera, the mechanisms used by these unusual animals for organelle transport is of considerable interest. Here I report on the possible mechanisms of organelle transport in the hexactinellid sponges *Rhabdocalyptus dawsoni* and *Aphrocallistes vastus*.

METHODS

Whole cell lysate, SDS-PAGE, and Western Blots:

Whole cell lysate was made from *Rhabdocalyptus dawsoni* and *Aphrocallistes vastus* by dissociating approximately 20 cm^3 of cleaned sponge tissue into a beaker through 100 μm Nitex mesh. The suspension of tissue was poured into several 50 ml sterile plastic centrifuge tubes and hand-centrifuged. The salt water was poured off and pellets of tissue combined in one 50 ml tube. To 5 ml of tissue 5 ml PEM buffer (PIPES, EGTA, $MgCl_2$) pH 6.9, 1mM PMSF (protease inhibitor) final volume, and 0.5% Triton X-100 were added, the mixture was finger-vortexed, and left on ice. After 5 minutes, 35 ml cold acetone was added, the mixture was finger-vortexed again, and left on ice for 30 minutes. The lysate was centrifuged at 2000 x g (4°C) for 30 minutes, after which the acetone was poured off and the pellet resuspended in approximately one volume of 2 X Laemmli Sample Buffer. The final suspension of solubilized tissue was aliquoted and stored frozen at minus 80°C until needed.

Whole cell lysate was run on a 7.5% SDS-Polyacrylamide gel, transferred to Immobilon P^{TM} membrane (Millipore, Bedford, MA) and incubated overnight (at 4°C) with the following antibodies: monoclonal anti-kinesin SUK4 (mouse host, IgG) (developed by J. Scholey and obtained from the Developmental Studies Hybridoma Bank, maintained by the Department of Pharmacology and Molecular Science, Johns Hopkins University School of Medicine, Baltimore MD, and the Department of

Biological Sciences, University of Iowa, Iowa City, Iowa), monoclonal anti-kinesin K1005 (mouse host, IgG) (Sigma, St. Louis, MO), monoclonal anti-cytoplasmic dynein M74-1 and M74-2 (mouse host, IgG)(a generous gift from W. Steffen, Institute of Biochemistry and Molecular Cell Biology, University of Vienna). Monoclonal anti-α tubulin (mouse host, IgG)(Amersham, Arlington Heights, Ill.) and monoclonal anti-ß tubulin (mouse host, IgG)(developed by M. Klymkowski and obtained from the Developmental Studies Hybridoma Bank) were used as positive controls since these antibodies were known to recognized proteins of the expected molecular mass of tubulin in the whole cell lysate in previous experiments. The primary antibody was omitted from one lane for a negative control. Blots were incubated for 30 minutes in a secondary goat anti-mouse (IgG (H and L)) alkaline phosphatase antibody, and were developed using the one step chemical substrate technique (NBT/BCIP, Pierce, Rockford, Illinois, Cat#34042).

Preparation of tissue cultures and light, fluorescence and video microscopy

These were as described in the general methods section, except for visualization of the endoplasmic reticulum. For this tissue was tweezed from the whole sponge and allowed to regenerate overnight in sea water. Pieces were incubated live in $DiOC_6(3)$ ($1\mu g \cdot ml^{-1}$) in sea water from a stock of ($100\mu g \cdot ml^{-1}$) in ethanol to label the endoplasmic reticulum. They were washed 3 times for 10 minutes each in sea water, mounted in the same, and viewed with a Leitz epifluorescence microscope. Other

preparations were fixed with 2% paraformaldehyde in PEM buffer for 30 minutes at 4°C, rinsed in PBS with 0.1% TX-100 for 30 minutes, and incubated for 30 minutes in ($1\mu g \cdot ml^{-1}$) $DiOC_6(3)$. These preparations were rinsed in PBS for 30 minutes and mounted in PBS-glycerol with n-propyl gallate for viewing by fluorescence microscopy.

Permeabilization experiments:

Numerous attempts were made to develop a lysed permeabilized tissue preparation which could be reactivated by the addition of ATP. The following buffers were used varying the type and quantity of detergent, and the pH, as listed in Appendix 1.

(1) "Electrode solution": KCl (400mM), $MgCl_2$ (2mM), $CaCl_2$ (1mM), $NaCl_2$ (50mM), HEPES (10mM), EGTA (11mM), NMG (58mM), HCl (28mM), pH7.5

(2) "Reticulomyxa solution": 5% hexylene glycol, sodium orthovanadate (1mM), 0.15% Brij 58, 50% PHEM (PIPES (30mM), HEPES (12.5 mM), EGTA (4mM), $MgCl_2$ (1 mM)), pH 7.0

(3) PEM: PIPES (50mM), EGTA (1mM), $MgCl_2$ (0.5 mM) pH 6.9

(4) PEG-GTX: 4% Polyethylene glycol MW 600, 10% glycerol, PIPES (10 mM), EGTA (5 mM), KOH (10 mM), KCl (27mM), 0.15% TX-100, pH 7.0

(5) PHEM: PIPES (50mM), HEPES (25mM), EGTA (10 mM), $MgCl_2$ (2 mM), pH 6.9

Buffers were added by gentle perfusion to an adherent tissue preparation on a glass coverslip inverted onto a glass slide and supported on two sides by plastic coverslip spacers with a vaseline-Parafilm adhesive mixture. The experiment was recorded by video microscopy with a Panasonic digital colour CCD video camera, processed with an OMNEX (Imagen Inc.) digital image processor, and recorded on a SONY super VHS video recorder. After tissue lysis, buffer without detergent was perfused through the preparation, followed by buffer with 1mM ATP. In some cases up to 10mM ATP was used in the reactivation buffer.

Drug treatments:

A stock concentration of 1 M N-ethylmaleimide NEM was made in 100% ethanol diluted in sea water to 1, 10, and 100 μM, and 1 and 5 mM. A stock concentration of 1 mM of the ionophore 4Br A23187 was made DMSO and diluted in sea water to 20 and 40 mM for use. Unlysed adhered preparations were perfused with NEM. The ionophore 4Br A23187 was perfused with and without EGTA and EDTA as described in the results. Controls were conducted with 3% ethanol or 4% DMSO. The experiment was recorded by video microscopy.

Rates of bulk transport:

Rates of movement were calculated for organelles moving a) individually both

continuously and by saltation, b) in the centre of bulk streams, c) at the edge of bulk streams, and d) erratically within lamellipodia, using the distance measurement module of the OMNEX (Imagen Inc.) digital image processor.

Negative stain electron microscopy:

Pieces of whole sponge were dissociated into a beaker, poured into a dounce homogenizer and homogenized by hand for 2 min. A drop of homogenized tissue was pipetted onto a formvar-coated electron microscope grid. After 15 seconds a drop of 1% Phosphotungstic Acid pH 7.0 was pipetted on the homogenized tissue. After exactly one minute the liquid was drawn off with number 1 Whatman filter paper. When dry the grid was viewed in a Hitachi transmission electron microscope.

Electron microscopy:

Tissue was fixed and processed for thin section electron microscopy as described in the general methods section.

Membrane transport:

To determine whether membrane transport of materials attached to the surface of adherent tissue preparations occurred, 1 μm fluorescent latex beads (Molecular

Probes, Eugene, OR) were dropped with a micropipette using a micromanipulator onto the surface of 24 hour-old adherent aggregates. Movements of beads on and in the tissue was filmed with video microscopy as described above.

RESULTS

1. Molecular Motors

Immunoreactivity was shown in whole cell lysate from *Aphrocallistes* with anti-β tubulin, anti-α tubulin, with both of the antibodies to cytoplasmic dynein, and possibly with anti-kinesin from Sigma (Fig. 17). The antibody to kinesin from Sigma recognized a high molecular mass (HMM) protein and proteins of approximately 60-65 kDa and several smaller proteins. SUK4 did not show immunoreactivity with proteins of the expected molecular mass for kinesin in *Aphrocallistes* whole cell lysate. Antibodies to the intermediate chain of cytoplasmic dynein M74-1 and M74-2 both recognized proteins of approximately 70 to 80 kDa.

Whole cell lysate from *Rhabdocalyptus* never produced a clear banding pattern on SDS-PAGE, possibly because the sponge has a debris-covered outer coat, which despite being cut off with scissors, might contaminate the lysate. No amount of centrifugation to remove the dirt gave good results, and consequently attempts to use this sponge for immunoblots were abandoned. In contrast, whole cell lysate from *Aphrocallistes* produced a clear banding pattern when stained with Coomassie blue (Lane 2, Fig. 17).

None of the buffers used in attempts to lyse and subsequently reactivate organelle transport in *Rhabdocalyptus* produced positive results (Appendix 1). Although some buffers appeared less damaging to the tissue than others, attempts

to reactivate organelle transport with 1-10 mM ATP usually caused the lysed tissue to wash away. The lysis of preparations with 50% PHEM pH 6.9, 5% hexylene glycol and 0.15% Brij 58 was the least destructive. Use of the same buffer without detergent but with 1 mM ATP in attempts to reactivate transport may have caused slight movement of organelles, but if so it was insufficient to permit subsequent pharmacological treatments which could have been used to test for mechanoenzyme specificities.

Since vanadate, an inhibitor of dynein motility at micromolar concentrations (Forman *et al.*, 1983), and AMP-PNP, an inhibitor of kinesin-driven motility (Brady *et al.*, 1985), do not penetrate the plasma membrane of living tissue, their effects on organelle transport in *Rhabdocalyptus* could not be assessed. Concentrations of 1 and 10 μM NEM had no immediate effect on streaming; 100 μM NEM caused streaming to stop gradually one minute after addition of the drug. Streaming could be reactivated after washing out the drug. One millimolar NEM caused instantaneous cessation of streaming and caused the membrane to lyse one minute after addition of the drug; 5 mM NEM stopped streaming instantly and stripped the membrane causing the preparation to tear away from the substrate. Controls with ethanol had no effect on tissue cultures.

Treatment with 20 μM of the ionophore 4Br A23187 caused the reversible cessation of streaming. Control treatment (4% DMSO) had no effect on tissue or streaming for up to 30 minutes, after which streaming continued but the tissue began to withdraw from the substrate. Thereafter streams became distorted and slowed to

a gradual stop. In some areas of the preparations movement continued for longer than 30 minutes. With 40 μM 4Br A32187 all streaming ceased within one minute. Tissue retracted from the substrate but did not detach. After washing out the ionophore, transport began first along tracks in thin areas of the preparation, and with time bulk streaming could be found throughout the preparation. When 40 μM of the ionophore was added to the preparation in 10 mM EDTA in ASW the tissue rapidly blebbed, and withdrew from the coverslip; streaming could not be reactivated. This concentration of EDTA in ASW without ionophore had no effect on the tissue, nor did EDTA with 4% DMSO. Identical results were achieved with 10 mM EGTA.

2. Rates of transport

Individual organelles moved both continuously and by saltation along visible tracks and flowed within streams at constant rates (Fig. 18). When in bulk streams organelles appeared to be carried by the flow. If a stationary obstacle, such as a spicule fragment, was encountered in mid-stream, the flow parted around it, slowing slightly at the edges of the hindrance. The mean rate of transport in streams which did not continuously transport large amounts of cytoplasm, but which from time to time thinned down to individual organelles was 1.86 $\pm$ 0.42 $\mu m \cdot s^{-1}$ (n=33). (Rates are given with standard error.) In large streams 10-15 μm wide the mean rate of transport at the edge of stream was 2.01 $\pm$ 0.44 $\mu m \cdot s^{-1}$, whereas the mean rate of transport in the middle of the stream was significantly slower at 1.71 $\pm$ 0.29 $\mu m \cdot s^{-1}$

(n=31, p=0.008). Movement of single organelles in thin areas followed visibly raised pathways, presumed to be microtubule bundles. The average rate of transport of individual organelles moving continuously was 2.15 ± 0.33 $\mu m \cdot s^{-1}$ (n=32; max=2.96, min=1.23). Individual organelles which moved by saltation, halting and then jumping forward, on average travelled faster at 3.6 ± 1.03 $\mu m \cdot s^{-1}$ (n=11; max=5.52, min=0.74). In large lamellipodia organelles moved far more slowly, at a mean rate of 0.32 ± 0.11 $\mu m \cdot s^{-1}$. They often changed direction, and appeared to jump forward as if by saltation (Figs. 18 and 19). This form of movement was similar to that most often seen in thin areas of regenerating tissue explants (see Leys and Mackie, 1994; Wyeth et al., 1996).

3. Mechanism of bulk transport

The adherent cultures had no membrane boundaries dividing streaming from stationary cytoplasm. In thin section transmission electron microscopy (TEM) streaming cytoplasm could be identified by the presence of bundles of microtubules which continued for great distances (Fig. 20). The surrounding cytoplasm contained mitochondria, nuclei, and membranous organelles. Non-streaming areas of the cultures could be identified in thin sections by the lack of microtubules and the presence of large numbers of archaeocytes, spherulous cells, and collar bodies (Fig. 21).

In cross-sections of former streams examined by thin section TEM

microtubule bundles were never found evenly distributed or randomly scattered throughout the tissue. Giant bundles of microtubules ran in shafts at some 5-10 μm intervals through streams, and many individual microtubules were at the surface of former streams just under the plasma membrane (Fig. 22 A,B). Some microtubules were found near organelles, but not all organelles had microtubules associated with them, and often several vesicles were associated with a bundle of microtubules. Scanning electron microscopy of lysed adhered preparations confirmed that microtubules were located just under the surface membrane (Fig. 22C). Polarity of microtubules could not be determined, as attempts to decorate bundles with exogenous tubulin in lysed preparations were unsuccessful.

Staining of either live or fixed preparations with $DiOC_6(3)$, a stain which preferentially incorporates into membranes (in particular the endoplasmic reticulum) based on charge differences, did not highlight any network which could be positively identified as the endoplasmic reticulum in *Rhabdocalyptus* preparations. In tissue explants viewed by fluorescence microscopy this dye highlighted streams of cytoplasm (Fig. 23A).

In horizontal sections viewed by TEM, formerly streaming cytoplasm was always associated with numerous mitochondria and with extensive elongated membranous organelles which lay just above the plane of microtubules (Figs. 23 B,C).

Negatively stained homogenized tissue from the whole sponge observed by transmission electron microscopy showed fibrous bundles traversing the supportive

grids and numerous organelles both associated with and separate from the bundles (Figs. 24 A,B). The larger organelles up to 5 μm in diameter often contained other material; in this way they resembled phagosomes known from thin section TEM. Some organelles were flattened on the side where they abutted fibrous tracts and were often associated with organelles not on the tracts (Fig. 24B). More often however, a membranous network surrounded the organelles attached to the tracts and connected them with other organelles (Fig. 24C). Similar membranous networks were seen around large organelles not attached to fibrous tracts.

4. Membrane transport

Latex beads pipetted onto the surface of adherent aggregates underwent Brownian motion in a plane of focus just above the tissue for up to 15 minutes. Gradually the beads descended on to the surface whereupon Brownian motion ceased, indicating attachment to the surface (Fig. 25A). Not all the beads were taken up by the tissue, but those that were changed appearance when internalized. They initially remained at the site of uptake. Uptake occurred irrespective of proximity to streaming cytoplasm. However, approximately 15 minutes after uptake some beads changed position and appeared to be caught up in nearby streams (Figs. 25 B-D). Some 30 minutes to one hour after adding the beads to the surface they were seen moving within many streams (Figs. 26 A-C). None of the beads which attached to the surface of preparations appeared to move while in that plane of focus.

Figure 17. Western blot analysis of *Aphrocallistes vastus* whole tissue lysate using antibodies to known motor proteins. Lane 1: molecular weight markers, Lane 2: Coomassie Blue stained whole cell lysate from a 7.5% SDS-PAGE gel, Lane 3: anti-β tubulin, Lane 4: anti-α tubulin, Lane 5: SUK4 anti-kinesin, Lane 6: anti-kinesin K1005, Lane 7: anti-cytoplasmic dynein M74-1, Lane 8: anti-cytoplasmic dynein M74-2, Lane 9: no primary antibody. Both antibodies to cytoplasmic dynein recognized proteins at approximately 70-80 kDa (arrowhead). SUK 4 (anti-kinesin) showed no recognition of kinesin in the sponge lysate, while K1005 recognized a high molecular mass protein and several proteins of less than 80 kDa.

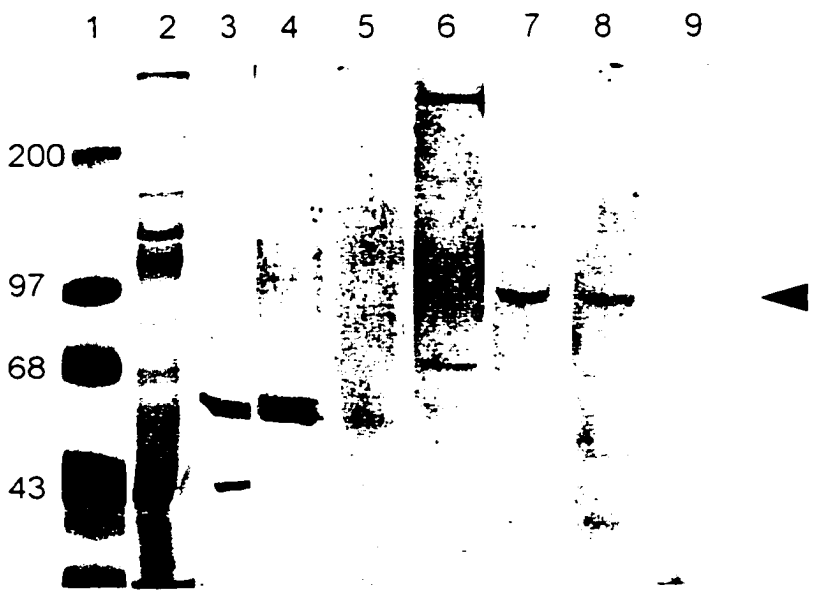
1
2
3
4
5
6
7
8
9
200
97
68
43

Figure 18. Rates of transport of four classes of organelles in adherent *Rhabdocalyptus* preparations. (A) Single organelles moving at a constant velocity but not in bulk streams. (B) Organelles moving at a constant velocity in the middle of bulk streams. (C) Organelles moving at a constant velocity at the edge of bulk streams. (D) Organelles moving by saltation within large lamellipodia (see figure 19). A total of 32 measurements were made at each location.

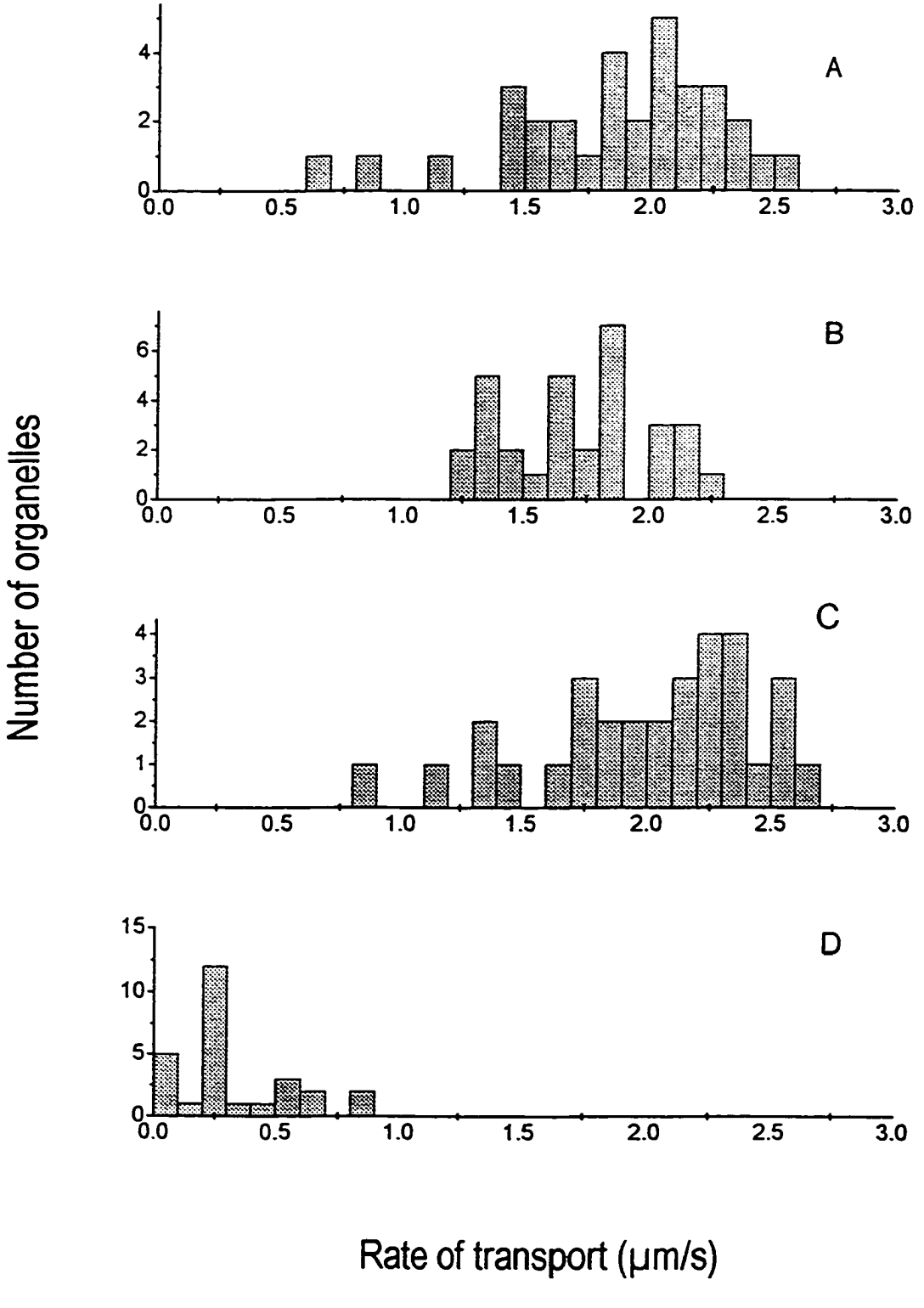
A
B
C
D
Number of organelles
Rate of transport (µm/s)
0.0
0.5
1.0
1.5
2.0
2.5
3.0

Figure 19. Saltatory movement of organelles in a broad lamellipodium from an adherent *Rhabdocalyptus* culture. Video microscopy. (A) A tracing from the monitor of a video recording showing organelles moving at different rates and in directions. Arrows indicate the starting position of organelles at T=0 and asterisks show the position of each organelle at 15 second intervals thereafter. (B) A frame from the video sequence showing the positions of organelles x, y, and z from the tracing in (A) at 15 seconds. Bar: 10μm.

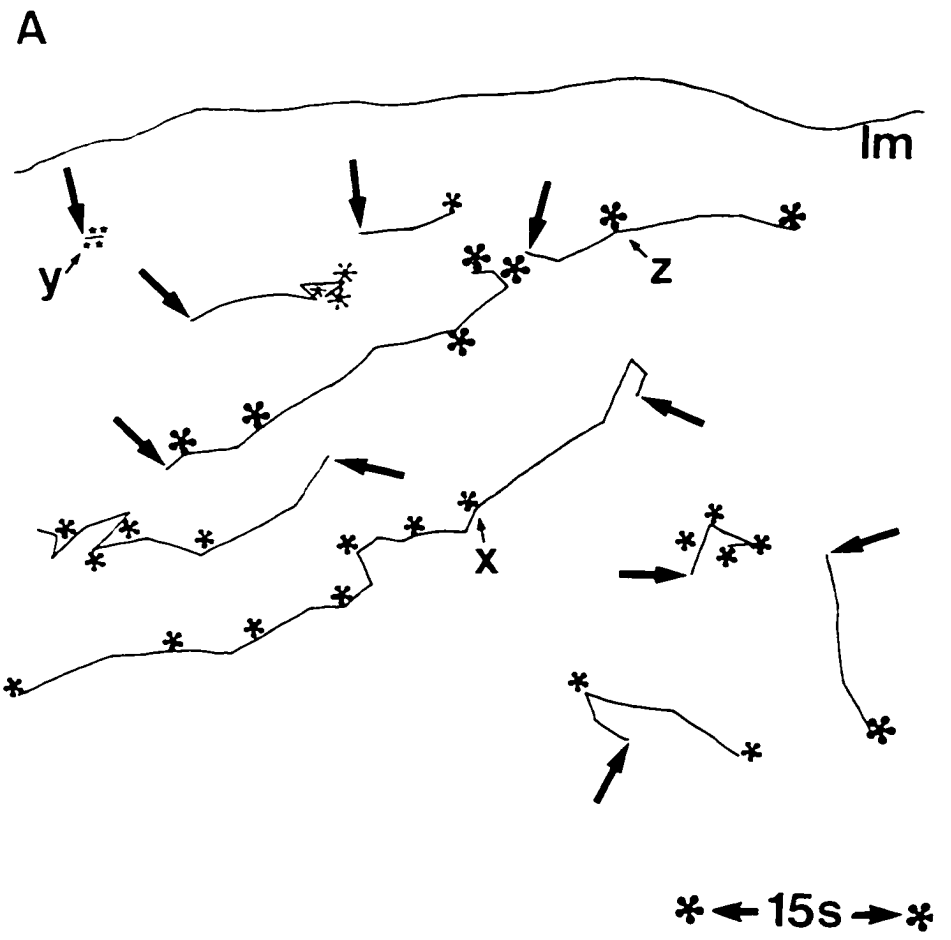
A
lm
y
z
x
15s

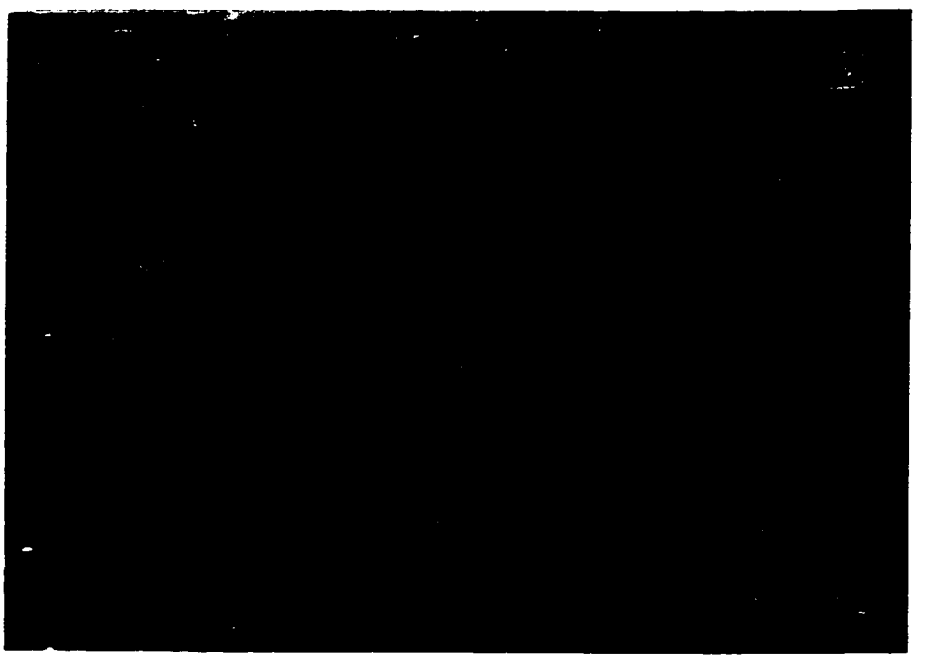

Figure 20. The ultrastructure of adherent tissue from *Rhabdocalyptus* showing an area which was streaming prior to fixation. Transmission electron microscopy. A horizontal section in the plane of streaming shows large bundles of microtubules (mts) traverse great distances while others (arrowheads) anastamose with or diverge from the central bundle of microtubules. Mitochondria (m), nuclei (Nu), membranous organelles (mo), and large vesicles (v) are associated with microtubule paths. Bar: 2μm.


m
mo
mi
mo
m
Nu

Figure 21. Features of stationary cytoplasm from *Rhabdocalyptus* tissue cultures. Transmission electron microscopy. (A) Large areas of the tissue cultures lack microtubule bundles, and contain instead numerous archaeocytes (ar), collar bodies (cb) with flagella (f) and microvilli, and spherulous cells (sc). Arrowheads indicated plugged junctions. Bar: 5μm. (B) Detail of a spherulous cell from an area of stationary cytoplasm. Nucleus (Nu), mitochondria (m), Golgi (g), inclusions (i), archaeocyte (ar), trabecular syncytium (ts). Bar: 1μm.

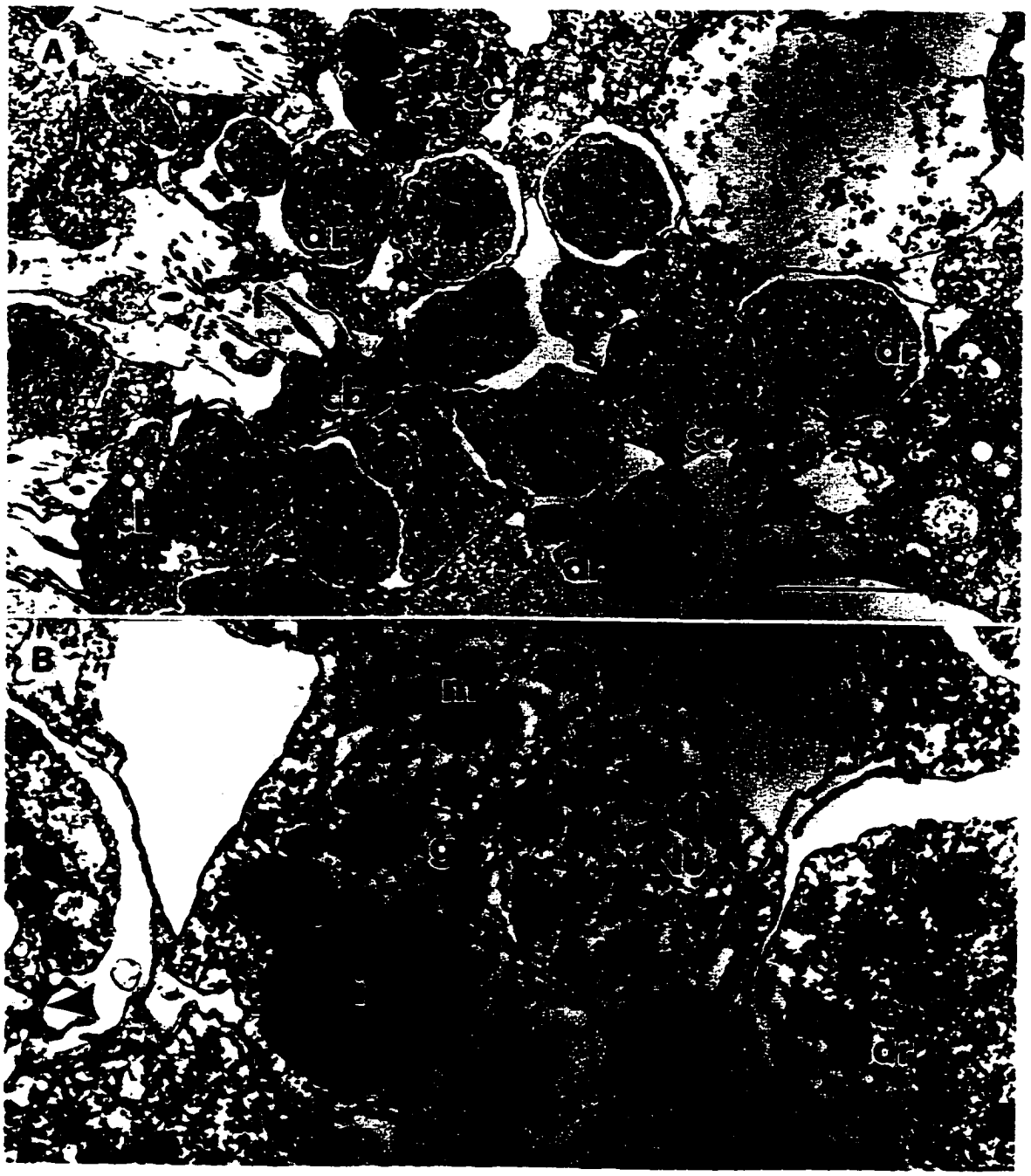
A
B

Figure 22. The distribution of microtubules in streams in adherent tissue cultures from *Rhabdocalyptus*. Transmission and scanning electron microscopy. (A) A cross section through a former stream shows that microtubules are bundled in a shaft which runs between the large black arrows (top and bottom) through the cytoplasm (small black arrows). Very few microtubules are found elsewhere. Similar shafts of microtubule bundles occur every 5 to 10 μm, presumably through areas of the cytoplasm which were streaming (also see fig 14, chapter II). Microtubule bundles are always associated with numerous mitochondria and with membranous organelles (mo), while archaeocytes (ar) and other large vesicles are not directly associated with the microtubules. Nucleus (Nu). Bar: 2μm. (B) Magnification of microtubules (arrows) in (A) lying under the surface membrane and associated with numerous membranous organelles (mo) and mitochondria (m). Bar: 1μm. (C) Scanning electron microscopy of preparations lysed for 1-2 minutes using PEM buffer with detergent revealed microtubules (arrows) scattered under the surface membrane (sm). Bar: 5μm.


A
sm
B
sm

Figure 23. Membranous networks are associated with streaming cytoplasm. Epifluorescence and transmission electron microscopy. (A) Labelling of the membranous network with $DiOC_6(3)$ in a regenerated tissue explant. The dye highlights streams (arrowheads) of cytoplasm running throughout the preparation. Bar: 100μm. (B and C) Horizontal sections (TEM) of former streams reveal that microtubules (arrows) are always found associated with nuclei and membranous organelles (mo). (C) In horizontal sections, the cytoplasm which had been streaming can be distinguished by the abundance of elongated membranous organelles (mo). Nucleus (Nu), archaeocyte (ar), mitochondria (m). B,C Bar: 2μm.

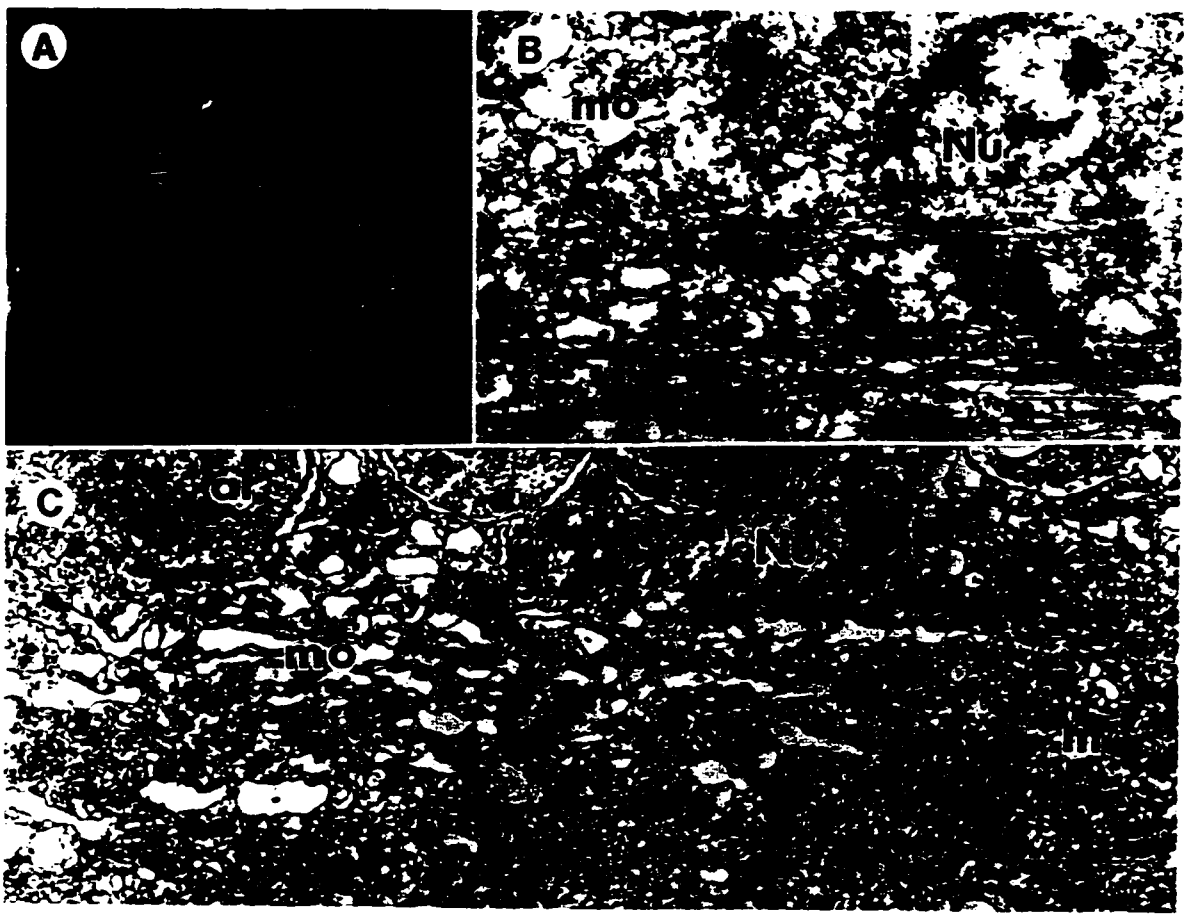
A
B
mo
Nu
C
a
mo
Nu
m

Figure 24. Evidence of a membranous network linking organelles to fibrous tracks in streams in adherent cultures from *Rhabdocalyptus*. Negative stain transmission electron microscopy. (A) Organelles (o) are flattened on the side they abutt fibrous tracts (black arrows). (B) Sometimes organelles away from the tracks appear to be linked directly (arrowhead) to those on the tracks. A,B Bar: 1μm. (C) More often membranous networks (mn) surround organelles which are directly associated with the fibrous tracks, forming a link (arrowhead) to organelles not associated with the tracks (shown by black arrows). Bar: 2μm.

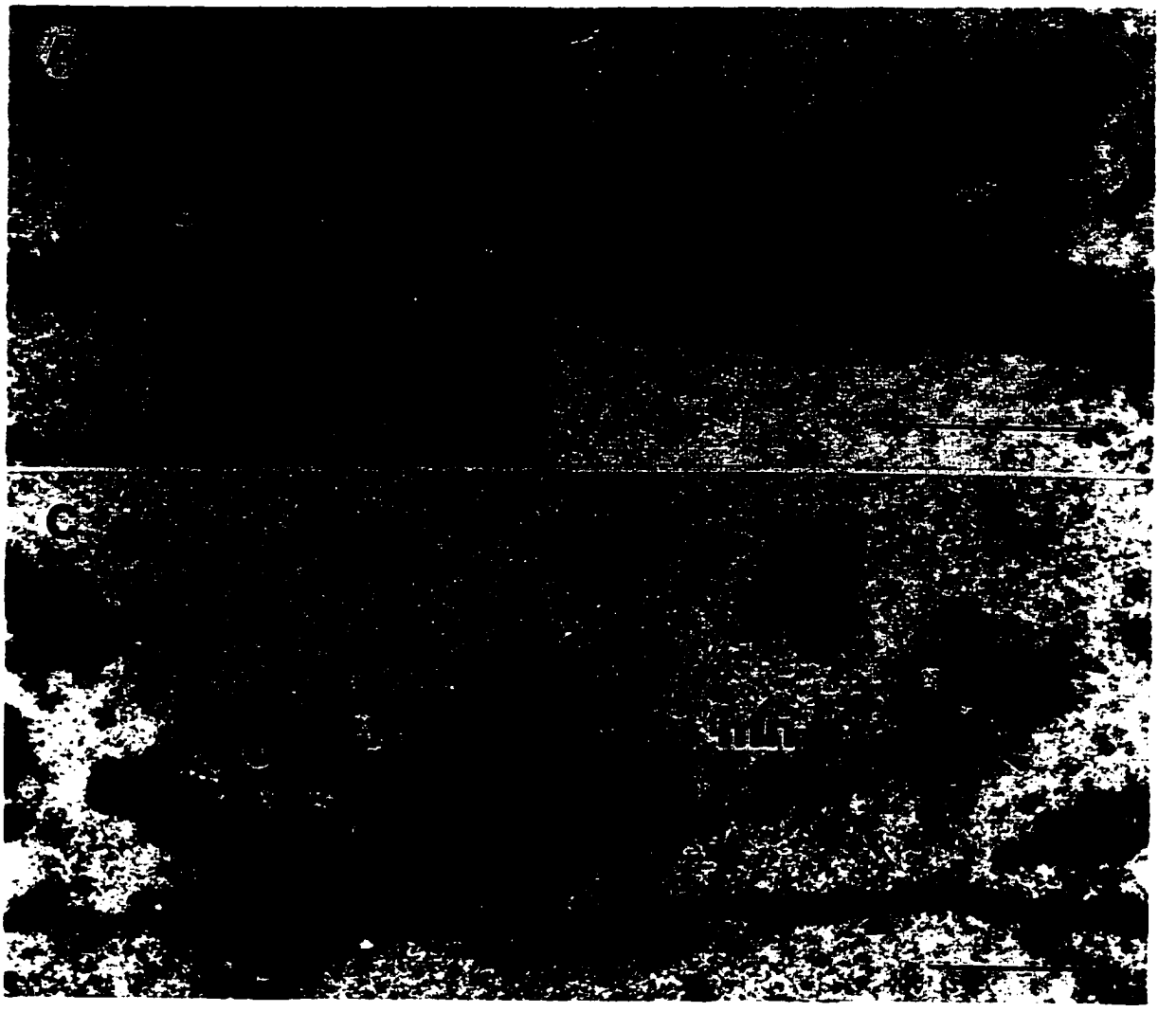

Figure 25. Uptake and transport of fluorescent latex beads by adherent aggregates from *Rhabdocalyptus*. Video microscopy. (A) Beads on the surface of adhered aggregates (Lb_o) undergo distinctive Brownian motion and are opaque compared to those which have been internalized (Lb_i). (B,C) Once internalized the beads (arrowheads) are slowly moved into streams, where they are transported at a constant rate of just over 2 $\mu m \cdot s^{-1}$. (D) Fluorescence microscopy of the same beads in (C). A-C Bar:10μm

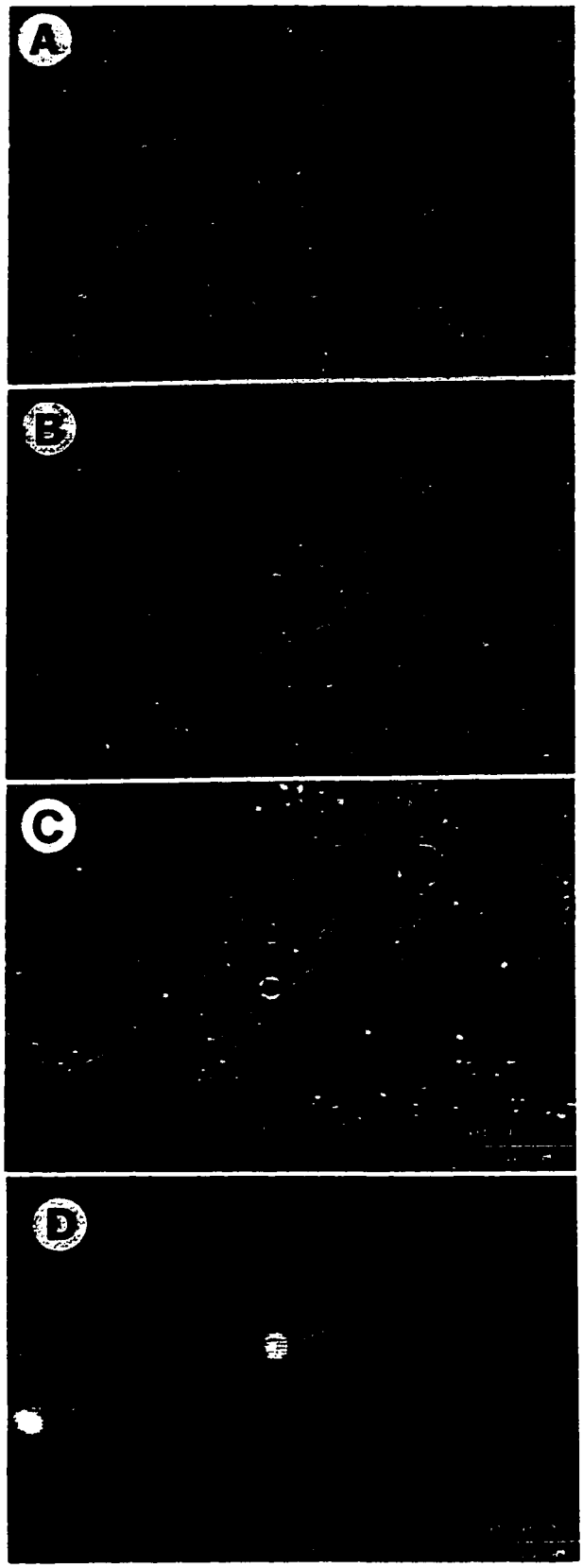
A
B
C
D

Figure 26. Transport of latex beads within streams in adherent cultures from *Rhabdocalyptus*. Video microscopy. (A-C) Latex beads (Lb, black arrows) are transported within streams at rates of just over 2 $\mu m \cdot s^{-1}$. Bar: 10μm.

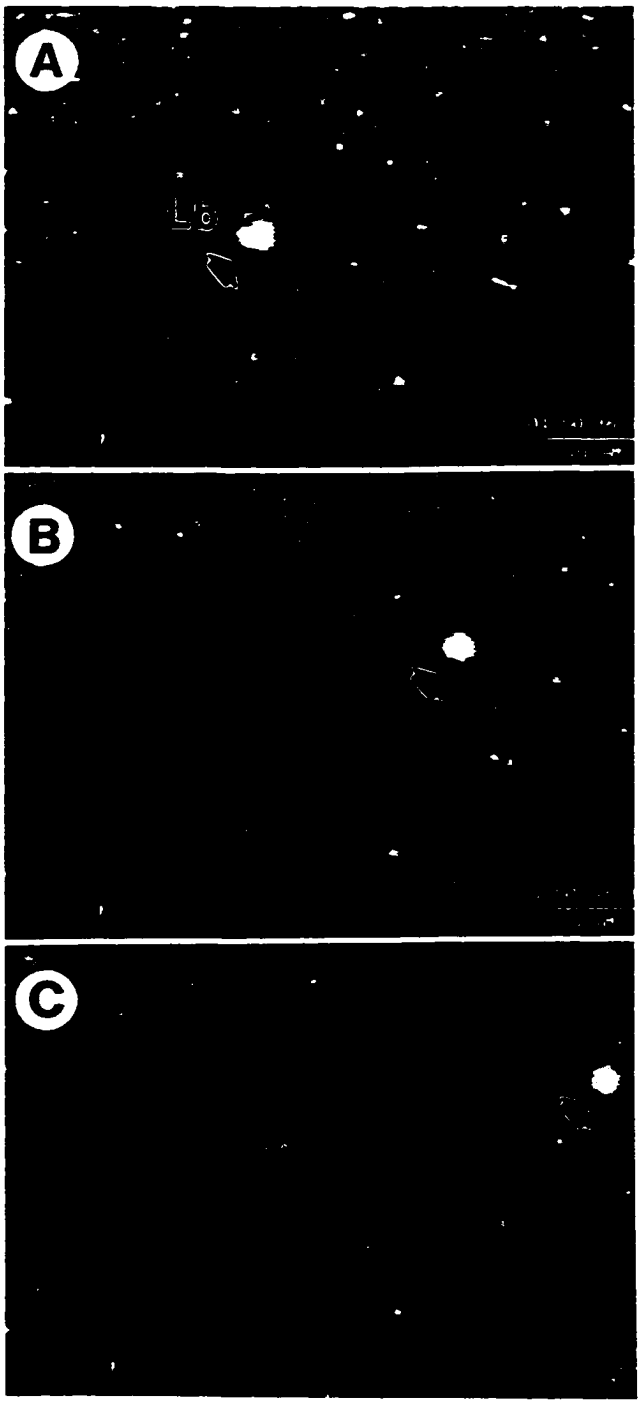
A
B
C

DISCUSSION

While some aspects of cytoplasmic transport in *Rhabdocalyptus* are clearly similar to trafficking of vesicles in nerve axons, others more closely resemble bulk cytoplasmic movements in *Amoeba* and the so-called shuttle streaming shown by *Physarum*. Colcemid and nocodazole treatment of adherent, streaming preparations from *Rhabdocalyptus* show streaming to be microtubule-based, and both indirect immunofluorescence with antibodies to tubulin and electron microscopy show that microtubules are abundant in streams (Leys, 1995). Furthermore, rates of organelle transport correspond to rates generated by microtubule-based motors in other systems. Preliminary biochemical evidence points to the presence of cytoplasmic dynein in *Aphrocallistes*, and it is likely this motor also exists in *Rhabdocalyptus* and other hexactinellids, given the similarity of the streaming processes observed. However, negative staining of homogenized cytoplasm suggests that rather than all organelles having direct links with microtubules, a membranous network links bulk cytoplasm to bundles of microtubules. If so, this mechanism could be responsible for the different rates of transport recorded from the centre to the edge of streams and might also account for the slower movement of cytoplasm around the edges of an obstacle such as a broken spicule piece.

1. Motors

Unfortunately it was not possible to reactivate streaming with ATP in

permeabilized cultures, so it was not possible to absolutely identify the motors involved. It appears that some essential ingredient is lost during permeabilization. Numerous variations of buffer osmolarity, pH, type and amount of detergent were tried, but motility could not be reactivated under any condition. Consequently, to determine whether particular motors were present or not, first whole mounts and western blots were probed with antibodies to both kinesin and cytoplasmic dynein, and second, ultrastructural evidence for transport mechanisms was sought.

Perhaps the most intriguing evidence regarding the mechanism of cytoplasmic transport is the finding of an immunoreactive band at the predicted molecular mass of cytoplasmic dynein in whole cell lysate from *Aphrocallistes*. Both antibodies to the intermediate chain of cytoplasmic dynein crossreacted with a protein in sponge lysate suggesting that dynein-ATPases may power cytoplasmic transport in hexactinellids. These antibodies are known to cross-react with chicken, *Xenopus*, and various mammalian cell lines (Killisch et al., 1995). In contrast, the lack of cross reactivity with SUK4 in whole mounts (data not shown) and in western blots suggests that the epitope for this antibody in sponge lysate differs significantly from that in sea urchin, or that hexactinellid tissue lacks kinesin altogether. SUK4 is known to cross-react with kinesin from mammals, sea urchin, and *Drosophila*, but not from squid (Ingold et al., 1988). In earlier experiments antibodies against kinesin from the ascomycete fungus *Neurospora crassa* also showed no cross-reactivity with proteins in the *Aphrocallistes* lysate. Kinesin from *Neurospora crassa* has heavy chains with a molecular mass of 105/108 kDa, shares 55% sequence similarity with motor domains

of other conventional kinesins, and can propel microtubules in *in vitro* assays (Steinberg and Schliwa, 1995), suggesting that kinesin may have had similar motor functions in very early eukaryotes. Although K1005 (anti-kinesin) recognized a variety of proteins in the sponge lysate, this antibody clearly did not recognize bands at the predicted molecular mass of kinesin in the sponge lysate.

It would be interesting if cytoplasmic dynein were responsible for organelle transport in hexactinellids. A dynein-like motor is involved in bidirectional transport of bulk cytoplasm along microtubules in the multinucleated protist *Reticulomyxa* (Euteneuer et al., 1988). Like *Rhabdocalyptus*, this protist can fuse with pieces torn from a conspecific, but organelle transport can be as fast as 20 $\mu m \cdot s^{-1}$ (Koonce and Schliwa, 1986). Furthermore, immunofluorescence studies have shown that cytoplasmic dynein is associated with cross-bridges between microtubules in *Allogromia*, a marine foraminiferan, which transports bulk cytoplasm at rates of greater than $10\mu m \cdot s^{-1}$ (Travis and Allen, 1981; Golz and Hauser, 1994).

In *Reticulomyxa* the great majority of microtubules are of uniform polarity, oriented with their plus ends distal to the cell body, implying that cytoplasmic dynein is capable of both plus- and minus-end directed movement (Euteneuer et al., 1989). Although the polarity of microtubules in *Rhabdocalyptus* could not be determined, flow within any one stream is unidirectional. Given the propensity of dynein ATPases to power minus-end directed or bidirectional motility, and of kinesin ATPases to power solely plus-end directed motility, it would be desirable to know the polarity of microtubules within streams. The inhibitory action of micromolar concentrations of

NEM, which at low concentrations inhibits dynein's ability to generate force and to bind to microtubules (Shimizu and Kimura, 1974; Mitchell and Warner, 1981), also supports the role of dynein in organelle transport in *Rhabdocalyptus*. Millimolar concentrations of NEM have no effect on kinesin driven motility (Vale et al., 1985b).

Given the similarity in structure and function at the molecular level of both cytoplasmic dynein and kinesin from protists and fungi to mammals, and our growing knowledge of the roles these proteins play in membrane traffic between the Golgi and endoplasmic reticulum (ER)(Lippencott-Schwartz et al., 1995), and bearing in mind that the ER and other vesicles are transported along microtubules by these proteins (Toyoshima et al., 1992; Walker and Sheetz, 1993), it would hardly be remarkable to find both motors in hexactinellids. The results confirm that at least one known molecular motor may exist in hexactinellids and the cross-reactivity shown by the anti-cytoplasmic dynein antibody used suggests that cytoplasmic dynein is well-conserved throughout the metazoa.

Although myosin motors were not sought in this study, it is conceivable that a triple motor mechanism could function in *Rhabdocalyptus*. Whereas rates of bulk streaming were uniform and correspond to rates of dynein or kinesin-driven transport in other organisms, individual organelles often moved haltingly. In giant lamellipodia rates of transport were very variable and average velocities far slower than those of bulk transport. These organelles often moved on invisible tracks and always unidirectionally, all characteristics which closely resemble organelle movement along actin as described in extruded squid axoplasm (Kuznetsov et al., 1992; Bearer et al.,

1993). Difficulties with labelling actin in adherent preparations (see Leys, 1995) prevented examination of the tracks on which these organelles moved, so their identification as actin, though plausible, remains unproven.

2. Calcium

The role of calcium in regulating cytoplasmic movements has been well established in plants and animals. In both algae and higher plants greater than 10^{-5} M Ca^{2+} irreversibly inhibits streaming, while between 10^{-7} and 10^{-6} M Ca^{2+} is required for motility (Williamson, 1975; Tominaga et al., 1983; Takagi and Nagai, 1986; Kohno and Shimmen, 1988; Grölig et al., 1988). Release of Ca^{2+} from the endoplasmic reticulum controls melanophore pigment aggregation (Thaler and Haimo, 1992), and Ca^{2+} gradients cause local solation of cytoplasm leading to streaming in both *Amoeba* and the slime mold *Physarum* (Ridgeway and Durham, 1976; Jansen and Taylor, 1993). Ca^{2+} gradients in pollen tubes have even been shown to cause deposition of vesicles at the pollen tube tip (Miller et al., 1992). The fact that relatively low concentrations of the ionophore 4 Br A23187 caused cessation of streaming in *Rhabdocalyptus* suggests that Ca^{2+} similarly affects cytoplasmic transport in hexactinellids. Similar calcium gradients may cause changes in viscosity of the cytoplasm in *Rhabdocalyptus* when streams turn sharp angles or encounter obstacles. However, considering the effect of the calcium ionophore on streaming, it is odd that no amount of mechanical disturbance (eg. poking with a wire electrode,

cutting, or tapping the preparation), which should allow calcium to enter the cytoplasm, caused streaming to stop (author, observation). This suggests that the tissue is highly effective at removing excess calcium from the cytoplasm, or sequestering it intracellularly.

3. Bulk cytoplasmic transport

Several lines of evidence indicate that transport of bulk cytoplasm in *Rhabdocalyptus* requires more than motor-driven transport of organelles along microtubules. In streams microtubules occur in bundles of 20 or more stacked from the surface membrane down to the where the tissue is anchored to the substrate. Although some lie singly here and there, and a number lie directly under the surface membrane in streams, they are certainly not randomly scattered throughout the streams. (There is no reason to suppose that some microtubules may depolymerize upon fixation, giving a false picture of the distribution.) However, an analysis of rates of transport of individual organelles, and of organelles at the edge and in the centre of streams, showed that isolated organelles move fastest, and that organelles at the edges of streams move significantly faster than organelles in the centre of streams. These observations imply that there is more drag in the centre of streams than at the edges, suggesting that microtubule bundles delimit the edges of streams. If microtubule bundles lay primarily in the middle of streams it is likely that a gradient in velocity opposite to that observed would exist; i.e. the fastest transport would occur

in the centre of streams and the slowest transport at the edges, where viscous drag with the non-moving cytoplasm should slow the stream down.

Since bundles of microtubules are not evenly distributed through streams it appears probable that organelles in bulk cytoplasm are linked to microtubule bundles via other organelles, or via a tubulovesicular network which is connected to microtubules and pulls the other components of the cytoplasm by viscous drag. Such a mechanism was shown to function in the 500 μm wide swaths of cytoplasm streaming in the characean alga *Chara* (Nothnagel and Webb, 1982; Kachar and Reese, 1988). Less extensive membranous networks can form spontaneously and track along microtubules in preparations with purified kinesin (Vale and Hotani, 1988). There is evidence for linkage of a membranous network to microtubules in axons (Droz *et al.*, 1975), fibroblasts (Terasaki *et al.*, 1986), algae (Menzel, 1994), and even in basal epithelial cells of fresh water sponges (Wachtmann and Stockem, 1992). However, attempts to label the endoplasmic reticulum in *Rhabdocalyptus* with $DiOC_6(3)$, as was done with some of the above organisms, were unsuccessful. In regenerating tissue explants at low magnification this dye highlighted streams of cytoplasm, but showed none of the detail seen in either fibroblasts (Terasaki *et al.*, 1986), or in the streaming cytoplasm of *Acetabularia* (Menzel, 1994). Considering the quantity of membranous vesicles in streams revealed by thin section TEM, it is not surprising that $DiOC_6(3)$ concentrated in streams in tissue explants.

Figure 27. A diagram of the proposed mechanism of bulk cytoplasmic transport in hexactinellid sponges. Organelles such as nuclei (n) and mitochondria (m) and a membranous network (mn) all associate with and are transported along microtubules (Mts) as indicated by the large black arrow. The membranous network may form specific links with other organelles and vesicles (v), or it may simply pull the other components of the cytoplasm along by way of the viscous drag generated by gelating proteins within the cytoplasm (ag).

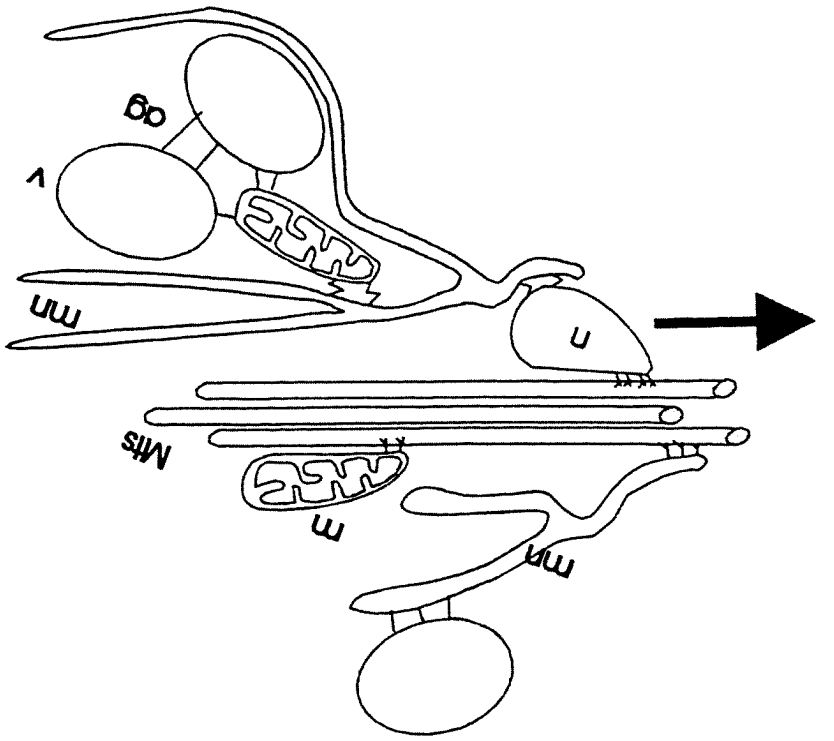
Go
N
uw
u
Mis
E
mn

Some evidence, however, that at least a partial network of membranous material links organelles to pathways of transport was found in negatively stained preparations of freshly homogenized sponge tissue. In this technique organelles are liberated from cells, but their associations are maintained as the cytoplasm does not disperse and organellar membranes are not lysed. These preparations showed individual organelles associated with long tracts, presumably microtubules. A membranous network was often associated with organelles on the tracts and frequently extended to other organelles. Although this evidence does not prove that all bulk streaming in *Rhabdocalyptus* involves the endoplasmic reticulum or a membranous network it does suggest that a linkage system is involved. The network seen appears less extensive than that found in characean algae, and in addition to a membranous network there are direct links between organelles.

Organelles could be linked by actin-related proteins or they could lie within a network of gelating proteins such as filamin and α-actinin. One indication that an actin gel may exist in bulk streams in *Rhabdocalyptus* is that foci of rhodamine-labelled actin remain after tissue lysis in preparations used for study of stress fibres and filopodia in adherent aggregates (Leys, 1995; Chp. II). These foci are reminiscent of the contracted extracts of *Dictyostelium* labelled with fluorescein-actin, which were induced by addition of calcium (Taylor and Fechheimer, 1982). Interestingly, identical foci of actin were described by Koonce and Schliwa (1986) in reactivated preparations of *Reticulomyxa*, where they were interpreted as evidence of an actin-based system for bulk cytoplasmic transport. The suggested interaction between

organelles, a membranous network, and microtubules to generate bulk streaming of cytoplasm is illustrated in figure 27.

4. Membrane transport

Finally, despite finding microtubules lying under the surface membrane of streaming adherent preparations, there is no evidence that these drive the kind of membrane transport used in feeding by some protists (Bowser and Rieder, 1985). Surface transport of foreign particles has been documented in the keratose demosponge *Dysidea* (Teragawa, 1986), but in that sponge sand grains and other debris are taken up by exopinacocytes, delivered into the dermal mesohyl, and transported towards areas where they are presumably used for structural support. Similarly, in *Rhabdocalyptus*, latex beads dropped on the surface membrane were not transported until internalized and moved into a stream. It is likely that microtubules at the surface of streams of cytoplasm use the membrane as an anchor when most of the cytoplasm in the stream is in motion.

SUMMARY

1. A protein that cross-reacts with an antibody specific for cytoplasmic dynein was found to be present in *Aphrocallistes vastus* whole cell lysate. Dynein powered

organelle transport is supported by experiments showing inhibition of motility by NEM.

2. The presence of kinesin could not be confirmed either by western blot analysis or immunofluorescence microscopy on whole mounts.

3. Rates of transport, the lack of directionality, and the saltatory manner of movement of organelles in lamellipodia suggest the possible involvement of myosin in organelle motility in both *Rhabdocalyptus* and *Aphrocallistes*.

4. Calcium was found to inhibit streaming. Cessation of organelle transport by ionophore treatment was reversible. Mechanical stimuli to adherent preparations had no effect on streaming.

5. A model of bulk streaming is proposed which utilizes transmission of drag forces to organelles from motor-associated vesicles on tracks via a membranous network. In support of this model, negative stain electron microscopy showed membranous networks connecting organelles to microtubules and revealed direct links between organelles.

7. No evidence was found for membrane surface transport. Latex beads dropped on preparations remained stationary when adhered to the surface membrane, but once internalized were transported in streams.

Chapter 4: FUSION AND CYTOPLASMIC STREAMING ARE CHARACTERISTIC OF AT LEAST TWO HEXACTINELLIDS. AN EXAMINATION OF LIVE TISSUE FROM *APHROCALLISTES VASTUS*.

INTRODUCTION

There is now substantial evidence that hexactinellid sponges are syncytial animals. Both early histological studies (Schulze, 1880, 1899; Ijima, 1901, 1904) and recent ultrastructural investigations (Reiswig, 1979a; Mackie and Singla, 1983b; Boury-Esnault and de Vos, 1988; Salomon and Barthel, 1990; Reiswig, 1991; Reiswig and Mehl, 1991; Boury-Esnault and Vacelet, 1994) show that these sponges consist of a single, multinucleated, giant cell (the trabecular syncytium) which is connected via perforated plugged junctions to cellular components (choanoblasts, archaeocytes, thesocytes, etc.). However, because the trabecular syncytium is an extremely delicate, reticulate network of tissue, and is draped like an irregular cobweb over the glass skeleton, the exact nature of the structure of its cytoplasm has been difficult to grasp with thin section transmission electron microscopy (TEM).

This is where live tissue cultures from *Rhabdocalyptus* dawsoni, a rossellid hexactinellid, have been instructive (Leys, 1995). In culture, dissociated tissue from *Rhabdocalyptus* aggregates by fusing membranes to form a giant multinucleated syncytium which contains the various cellular components still connected by plugged junctions to the syncytial tissue. Within the single outer membrane of these cultures, the syncytial tissue is organized into pathways of constantly moving cytoplasm, presumably transported along bundles of microtubules, and areas of stationary cytoplasm, presumably corresponding to groups of the cellular components such as archaeocytes, thesocytes, and spherulous cells. Observations from small regenerating

tissue fragments or explants from *Rhabdocalyptus* show that similar cytoplasmic streaming can be seen along strands of the trabecular syncytium (Leys and Mackie, 1994).

Although it is to be expected that other hexactinellids can also form giant syncytia in culture, and would also transport bulk cytoplasm within the trabecular syncytia, reflecting their syncytial composition when whole, there is no information on live tissues from any other hexactinellid. The lack of such studies reflects the difficulty involved in collecting and maintaining hexactinellids alive in sea water aquaria, and in carrying out in vitro research on these animals. Due to their preferred deep water habitat, the majority of specimens are collected either by dredging or by submersible. Unless there is direct access to a cooled, flow-through, sea water system, it is not possible to maintain these sponges alive.

The presence of hexactinellids within SCUBA range (30-50 m) on the west coast British Columbia, Canada, has been known for some time (Fraser, 1932), but it was not until the late 1970's that their unusual accessibility was taken advantage of when Reiswig (1979a) looked at the histological organization of *Aphrocallistes vastus* and *Heterochone calyx*. Since that time *Rhabdocalyptus dawsoni*, which is the most readily accessible of shallow water hexactinellids in British Columbia, has been targeted for studies on physiology (Lawn et al., 1981), ultrastructure (Mackie and Singla, 1983b), ecology (Marliave, 1992; Reiswig, 1990), and most recently for video microscopy of living tissues (Leys, 1995; Wyeth et al., 1996).

In order to confirm that live tissues and aggregates from another hexactinellid

- one whose gross morphology is substantially different from that of *Rhabdocalyptus*, in having a fused, dictyonal skeleton - also form giant multinucleated syncytia and undergo cytoplasmic streaming, in this chapter I compare the cytological organization of tissue cultures and of spicule preparations from *Aphrocallistes vastus* with that described previously for its relative *Rhabdocalyptus* (Leys, 1995).

METHODS

Specimen collection:

Specimens of *Aphrocallistes vastus* were collected by SCUBA from 35-40 m depth, the uppermost limit of the population, and the lowest limit of SCUBA, permitting a maximum of 6 minutes work, in Saanich Inlet, British Columbia, Canada. Pieces were cut from mitten-like extensions of the main cone using a sharp knife, and transported in bags of sea water to aquaria at the University of Victoria, British Columbia.

Preparation of aggregates, video microscopy, immunocytochemistry, and electron microscopy

These are described in the general methods section.

RESULTS

1. Description of specimens

Aphrocallistes has a strikingly different morphology from *Rhabdocalyptus*. Unlike *Rhabdocalyptus*, its skeleton is fused into a rigid, permanent support. *Aphrocallistes* grows in the form of an expanding hollow cone, by adding tissue and skeleton first as a limp, flexible framework which appears to sag and bend under the weight of the new tissue. The body wall is generally less than one centimetre thick. Large individuals can reach a metre in height and, depending on the undulating shape, at places they may reach a metre in width. This sponge is free of all debris, and has a creamy yellow colour.

2. Adhesion and spreading of cultures

Dissociated tissue from *Aphrocallistes* adheres to substrates containing Concanavalin A or tissue extract from conspecifics, and to a lesser extent to tissue extract prepared from *Rhabdocalyptus*. Pieces of tissue adhered within 5-30 minutes of plating and typically spread a broad lamellipodium around what thin section electron microscopy confirmed were either uni- or multi-nucleate pieces of cytoplasm (Figs. 28 a-c). The adhered preparations showed extensive lamellipodial ruffling and filopodial movement as described for *Rhabdocalyptus* cultures (Fig. 28c). Lamellipodial

spreading brought separate tissue pieces into contact, and fusion of pieces occurred approximately 1 hour after plating. Occasionally adherent pieces became elongated and migrated considerable distances across the coverslip until another spread tissue piece was encountered (Fig. 28d). The advancing edge of such pieces was characterized by a semi-circular lamellipodial margin, much like that of keratocytes in culture (Fig. 28e).

In some instances unidirectional streaming or swirling of the cytoplasm could be seen in pieces which had attached to the coverslip but which remained spherical rather than spreading. Generally, however, the tissue pieces adhered and spread, and the cytoplasm soon began circumnavigating the centre of the piece. Spreading tissue pieces grew in diameter as new tissue was incorporated, and after 12-24 hours, streams of continuously moving cytoplasm wound for distances of up to several centimetres in length in the adherent cultures. The mean rate of transport of organelles and bulk cytoplasm in *Aphrocallistes* was 1.82 ± 0.15 $\mu m \cdot s^{-1}$ (SE)(max: 2.08, min: 1.47). This rate was not significantly different from the average rate of transport in *Rhabdocalyptus* (2.15 ± 0.33 $\mu m \cdot s^{-1}$) ($p << .01$).

When viewed with differential interference contrast microscopy the contents of the cytoplasm appeared different from those of *Rhabdocalyptus* cultures. In *Aphrocallistes* individual organelles were harder to identify in the streaming cytoplasm although, surprisingly, streams appeared less dense on the whole. Nuclei, labelled with Hoechst #33342, flowed within streams in *Aphrocallistes* cultures (Fig. 29a), although more nuclei were stationary than moved in streams compared to cultures

prepared from *Rhabdocalyptus*. The movement of bulk cytoplasm in cultures from both species was similar in that streams became congested when an obstacle such as a piece of broken spicule was encountered, and stopped, turning 90-180 degrees upon reaching the edge of the preparation.

3. Cytoskeletal architecture

The cytoskeleton of tissue pieces fixed one hour after plating consisted of actin-dense filopodia, as shown by labelling with rhodamine phalloidin (Fig. 28f), and a tangled web of microtubules, shown by labelling with anti-tubulin antibodies (Fig. 28g). Although aggregates made from *Aphrocallistes* adhered less strongly than aggregates from *Rhabdocalyptus*, making it difficult to carry a 24 hour-old preparation through all the procedures for immunocytochemistry, no obvious differences could be discerned from the organization of the cytoskeleton in day-old adhered *Rhabdocalyptus* aggregates.

In cross sections of formerly streaming cytoplasm from *Aphrocallistes*, microtubules could be clearly identified adjacent to both empty vesicles and large electron dense vesicles (Fig. 29b). Thin sections cut horizontally in the plane of streaming from cultures of *Aphrocallistes* showed bundles of 10 to 20 microtubules which traversed the entire grid (Fig. 29c). Microtubules were more distinct than in *Rhabdocalyptus* cultures, and spacing between microtubules in bundles was estimated to be one microtubule width (20-30 nm); there were no clearly repeating cross

bridges joining neighbouring microtubules. In confirmation of light microscopic observations the streaming cytoplasm was found to contain fewer nuclei, phagosomes, and archaeocytes than that of *Rhabdocalyptus*, which may have contributed to the improved preservation of microtubules by allowing better penetration of the fixative. Instead, streams in *Aphrocallistes* cultures were packed with numerous clear vacuoles of varying shapes and sizes, many electron dense spheres, and some mitochondria.

In areas of the tissue which presumably were not streaming, there were many enucleate collar bodies still connected to choanoblasts by perforate plugged junctions (Fig. 29d). Septate junctions, as described by Mackie and Singla (1983b), were often adjacent to plugged junctions and also joining collar bodies to choanoblasts. Centrioles were common in archaeocytes and choanoblasts, but were never seen in the multinucleate cytoplasm (Fig. 29 e,f).

4. Tissue explants

Shavings from the whole sponge placed under a coverslip on a slide regenerated overnight to form a new dermal or outer membrane. In parts of these preparations which were sufficiently thin for video microscopy, numerous individual organelles moved haltingly in thin areas of the tissue which stretched between spicule pieces (Fig. 30 a-c). Wide streams of moving cytoplasm could readily be seen traversing an entire centimetre-long preparation (Fig. 30 d,e).

Figure 28. Early aggregates from *Aphrocallistes vastus* upon adhesion and spreading of dissociated tissue to coated substrates. Video and fluorescence microscopy. (a-c) Minutes after plating dissociated tissues on tissue extract, large pieces adhered and spread a broad skirt-like lamellipodium. These lamellipodia often showed ruffling as though there was movement of the membrane from the leading edge backwards (c). Scale bars (a-e): 10μm. (d) Some pieces became elongate and began migrating across the coverslip. (e) The advancing edge of these pieces was often characterized by a semicircular lamellipodial margin (lm). (f) The actin cytoskeleton labelled with rhodamine phalloidin in an adhered aggregate approximately one hour after plating tissue. (g) Microtubules labelled with antibodies to α-tubulin (Amersham) in a one-hour-old adhered aggregate. Scale bars (f-g): 20μm.

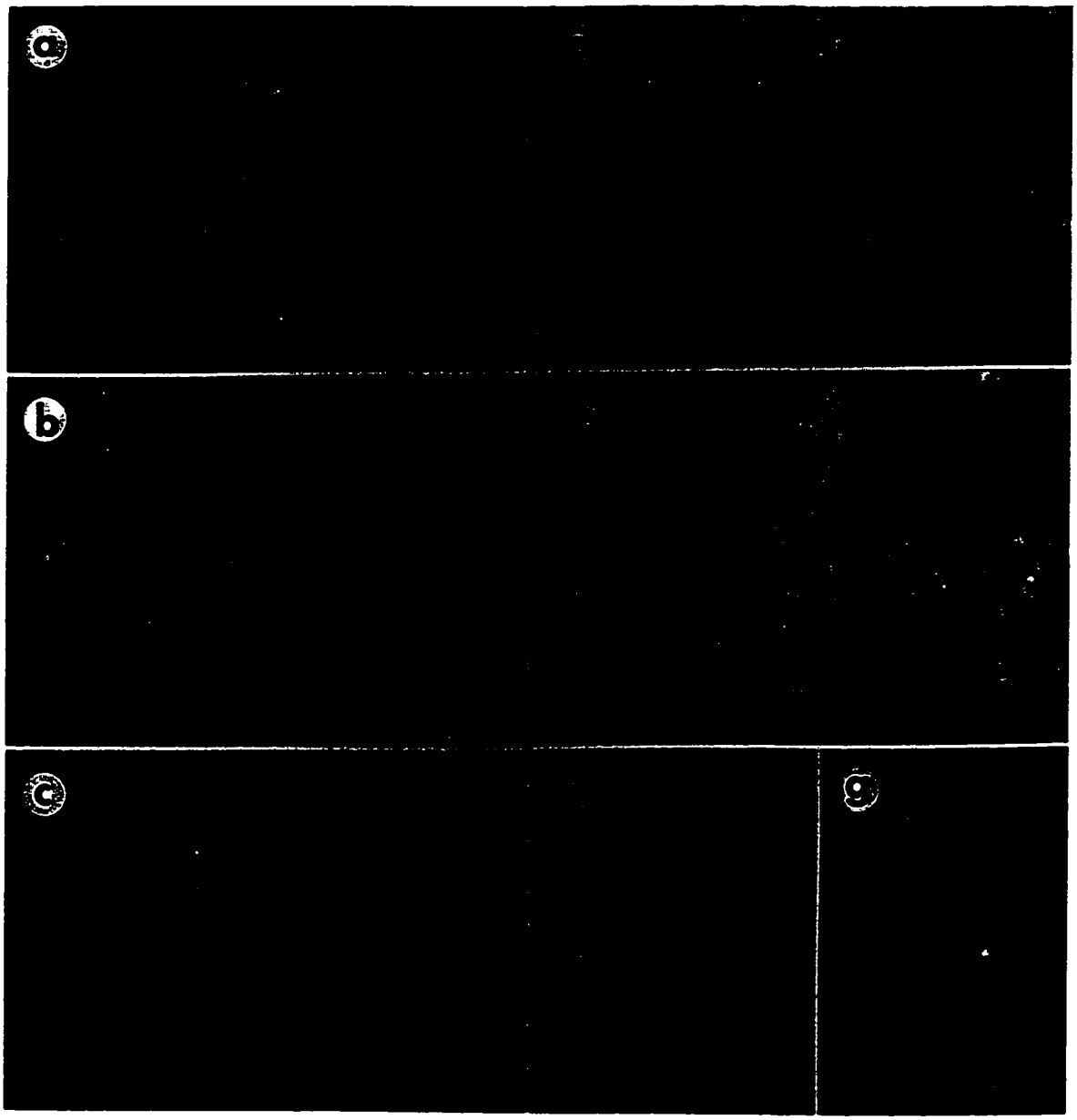
a
b
c
g

Figure 29. Characteristics of 24-hour-old adhered aggregates from *Aphrocallistes vastus*. Epifluorescence and transmission electron microscopy. (a) Nuclei labelled with Hoechst #33342 in streaming cytoplasm left a path showing their movement during a 30 second time exposure with epifluorescence microscopy. Scale bar: 10μm. (b) Microtubules in a cross section of formerly streaming cytoplasm were adjacent to large electron dense vesicles and numerous clear or empty vesicles. Scale bars (b-f): 0.5μm. (c) Horizontal sections of a path of formerly streaming cytoplasm revealed large bundles of microtubules associated with membranous organelles (mo) and electron dense vesicles (dv). (d) A collar body (cb) and choanoblast joined via a perforated plugged junction (arrow) were representative of the cytoplasm which was presumably stationary. Material can be seen traversing the two pores in the plugged junction. (e,f) Planes sectioned on either side of the plugged junction (black arrow) shown in (d) showed further pores within the junction and revealed centrioles (open arrows) located on either side of the plugged junction.

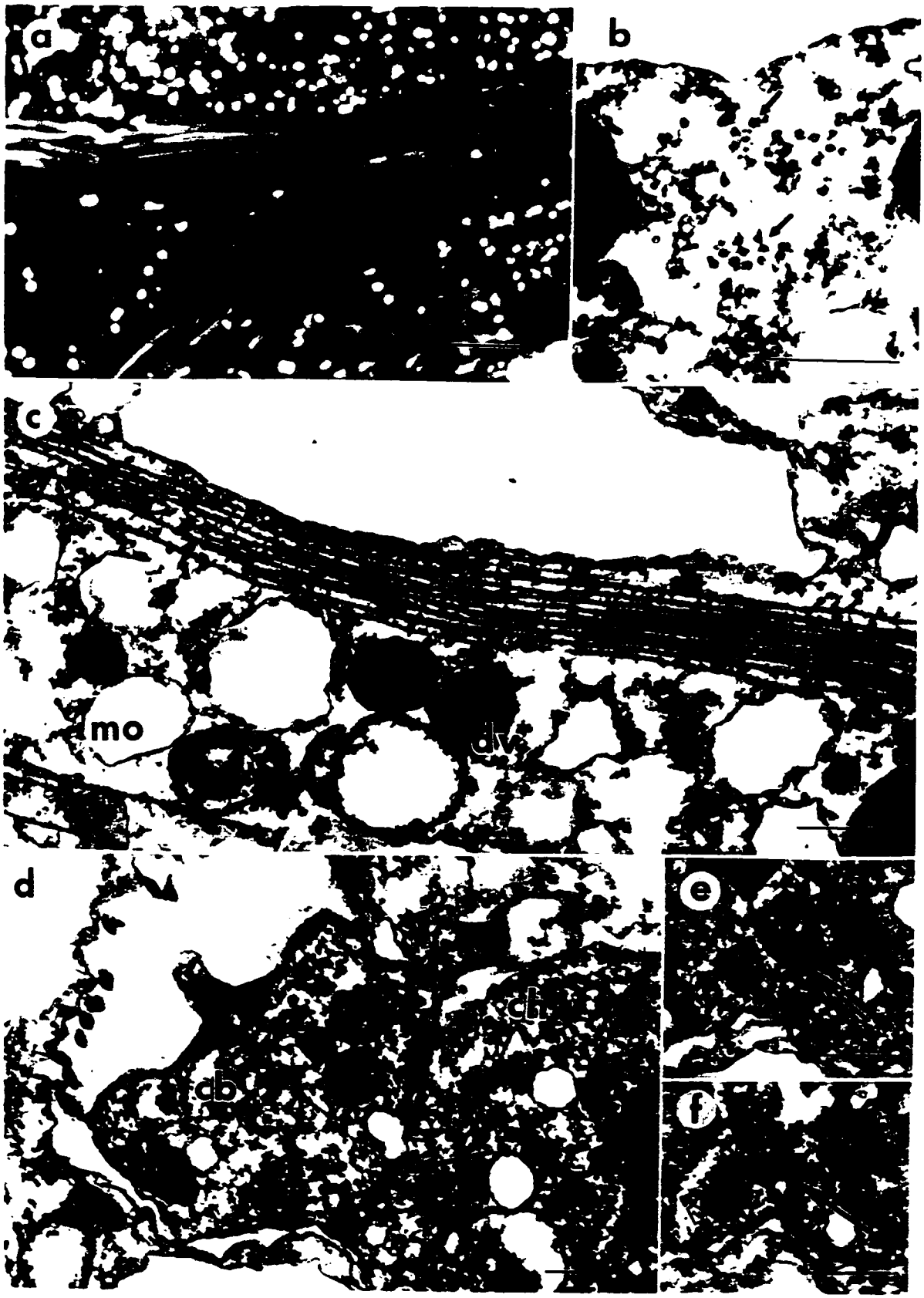
a
b
c
mo
dv
d
db
db
e
f

Figure 30. Organelle transport in regenerating tissue explants from *Aphrocallistes vastus*. Video microscopy. (a-c) Saltatory transport in thin areas of the trabecular syncytium which bridge spicules is far slower than transport of bulk cytoplasm in streams (d,e). (Arrow = vesicle). Time a-c: 0, 30, 60s; d,e: 0, 15s. Bars: 10μm.

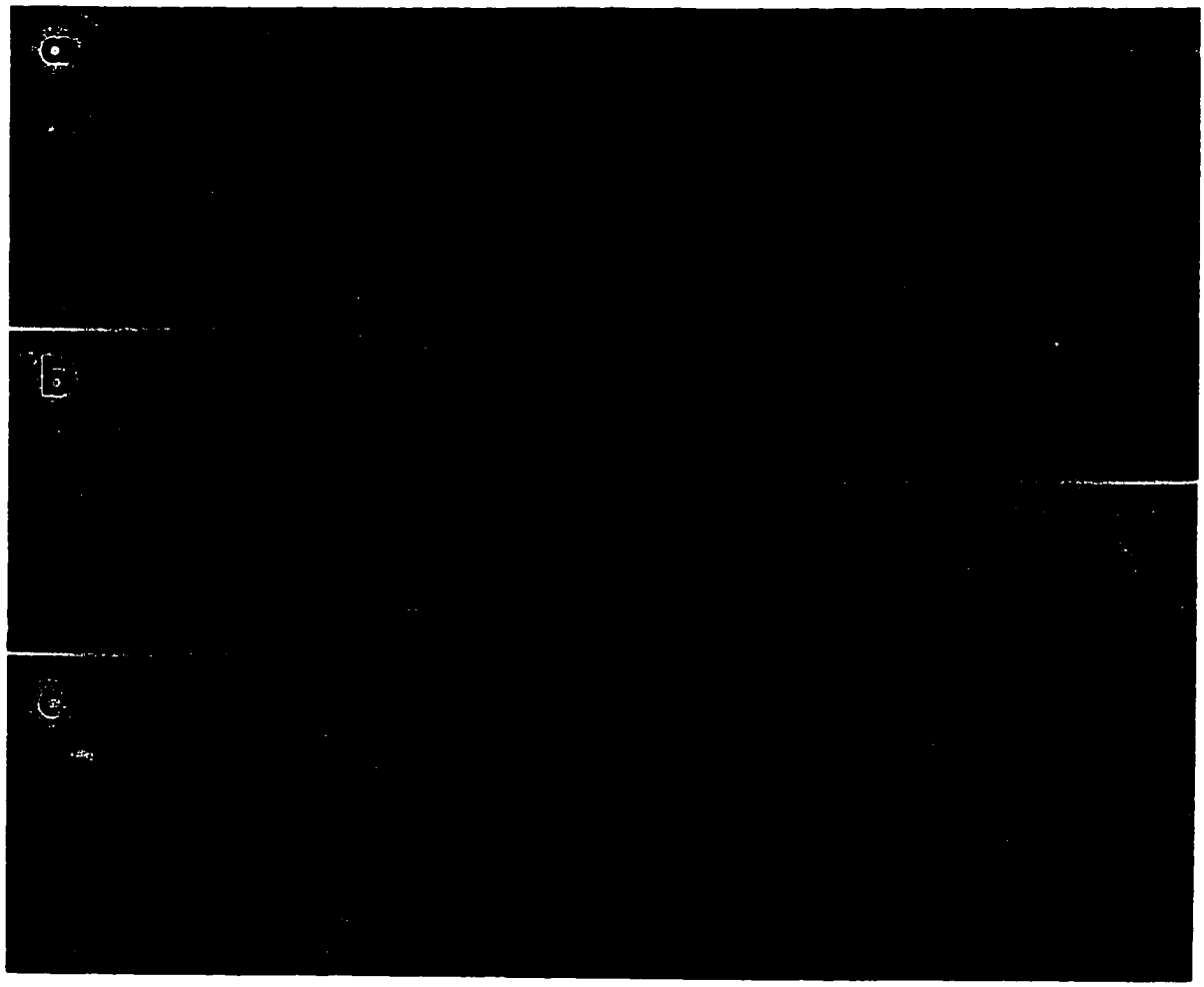

DISCUSSION

1. Tissue dynamics and cytoskeletal organization in *Aphrocallistes vastus*.

Dissociated tissue from *Aphrocallistes vastus* adhered to both natural and artificial substrates in culture. The tissue fused to form giant multinucleate tissue masses in which individual organelles and bulk cytoplasm were transported in extensive streams in a manner identical to that seen in cultured tissue from *Rhabdocalyptus* (Leys, 1995).

Tissue fusion, cytoskeletal architecture, and rates of organelle transport were comparable in every way to their counterparts in cultured tissue from *Rhabdocalyptus*. The adhered cultures of the two species differed only in the content of the streams of cytoplasm, which was apparent by both light and electron microscopy. Whereas in *Rhabdocalyptus* streams commonly contained numerous mitochondria, phagosomes, archaeocytes, Golgi systems, numerous nuclei, and empty vesicular or membranous material, thin sections of *Aphrocallistes* revealed that streams contained vast amounts of membranous organelles, few mitochondria, few nuclei, and numerous electron-dense, spherical granules. Since the outside of *Rhabdocalyptus* is covered in debris and *Aphrocallistes* is quite clean it is possible that despite the fact that the outer spicules were cut off prior to dissociation of *Rhabdocalyptus* tissue there may be more debris for this sponge to phagocytose during aggregation. Adherent tissue cultures from both species contained numerous archaeocytes, thesocytes, spherulous cells, and

choanoblasts in areas of the cytoplasm which were presumably stationary prior to fixation of the tissue. All these cells were connected either to each other, or to the multinucleate cytoplasm, via perforate plugged junctions.

The similarity in rates of organelle transport and amount of membranous material found in streams of both species suggests that similar mechanisms involving linkage to microtubules by membranous networks or actin gels (Chp. III) underlie motility in both sponges. Furthermore, rates of spreading of dissociated tissue, and the time at which membranes first encounter each other and fuse during aggregation, were similar in both species.

2. 'Cord syncytia' and cytoplasmic streaming

When Reiswig (1979a) first examined the histology of *Aphrocallistes vastus* using electron microscopy he confirmed the syncytial nature of trabecular tissues in hexactinellids and described for the first time the primary and secondary reticula, components of the trabecular syncytium which surround and possibly support choanoflagellate structures in the flagellated chambers.

Another characteristic he described was a 5-10 μm swath of uniformly staining multinucleate cytoplasm which ran for hundreds or thousands of micrometers, anastomosing and forming "intersecting arrays in both the subdermal and subgastral trabeculae" (Reiswig, 1979a). This feature, which he termed the "cord syncytia", may have escaped notice by earlier sponge workers or have been grouped with the

structures they called trabeculae. Wider (up to 30 μm diameter), albeit less abundant, swaths of dense cytoplasm were later seen in *Rhabdocalyptus* (Mackie and Singla, 1983b) and may occur in all hexactinellids, in differing thicknesses. For example, in *Oopsacas* cytoplasmic "strands" (Boury-Esnault and Vacelet, 1994, Fig. 4) were found linking the external surfaces of adjacent flagellated chambers. That cord syncytia most probably correspond to actively streaming swaths of multinucleate cytoplasm can be seen in regenerating tissue explants (Leys and Mackie, 1994; and this chapter). The lack of function ascribed to these paths of cytoplasm in earlier studies can be blamed on inadequate fixation. Using the fixation protocol of Mackie and Singla (1983b), microtubules are only preserved in flagella. But by using a fixative designed to preserve a highly labile cytoskeleton (Harris and Shaw, 1984) extensive bundles of microtubules are revealed in all streams of formerly moving cytoplasm.

The role of cytoplasmic streams in transporting nutrients taken up by the trabecular syncytium in the vicinity of flagellated chambers (Wyeth et al., 1996) demonstrates that the physiology of hexactinellids differs vastly from that of other sponges. Nutrient transport in demosponges is by motile amoebocytes (Kilian, 1952; Imsieke, 1994). There is one report of cytoplasmic streaming seen during reaggregation in *Microciona prolifera* (Reed et al., 1976). However, because scanning electron microscopy of these aggregates demonstrated that they were cellular, it is likely that the streaming referred to was no different from the movement of individual organelles along microtubules which occurs in all cells.

Although *Rhabdocalyptus* and *Aphrocallistes* are the only hexactinellids in

which cytoplasmic streaming has been observed, and in which streaming in live tissues can be correlated with cord syncytia in preserved specimens, it is likely that cytoplasmic streaming, and hence the cord syncytia, are characteristics of all hexactinellids.

3. Hexactinellid features

According to their findings from a thorough ultrastructural survey of whole tissue from *Rhabdocalyptus*, Mackie and Singla (1983b) defined the features which characterize hexactinellids as 1) syncytial rather than cellular tissues, 2) lack of pinacocytes, 3) thin collagenous mesohyl, 4) plugged cytoplasmic junctions between morphologically distinct tissue types, 5) enucleate collar bodies, 6) primary and secondary reticula in large cup or thimble shaped flagellated chambers, and 7) triaxial spicule symmetry with square axial spicule filaments. From further, more recent, ultrastructural investigations of other hexactinellids, using similar fixation protocols, we are aware of only minor differences from this general plan. In *Caulophacus cyanae* it was felt that plugged cytoplasmic junctions were only seen at the beginning of the budding off of collar bodies (Boury-Esnault and De Vos, 1988). *Farrea occa* has numerous rod shaped bacteria in the mesohyl and an additional membrane, termed the inner membrane, which extends from the secondary reticulum into the flagellated chamber, and occasionally encloses the tips of the flagella (Reiswig and Mehl, 1991). *Oopsacas minuta* also possesses abundant thread-like

bacteria, adjacent to the collar of collar bodies, and a fine inner membrane above the secondary reticulum (Boury-Esnault and Vacelet, 1994). Finally, in *Dactylocalyx* neither a secondary reticulum nor dense perforate plugs were found (Reiswig, 1991), although their presence could not be entirely ruled out by the author.

There is evidence that the inner membrane may be a feature of a small percentage of flagellated chambers in all hexactinellids, and that it may correspond to central cells in flagellated chambers of cellular sponges (Reiswig and Mehl, 1991, and author observation). Moreover, the description of central cells from at least one demosponge (Langenbruch and Jones, 1989) corresponds surprisingly well to the secondary reticulum of hexactinellids. More information is needed on the structure and function of the primary and secondary reticula in hexactinellids, and of central cells in demosponges, before it can be concluded that either are characteristic of their respective groups.

The new information on live tissues from two hexactinellids shows that the basic cytological organization of these sponges differs substantially from that of cellular sponges. The formation of a giant cytoskeleton during aggregation of dissociated tissues, and the transport of bulk cytoplasm, including nuclei, in live tissues from more than one hexactinellid, appear to be characteristics unique to this group of sponges. Since the cord syncytia appear to be a uniquely hexactinellid feature, as is their role in the transport of nutrients and in tissue regeneration and morphogenesis in these sponges, I suggest that the presence of these structures should be added to the above list of features which characterize hexactinellids.

Chapter 5: IMPULSE CONDUCTION IN *RHABDOCALYPTUS DAWSONI*

INTRODUCTION

Sponges pump water through canals in their body wall to feed. The feeding current is generated by flagellated cells, called choanocytes, which line invaginations of the canal systems, termed flagellated chambers. Field experiments on tropical demosponges have shown that some sponges are able to adjust their pumping rate, diurnally, in response to tidal changes (Reiswig, 1971), or in response to sediment in the water (Gerrodette and Flechsig, 1979). Since cellular sponges are considered to lack both gap junctions, which would enable electrical signals to propagate between cells, and nerves (Mackie, 1984), it has been suggested that these sponges might control flow by local contractions of the oscula, contracting flagellated chambers, or by local inhibition of choanocyte beating by central cells, all of which would generate a very slow behavioral response. Indeed, contractions in cellular sponges have been reported to occur at some 10-20 $\mu m \cdot s^{-1}$, approximately the rate of a calcium wave in astrocytes (Nedergaard, 1994).

Hexactinellid sponges, however, are capable of much faster responses. This is the only group of the Porifera in which rapid propagation of arrests of the feeding current has been recorded (Lawn et al., 1981; Mackie et al., 1983). *Rhabdocalyptus dawsoni* arrests its feeding current upon mechanical or electrical stimulation, both in the field and in laboratory experiments (Mackie et al., 1983). The arrest is thought to prevent the animal from clogging its tissues with sediment disturbed by an intruder. Previous evidence has shown that the arrests are all or none, and rates of

propagation across the body wall, measured using two thermistor flow meters placed at a known distance apart over excurrent canals, averaged 0.26 $cm \cdot s^{-1}$. Unlike cellular sponges, the tissue of hexactinellids is connected in a giant syncytium, called the trabecular reticulum (Mackie and Singla, 1983b). The choanosome - tissues including the flagellated chambers - consists of flagellated enucleate processes (collar bodies) of nucleated mother cells (choanoblasts), suspended in a perforated sheet of the trabecular reticulum, the primary reticulum (see Fig 8. Chp II). Although the collar bodies and choanoblasts are distinct from the syncytial tissues, they are joined to the trabecular reticulum by cytoplasmic bridges which contain a unique, osmiophilic, perforate, plugged junction (see Mackie, 1981).

Because of the thinness of hexactinellid tissue - the largest strands of the trabecular reticulum are only some 20 μm thick, and the atrial and dermal membranes (the exposed inner and outer layers of the sponge) are less than one micron in diameter each - it was not previously possible to record directly from the sponge. Consequently propagation by a chemical or mechanical process could not be entirely ruled out.

In this chapter I describe a new preparation developed specifically for sponge electrophysiology which has made it possible to record an action potential from *Rhabdocalyptus dawsoni*. This is the first action potential ever recorded from a sponge. The work described in this chapter was done in collaboration with George Mackie.

METHODS

Flow recordings

Recordings of flow through the sponge were made using a thermistor flow probe (La Barbara and Vogel, 1976) mounted on a stand with the tip of the probe just inside the osculum of a sponge in a darkened sea water tray. Records of flow were made during 24 hours from 12 sponges. The rate of flow was calibrated by recording flow through a tube of known internal diameter while collecting the water via an overflow hose to calculate the volume of water moving per minute.

Mechanical stimuli (gentle prodding), and increased sediment load were used to attempt to cause the sponges to arrest. Sediment load was increased by introducing approximately 500 ml of sediment collected from the same habitat as the sponges, into the tank containing the animals (approximately 100 L total volume) so as to make the water murky. Despite the flow from hoses in the seawater tray, the water in the tank remained murky for more than 5 minutes.

Construction of aggregate grafts

Aggregates were made as described in Chapter I, using a large amount (8-10 pieces ca. $1cm^3$) of dissociated tissue and one or two coverslips coated with Concanavalin A (Con A) in a 5 cm diameter petri dish to promote adhesion and aggregation of

large balls of tissue. After 12-24 hours aggregates had rounded off and detached from the substrate. Aggregates measuring some 3-20 mm in diameter were gently pipetted, using the broad end of a pasteur pipette, on to the atrial side of slabs of body wall from the same individual from which the aggregates were made. The pieces of sponge were either pinned with stainless steel insect pins on to Sylgard (Dow Corning) coated dishes, or placed unpinned, atrial side up, in marked dishes in a flow through sea water tank.

Extracellular recording

Without removing the sponge piece from sea water, slabs of sponge with grafts were moved to the recording set up - a Sylgard-coated plexiglass dish ca. 15 x 15 cm with flow through sea water. A polyethylene suction electrode (ca. 80-100 μm internal diameter) coated with Con A was pushed onto the graft and slight suction was applied with a 1 ml plastic syringe attached to polyethylene tubing. This caused a small amount of the graft tissue to pull up into the electrode tip (Fig. 1). Bipolar platinum stimulating electrodes insulated close to the tip were pushed into the body wall several centimetres away from the graft. Flow was recorded from the slab of sponge with a thermistor flow probe, positioned over an exhalant canal on the atrial side beside the graft. Single or double stimuli of 50-80 ms duration and 80-100 V amplitude were applied using a stimulation isolation unit to allow reversal of polarity. Signals were amplified using a capacity coupled preamplifier and displayed on a

digital oscilloscope, with the polarities arranged so that negative-going events were in the up direction. Photos of traces were taken with a polaroid camera.

Figure 31: Diagram of a sponge graft fused to the pinacoderm (p) of the atrial side of a slab of sponge. Cytoplasm from the graft (g) is fused with cytoplasm from the sponge piece. The curved arrows indicate the flow of current through the sponge, generated by the flagellated chambers (fc) which are suspended by the trabecular syncytium (ts). The stimulating electrodes (se) were inserted into the atrial wall several centimetres from the thermistor flow probe (fp) and the recording electrode (re).

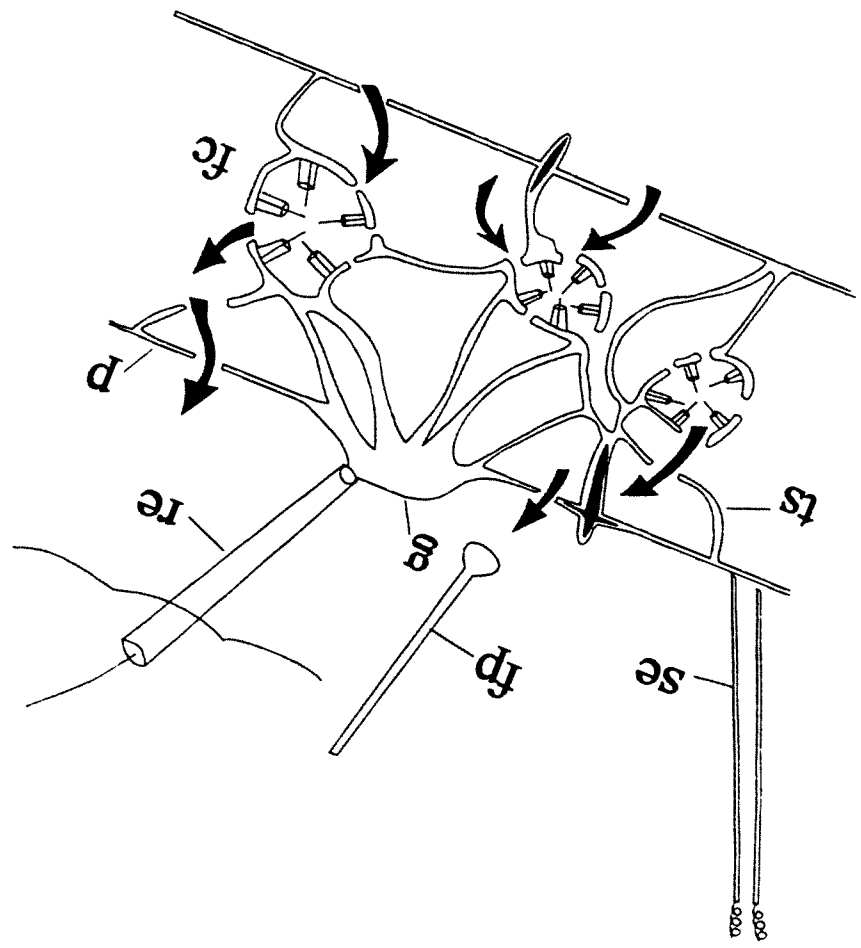
fc
p
re
g
fp
se
ts

RESULTS

1. Spontaneous pumping behaviour

Flow recordings were made over 12-36 hours from 12 different sponges. Two sponges pumped almost continuously for 24 hours, but most animals arrested their feeding current sporadically. None of the sponges showed any visible diurnal rhythm to the arrests. A typical unelicited arrest of flow lasted some ten minutes before the sponge began pumping once again (Fig. 2A). During such arrests, the sponge initially ceased pumping for less than one minute, and then resumed pumping, and almost immediately arrested again for up to ten minutes.

When pumping, all sponges responded to mechanical stimuli (e.g. prodding), and to an increase of sediment in the water (Fig. 2B). A typical response to a sudden increase in sediment was an initial partial arrest of the feeding current, followed approximately 1-5 minutes later by a full arrest of the current. In some instances the sponge appeared to attempt to begin pumping again several times, before uninterrupted pumping resumed. The rate of flow through sponges was calculated for three animals of approximately 15 cm length, but of different volumes to be 0.85 $cm \cdot s^{-1}$, 0.85 $cm \cdot s^{-1}$, and 1.19 $cm \cdot s^{-1}$ (mean rate of flow: 0.96 $cm \cdot s^{-1}$). The rate of pumping by these sponges after recovery from arrest caused by sudden increase in sediment load was 0.76, 0.50, and 0.96 $cm \cdot s^{-1}$ respectively for the above sponges, a reduction on average of 32 percent of the previous pumping rate.

2. Homografts

Aggregates adhered and grafted on to the atrial side of a piece of the body wall from the same sponge from which the aggregate was made. After 12 hours aggregates had fused with the sponge pieces (Fig. 3A) and after 24 to 36 hours, streams of tissue could be seen with the naked eye, running down off the aggregate into the tissue of the sponge (Fig. 3B). Within 3-4 days the aggregate tissue was entirely resorbed into the tissue of the sponge. At this time the atrial wall had a dense, creamy colour, but after one week there was no sign of either aggregate or graft on the sponge piece. Allografts were attempted but the aggregates failed to fuse with the test sponge.

3. A propagated action potential

When stimulated electrically each evoked arrest of the feeding current was preceded by an action potential, recorded from the graft (Figs. 4a,b). The rate of propagation of the event, calculated by determining the distance travelled between the stimulus and the crossover point of the action potential, divided by the time taken to travel that distance, was 0.18 ± 0.17 cm$\cdot s^{-1}$ ($n=18$). The duration of the action potential was approximately 5 seconds. A second stimulus given during an arrest either prompted another action potential and summation of the effectors (Fig. 4b), or (on one occasion) when the flow was fully arrested, the second stimulus caused another action potential but no further response from the sponge. The conduction system has

a long refractory period, probably between 30 and 40 seconds, but precise measurements were not made.

Figure 32. Spontaneous pumping in *Rhabdocalyptus dawsoni*. (A) A trace from a 24 hour recording from a sponge kept in a darkened sea water tray showing an unelicited or natural arrest. The flow record reads from left to right. The sponge arrested its feeding current for some 5 minutes, began pumping again, only to arrest for 2-3 more minutes before resuming uninterrupted pumping. (B) When sediment was introduced into the tank (at the arrow), the sponge began a series of arrests of pumping, before a complete arrest was achieved. Pumping was not resumed for some 20 minutes, at which time the sponge started and stopped pumping several times before normal pumping continued. Bar: 5 minutes for both A and B.

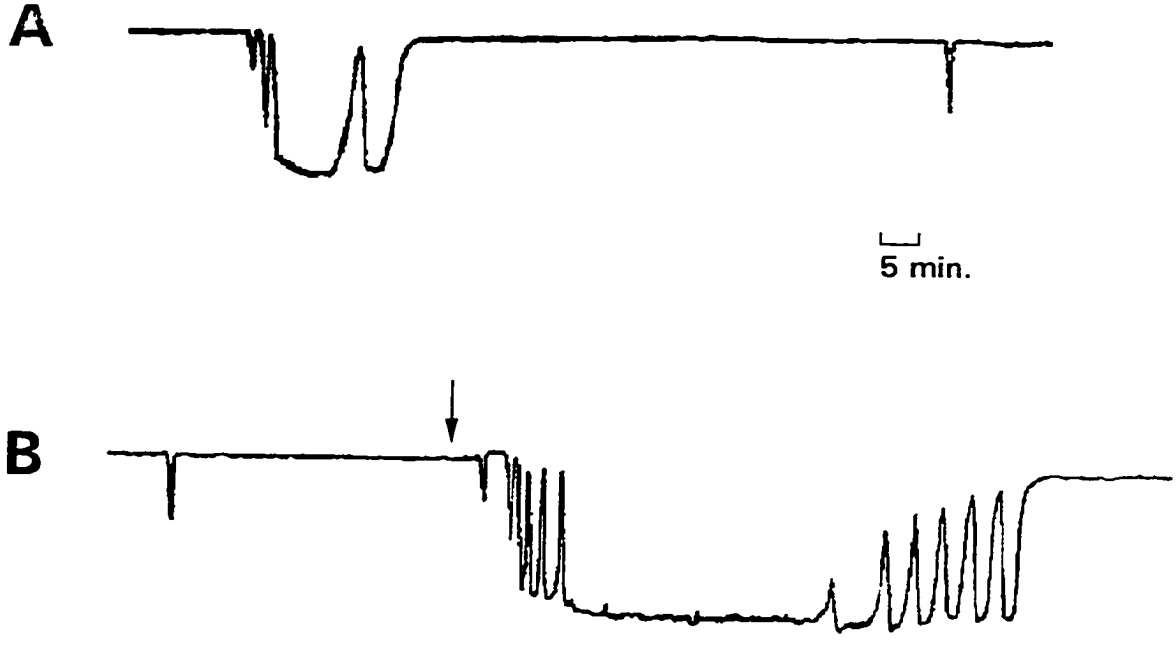
A
5 min.
B

Figure 33. Homografts on *Rhabdocalyptus dawsoni*. Light microscopy. (A) Aggregate grafts (arrowheads) fused on to the atrial side of a piece of the body wall of a sponge. O, osculum. Bar: 0.5 cm. (B) A magnified view of grafts (g) from A, above, showing streams of cytoplasm (arrowheads) flowing into the tissue of the body wall of the 'mother' sponge. Arrows indicate streams of cytoplasm in the trabecula syncytium of the sponge piece. Bar: 0.5 cm.

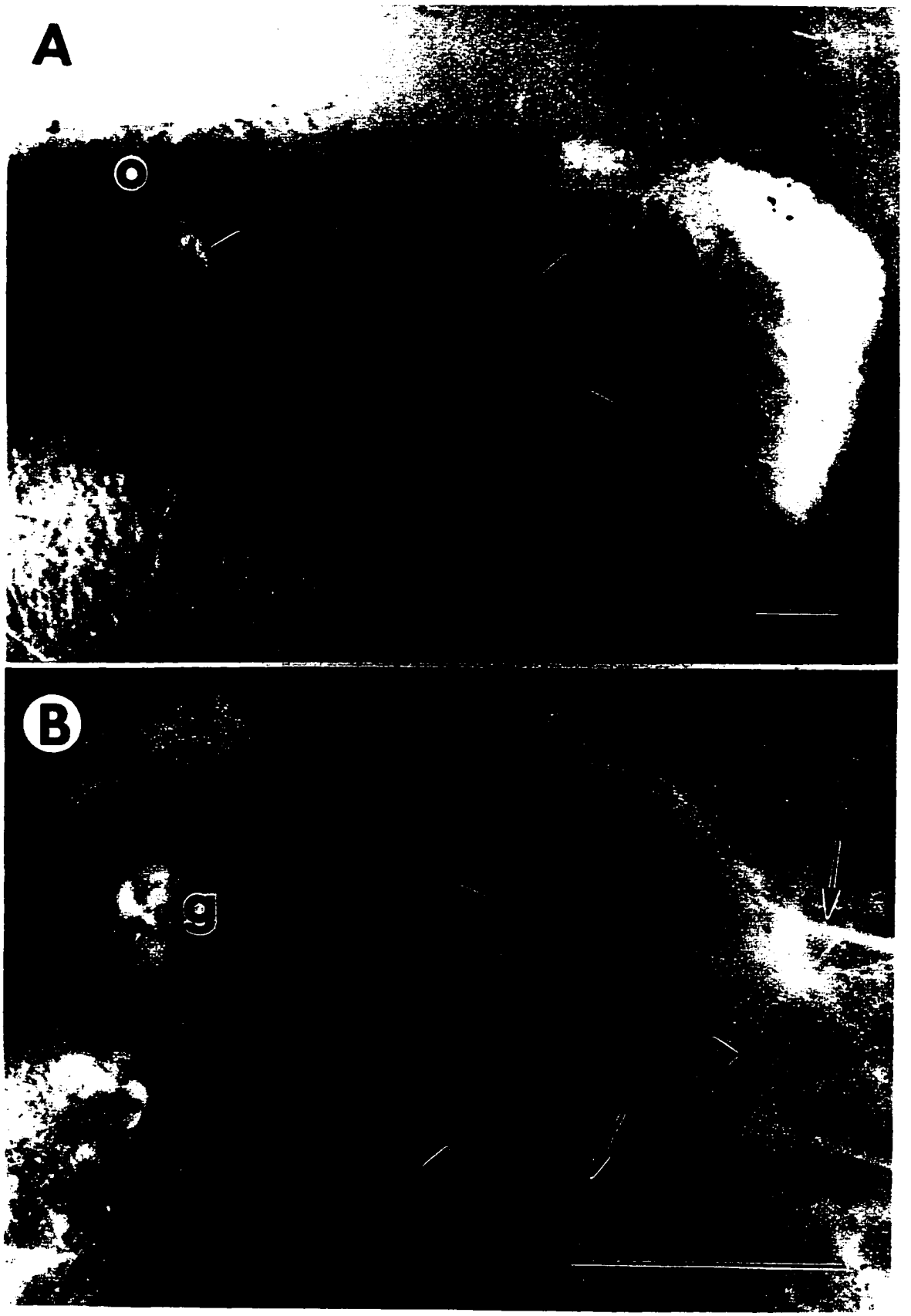
A
B

Figure 34. An action potential in *Rhabdocalyptus dawsoni*. (a) The upper trace shows an action potential and the lower trace shows the simultaneous recording of flow through the atrial wall of the sponge. A stimulus, marked by the asterisk, elicited an action potential which propagated through the sponge, immediately prior to the cessation of water flow through the sponge. The scale refers to the upper tracing of electrical current, and indicates 0.1mV on the vertical axis and 5s for (a) and 10s for (b) on the horizontal axis. (b) A second action potential could be elicited 40 s or longer after a first action potential had already caused the cessation of pumping.

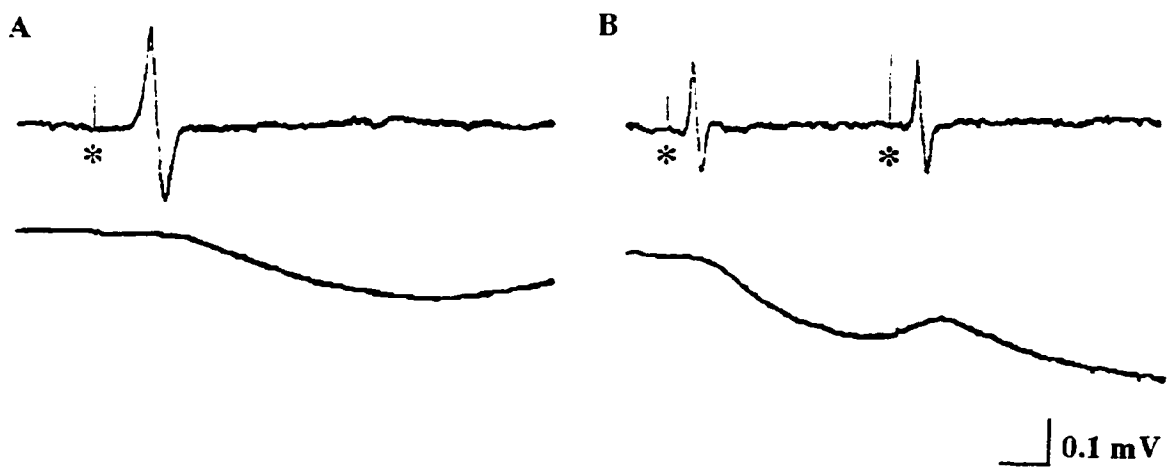
A
B
0.1 mV

DISCUSSION

1. The action potential

The results presented here show the first action potential ever recorded from a sponge. The implications of this are substantial. Firstly, it is clear that the syncytial tissues of *Rhabdocalyptus dawsoni* are able to conduct electrical signals which cause the cessation of the feeding current. In this respect, hexactinellids differ fundamentally from cellular sponges which have neither nerves, which would carry signals over long distances, nor gap junctions between adjacent cells, which would permit the non-nervous propagation of electrical events (Pavans de Ceccatty, 1989). Secondly, the conclusive demonstration that the propagation of electrical signals occurs in sponge tissue has implications for the evolution of excitability in the metazoa.

The rate of propagation of the action potential approaches the velocity of action potential propagation in some invertebrate epithelia (Mackie, 1965; Anderson, 1980) and nerve nets (Mackie and Meech, 1985) and agrees well with the rate of propagation calculated previously for propagated arrests of the feeding current in *Rhabdocalyptus* (Mackie et al., 1983). The slow speed of conduction may be explained in part by the circuitous route an action potential must travel through the tissue, but other factors, including channel density and core resistance would affect conduction velocity, and are at present unknown. The ionic basis of the action

potential has not been explored. Calcium and potassium channels are found in protists, whereas sodium channels first appear in Cnidaria (Hille, 1992). Possibly therefore, we are dealing with a calcium spike. Unfortunately, it was not possible to record with two extracellular electrodes from the preparation which would have allowed us to calculate the rate of propagation of the event more accurately, nor were we able to record intracellularly from the grafts, which would provide the true wave form of the event, undistorted by capacitative coupling.

Attempts to record electrically propagated events from reaggregated tissue using intracellular electrodes both in previous work and during this thesis work have been unsuccessful. The sponge membrane does not seal well around the electrode, so that successful penetrations were achieved fewer than half a dozen times. At these times the membrane potential recorded was about -45 mV, but the seal was not stable for more than a few minutes at most, so information on trans-membrane potential changes of the tissue could not be obtained (Leys, unpublished). The present experiments suggest that coating intracellular electrodes with Con A might be a useful approach.

The propagated action potential is probably independent of the effector, as suggested by the single recording of a propagated action potential during an arrest, which indicates that the tissue is excitable even though the effectors (flagella) are no longer able to respond because they have ceased moving already. Although it has not yet been shown conclusively that flagella cease beating after a stimulus and upon propagation of an action potential, contractions of the atrial and dermal pores do not

occur (data not shown) when the feeding current ceases, ruling out the role of these apertures as effectors. Contraction of the prosopyles - pores in the primary reticulum which supports the flagellated collar bodies and through which water passes into the flagellated chambers - remains possible. However, it is more likely that propagated electrical events cause the entry of calcium into collar bodies causing flagella arrest as in ciliate protozoa (Schmidt and Eckert, 1976; Moss and Tamm, 1987) and the tunicate branchial sac (Mackie et al., 1974). Active pumping of calcium out of the cytoplasm would restore levels to normal, allowing flagella to resume beating.

2. Pumping behaviour

It was assumed in previous work that the sponge uses the arrest to prevent clogging of its incurrent canals in response to increased sediment in the sea water (Mackie et al., 1983), although this hypothesis was not tested at the time. Here it is shown that artificially high levels of sediment introduced into the sea water do cause a complete arrest of the feeding current. The sponge's typical response to a sudden increase in sediment is much like an autonomous arrest. Initially the sponge stops pumping, attempts to pump once again, stops again, and so on, until it gives up altogether for some ten minutes, or until the water appears clear of sediment. The reduced rate of pumping in sponges which had arrested because of sediment suggests that either beating of flagella is hampered by sediment which entered or not all flagella begin beating at once.

The fact that there is no apparent diurnal rhythm to pumping and arrests in sponges kept in flow-through sea water tanks in the dark suggests that the arrest response must be specifically evoked, that is, the arrest response has evolved for a particular purpose. Since *Rhabdocalyptus* is particularly filthy on the exterior, and *Aphrocallistes vastus*, another hexactinellid found in the same habitat in local waters, is completely free of debris, it would be interesting to see if the latter sponge has the same arrest response, despite the unlikely event that the movement of other animals would dislodge sediment clogging its incurrent canals. Nonetheless, all hexactinellids live on sediment-rich substrates which would no doubt occasionally be stirred by the movements of other invertebrates and fish, generating the need for a protective response to clogging of the feeding system. It is possible that in the absence of motile archaeocytes (Mackie and Singla, 1983b), which would carry out cleaning of the canal system in cellular sponges (see Simpson, 1984), an alternative mechanism to prevent clogging has developed. It is probable that the syncytial tissue structure found in all hexactinellids makes them all capable of coordinated propagation of electrical events.

GENERAL DISCUSSION

Due to the deep water habitat of hexactinellid sponges practically all the information we have about these unusual animals comes from preserved specimens. Though we now have a better understanding of the habitat and ecology of hexactinellids from underwater photography, both by SCUBA and submersible on shallow and deep water species respectively, and from *in situ* measurements of feeding (Reiswig, 1990), the only experimental work to use live hexactinellids in the laboratory prior to this study deals with the physiology of *Rhabdocalyptus dawsoni* (Lawn et al., 1981), a species found in relatively shallow waters of British Columbia's fjords. The remarkable results from that study, which demonstrate that hexactinellids are the only sponges that possess a conduction system allowing them to stop their feeding current, shows how productive work on these animals can be. The discovery of another population of hexactinellids in a shallow submarine cave in southern France has also resulted in both *in vivo* and *in vitro* studies of that species (Vacelet and Boury-Esnault, 1994; Perez, 1996). However the general inaccessibility of hexactinellids in most parts of the world, and the difficulties of keeping them in good condition in the laboratory, even in British Columbia, explains why some rather obvious and intriguing questions about the cell biology of these syncytial animals were not followed up until now. The work I have presented in this thesis involves the first use of *in vitro* models to explore aspects of hexactinellid cell biology.

I have described a new method for culturing dissociated sponge tissue which

could be useful if applied to the culture of other marine invertebrate tissues. The mechanism of adhesion is species specific and probably involves calcium dependent adhesion of membrane-bound molecules, possibly carbohydrates or proteoglycans. Adhesion of hexactinellid tissues to natural or commercial substrates improves after wounding, but all individuals adhere poorly during winter months, November through April. From field studies I have been able to determine that the difficulty in obtaining aggregates in the laboratory during these months corresponds to a seasonal regression in which *Rhabdocalyptus* sloughs its outer spicule coat.

During aggregation hexactinellid sponge tissues fuse to form a giant, multinucleate syncytium; fusion of membranes can be observed by video microscopy and exchange of cytoplasm is corroborated by dye exchange. These are the only members of the Porifera which fuse during aggregation. The cytoskeleton of giant syncytial aggregates is quite remarkable. The actin cytoskeleton forms stress fibres across and around the edges of fused syncytia, and bundles of actin microfilaments make up large blunt filopodia which anchor the tissue to the substrate. Large bundles of microtubules weave throughout the tissue, forming the pathways for organelle transport.

Adherent cultures from two species of hexactinellid, *Rhabdocalyptus dawsoni* and *Aphrocallistes vastus*, possess clearly visible streams of bulk cytoplasm in which organelles, including nuclei, flow at rates of ca. 2 $\mu m \cdot s^{-1}$ along microtubule bundles. Cytoplasmic streaming is also visible in regenerating tissue explants, which, because the tissue has not been dissociated, perhaps more accurately reflect the organization

of tissue in whole animals. Western blot analysis shows that the tissue lysate from *Aphrocallistes* contains a protein which crossreacts with antibodies to cytoplasmic dynein but so far no evidence has been found for kinesin. Evidence for a membranous network near microtubule bundles in both species suggests that organelles in bulk cytoplasm are hauled along by the membranous network which presumably tracks along microtubule bundles. There is some indication that organelles may also be linked to microtubules by a network of actin. Similar mechanisms of transporting bulk cytoplasm have been found in characean algae (Kuroda, 1990) and in the multinucleate foraminiferan *Reticulomyxa* (Koonce et al., 1986).

It was also demonstrated both in this study (Chp III), and in a related project (Wyeth et al., 1996), that streams can function in transporting phagocytosed particles. This implies that hexactinellids employ a substantially different mechanism of nutrient distribution from that used by cellular sponges. It is proposed that cytoplasmic streams or cord syncytia, so named by Reiswig (1979a), be considered an identifying character of the Hexactinellida.

Finally, I present records of propagated electrical events that travel through the sponge prior to an arrest of the feeding current in *Rhabdocalyptus*. Although previous work strongly suggested hexactinellids were capable of propagating behaviorally meaningful electrical signals, direct recording of an action potential had not been achieved. By grafting aggregates back on to slabs of the sponge from which they were made, propagated action potentials were recorded after electrical stimuli.

The rate of propagation of electrical impulses, 0.18 $cm \cdot s^{-1}$ in *Rhabdocalyptus*, is approximately one order of magnitude slower than conduction in epithelia (Mackie and Singla, 1983a) and myocyte networks (Mackie and Singla, 1989) of tunicates. The impulse conduction can be explained by the finding that the tissues are syncytial and there are no membrane barriers to be crossed.

Some fundamental questions remain regarding the mechanism of fusion, the site of microtubule nucleation in syncytial cytoplasm, the role of cytoplasmic streaming in regeneration, the developmental potential of syncytial aggregates, and the role of archaeocytes in differentiation. It has yet to be demonstrated that archaeocytes are incapable of motility; if they are non-motile, and if they are not involved in either nutrient distribution or regeneration, the function of archaeocytes in hexactinellid tissue needs to be clarified. Finally, the ionic basis of impulse conduction in hexactinellids needs to be investigated.

The inherent difficulty of working with hexactinellid tissue has prevented me from answering these questions, but I would like to address some of these areas here, including some unpublished results (referred to as author: unpublished), which on their own are insufficient to warrant treatment as a separate chapter.

A) Fusion

During aggregation by dissociated tissues from *Rhabdocalyptus* the syncytium forms by fusion of uni- or multi-nucleate pieces of tissue, not by incomplete cytokinesis.

Whether this mirrors the developmental process is unknown. It is suggested that hexactinellid larvae may be cellular (Boury-Esnault and Vacelet, 1994), although plugged junctions were found between cells in the larvae. Whether the syncytial tissues of the sponge form by fusion of cells in the embryo or whether they arise by incomplete cytokinesis, and similarly produce the cellular components by separating nuclei and cytoplasm with membrane barriers and plugged junctions, is not yet known. There are examples of both kinds of processes in the animal kingdom, some of which (eg. myocyte fusion, viral mediated fusion) are heavily exploited as models for study of membrane fusion (Yanagimachi, 1988; Wakelam, 1988; Frey et al., 1995), and fusion specialists have already expressed great interest in the mechanism of membrane fusion in hexactinellids (Steggeman, personal communication).

From thin section transmission electron microscopy Pavans de Ceccatty and Mackie (1982) and Mackie and Singla (1983b) suggested that the osmiophilic plugged junctions, which separate cellular and syncytial cytoplasm, were formed between the Golgi and the nucleus and transported to the membrane for insertion into a cytoplasmic bridge. Their role, it was suggested, was to allow separation of function in an otherwise syncytial organism. I have no further information on the formation of plugged junctions, and see no reason why this hypothesis is not still correct. Nonetheless, without a clearer picture of how the plugs are formed and inserted into the membrane it is difficult to say whether cellular components are formed from the syncytial tissue, or whether cellular components adhere to and fuse with the syncytial tissue and plugged junctions form in the adjoining membrane afterwards. It would be

very useful to determine what the plugged junction consists of, whether it is related to other intercellular junctions in algae, plants, or animals, and which of these two hypothetical methods of formation is correct.

An interesting observation is that during aggregation of hexactinellid tissues fusion appears to occur between lamellipodia of large, well spread, multinucleated tissues, but not with what appear to be smaller spherical components, which tend to form only thin, elongated pseudopodia. Thin section electron microscopy of the tissue one hour after plating dissociated tissues suggests that the cellular components (archaeocytes, thesocytes, and spherulous cells) never fuse with the multinucleated tissue, except by forming cytoplasmic bridges which may become plugged with perforate junctions (author: unpublished). This implies that the membrane receptors presumed to be involved are retained on these cellular components after dissociation, and allow them to be incorporated into the multinucleated tissue rather than being either rejected or fused with. It would be useful to be able to divide hexactinellid tissue into archaeocyte and multinucleated syncytial fractions so as to examine fusion by both fractions. During earlier efforts to fractionate tissue using Ficoll gradients I found that archaeocytes did not readily separate out. It is possible that dissociated syncytial pieces have the same weight as archaeocytes and that this prevents the separation of these tissue types. Alternatively, regenerating tissue explants may be a better preparation in which to look for mitosis and the formation of new tissues. This question certainly merits further work.

B) Microtubule polarity and MTOCs

Microtubule organizing centres (MTOCs, sometimes known as centrosomes and distinguished by two centrioles) are the hub of microtubule assembly in all eukaryotic cells, anchoring microtubules (MTs) by their slowly growing minus ends to allow the fast growing plus ends to extend outwards into the cell (Joshi, 1993). In adhered aggregates from hexactinellids, centrioles were only seen in archaeocytes and choanoblasts; even using serial thin section transmission electron microscopy none of the nuclei in the multinucleate trabecular syncytium was ever found associated with centrioles (Chapter IV), although it is possible that centrioles exist near microtubule bundles but are inconspicuous. The question is where and how do the microtubules in streaming cytoplasm nucleate? Unlike other multinucleated syncytial organisms, in culture *Rhabdocalyptus* tissue lacks an inherent polarity. There is no cell body as there is in the freshwater foraminiferan *Reticulomyxa*, for example, from which streaming cytoplasm initially emerges giving MTs a uniform polarity (Euteneuer *et al.*, 1989). Nonetheless, MT assembly in *Reticulomyxa* is known to be centrosome independent, and although gamma tubulin - a component common to all MTOC whether in the centrosome or not - shows 72% sequence similarity to other gamma tubulin sequences, the location of gamma tubulin in *Reticulomyxa* has not yet been shown (Kube-Granderath and Schliwa, 1995).

In neurons MTs are nucleated at the cell body and subsequently transported into the neurites (Yu *et al.*, 1993). Consequently there is a strong case for a single

location of MT assembly generating the uniform polarity seen in *Reticulomyxa*. Considering that there is no central cell body in *Rhabdocalyptus*, no such argument can be made about MT assembly or polarity in this sponge. It is possible that the archaeocytes play a central role in organizing the cytoskeleton of syncytial cytoplasm. However, there are areas in the dermal and atrial membranes which apparently are quite distant from any archaeocytes. *Rhabdocalyptus* may have nodes of gamma tubulin randomly distributed throughout the tissue. Determining their location will be pivotal in understanding the organization of hexactinellid tissue. Unfortunately my attempts to obtain antibodies to gamma tubulin, which is not commercially available, were unsuccessful.

A second and vital role of MTOCs is organization of the spindle poles during cell division. As might be expected from the places where centrioles were found, mitosis was only seen in archaeocytes by thin section EM of tissue, and only in tissue from whole animals; no mitotic figures were found in adherent spread aggregates. Since syncytia in some cases fulfil the role of synchronizing development, including synchronization of mitotic divisions of nuclei (eg. *Drosophila* embryos), it might seem possible that nuclei in the trabecular syncytium undergo synchronous division. However, in the case where an archaeocyte was found undergoing mitosis in thin section, none of the other nuclei connected cytoplasmically (i.e. via plugged junctions) were dividing. It is possible that unlike the nuclei of archaeocytes, the trabecular nuclei are terminal and do not divide, or that they divide synchronously, which is why one never sees divisions. A similar case is found in myocytes where the

nuclei do not divide once cells have fused (Wakelam, 1988). It is even possible that the nuclei in trabecular tissues represent nuclear fragments such as those found in cells undergoing apoptosis (Earnshaw, 1995), except that trabecular nuclei in *Rhabdocalyptus* show no signs of degeneration and are consistent in size and contents in all transmission electron microscope observations, and react consistently with the vital dye Hoechst #33342. Certainly this would be an interesting problem to follow up.

C) The role of streams in regeneration

Streams of cytoplasm in adherent aggregates sculpt the preparation over time until fewer and larger streams flow between large hillocks of stationary tissue. Similarly, tissue explants tweezed from the whole animal begin a process of regeneration almost immediately. Rather than withdrawing from wounded areas, new tissue begins to stream out along torn spicule edges and within 12-24 hours has formed an outer membrane around the entire spicule preparation (Leys and Mackie, 1994). Wyeth et al. (1996) note that early regenerating tissue explants have far more streams than later preparations, which suggests that streams play a vital role in the regeneration of wounded tissue and the formation of the outer membrane which reestablishes the boundary of the tissue with the outside environment. Such pieces can continue in time to develop a new osculum, in essence becoming a functional sponge (Leys, unpublished).

Streaming may also be central to ongoing remodelling in whole animals. Both *Rhabdocalyptus* and *Aphrocallistes* possess inner membranes in a portion of their flagellated chambers. This membrane reaches down and joins with the secondary reticulum, and can even enclose the flagella in pockets, apparently blocking the flow of water. Specimens kept in laboratory aquaria for periods of several weeks lack a secondary reticulum. Instead the inner membrane joins with the primary reticulum, compartmentalizing each collar in what appear to be former flagellated chambers (author: unpublished).

Between 6 and 10 percent of flagellated chambers of sponges fixed immediately upon collection contain inner membranes (author: unpublished); the same percentage found occupied by central cells in demosponges. The increase in the number of chambers with inner membranes when animals are kept in aquaria for several weeks prior to fixation seems to indicate that the membranes in hexactinellids may remodel chambers when either flow patterns are changed or food resources are limited. The proposed formation of an inner membrane during remodelling in *Rhabdocalytpus* is diagrammed in Fig 35. Cytoplasmic streaming no doubt plays an essential role in the remodelling process. The function of central cells in remodelling demosponge flagellated chambers needs to be investigated before one can comment on the functional similarity of these structures in all Porifera.

Figure 35. An illustration of the hypothesized formation of the secondary reticulum and inner membrane in flagellated chambers of hexactinellid sponges. (A) Collar bodies with no secondary reticulum. (B) Collar bodies with a secondary reticulum, part of the trabecular syncytium which extends up from the primary reticulum. (C) An inner membrane extends down to join the secondary reticulum surrounding the microvilli of collar bodies. (D) Collars and flagella are completely engulfed by the inner membrane/secondary reticulum and are only visible within pockets of membrane. Collar body (cb), choanoblast (chb), primary reticulum (1^{o}r), secondary reticulum (2^{o}r), trabecular syncytium (shaded region), inner membrane (im), flagellum (f), microvilli (mv), collagen (co).

Figure 35. An illustration of the hypothesized formation of the secondary reticulum and inner membrane in flagellated chambers of hexactinellid sponges. (A) Collar bodies with no secondary reticulum. (B) Collar bodies with a secondary reticulum, part of the trabecular syncytium which extends up from the primary reticulum. (C) An inner membrane extends down to join the secondary reticulum surrounding the microvilli of collar bodies. (D) Collars and flagella are completely engulfed by the inner membrane/secondary reticulum and are only visible within pockets of membrane. Collar body (cb), choanoblast (chb), primary reticulum (1^{o}r), secondary reticulum (2^{o}r), trabecular syncytium (shaded region), inner membrane (im), flagellum (f), microvilli (mv), collagen (co).

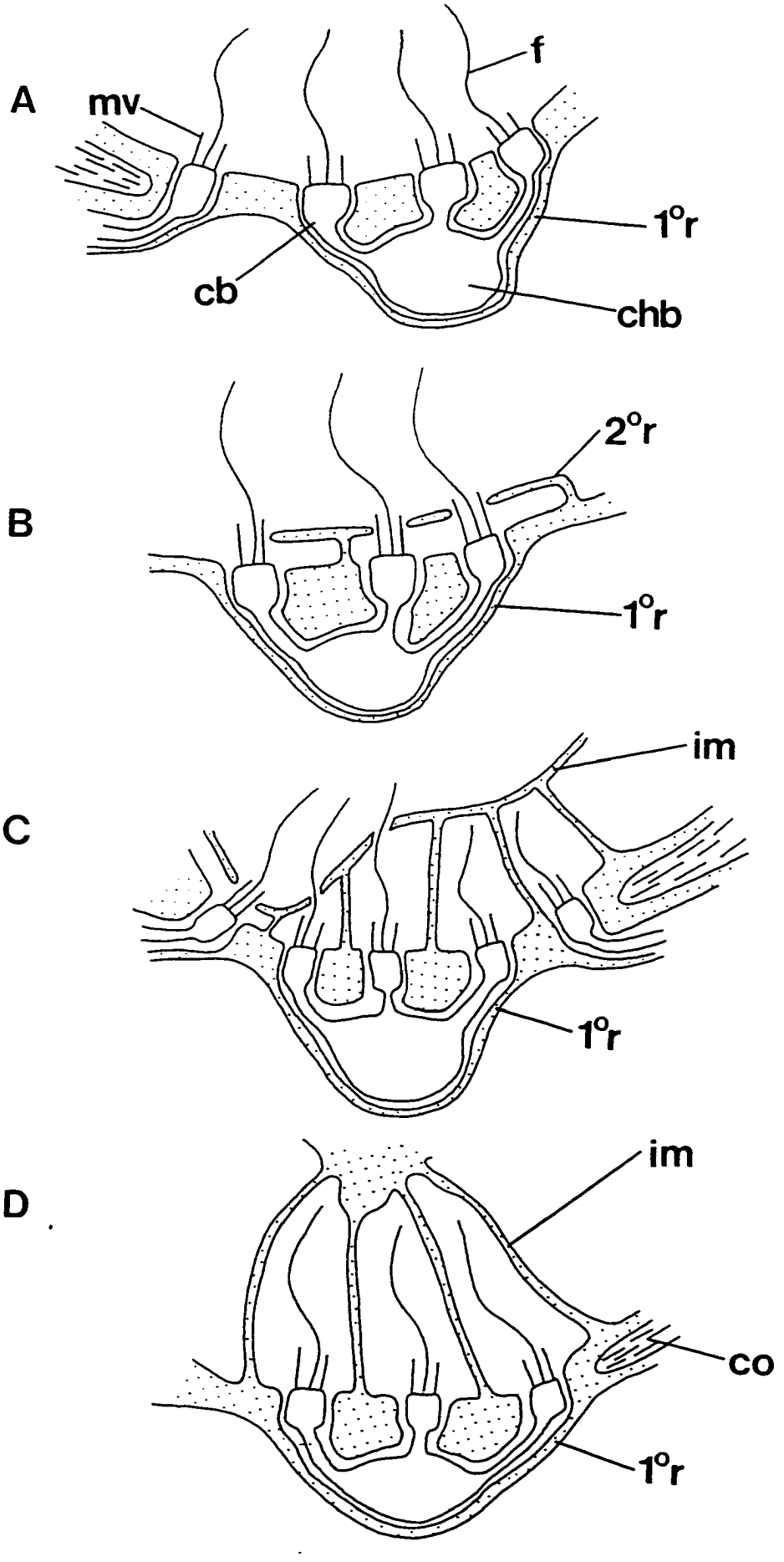
A
mv
f
1°r
cb
chb
B
2°r
1°r
C
im
1°r
D
im
co
1°r

D) The role of archeocytes in hexactinellid sponges

In cellular sponges archaeocytes are totipotent; some develop into germ cells for reproduction, and others become amoeboid to transfer nutrients to other parts of the sponge. Preliminary results from a study of paraffin sections from *Rhabdocalyptus* fixed monthly through the year support earlier observations from other hexactinellids (Ijima, 1904; Boury-Esnault and Vacelet, 1994) that congeries of archaeocytes also develop into germ cells in hexactinellids (author: unpublished). However, there is no indication that archaeocytes are motile (although occasionally it appears that they can be transported within streams in aggregates), which again suggests they are not the means of nutrient transport in these sponges.

Archaeocytes also appear to be the only cellular components of the hexactinellid tissue that undergo cell division (author: unpublished). Whereas Brien (1937) proposed that dissociated sponge cells retained their identity during aggregation, other researchers observed that some cell types disappeared during reaggregation and were reformed from archaeocytes (Borojevic and Levi, 1964; Bagby, 1972). Buscema and others (1980) demonstrated definitively that whole sponges could regenerate from preparations of purified archaeocytes, and that this cell type alone was capable of regenerating other sponge cells.

I have attempted to culture hexactinellid sponges from aggregates over the last four years by rearing aggregates in sterile sea water (0.45μm millipore filtered) that was changed daily, with and without antibiotics, under both light and dark conditions,

and by keeping them in darkened tanks in unfiltered sea water brought in from 20m depth at the Bamfield Marine Station. Only twice did I manage to have aggregates develop into a small sponge with a distinct dermal membrane and osculum from which a flow of water was visible (author: unpublished). The majority of aggregates kept in unfiltered sea water survive for up to two weeks before dying, which is similar to the results of Pavans de Ceccatty (1982). Those aggregates kept in filtered sea water survived much longer, some for up to 2 months, but without further development. It is possible that development requires a critical number of archaeocytes, as shown to be the case for cellular sponges (Buscema et al. 1980).

Video microscopy suggests archaeocytes play a passive role in aggregation. They are drawn into the centre of aggregating tissues and the syncytial cytoplasm is responsible for finding other tissue pieces, for fusion, and ultimately for expansion of the aggregate. However, presumably growing streams require a growing number of microtubules, and it is possible that the centrally located archaeocytes serve the role of tubulin producers. Aggregation experiments using purified archaeocyte preparations would certainly be worth conducting with hexactinellid tissue.

E) Impulse conduction in *Rhabdocalyptus dawsoni*

The ability to record electrically propagated events from aggregate grafts suggests that the grafts are fused with the syncytial tissues which are the pathways for conduction. However, if the graft membrane is excitable then it seems that one

should be able to record from detached aggregates, unless the ion channels are in an inactive state, or perhaps are not abundant enough. The inability to record from detached aggregates seems to imply that only when the aggregate is on a physiologically active piece of sponge and fusion of membranes between graft and sponge piece occurs are channels activated or developed.

In Chapter V I suggested that impulse propagation may be by way of a calcium spike because sodium channels first appear in the Cnidaria. However, a thorough search for sodium channels in the Porifera has not been conducted. Furthermore, it is always assumed that cellular sponges are incapable of impulse conduction because they lack gap junctions or similar aqueous channels connecting adjacent cells. Records of propagated contractile responses as fast or faster than conduction in *Rhabdocalyptus* have recently been brought to my attention (Reiswig, 1979b). The mechanism of these responses requires investigation before other Porifera are declared incapable of electrically propagated events.

What does this say about the evolution of excitability in the metazoa? Firstly, the Porifera are well established as metazoans based on developmental, morphological, and molecular data from demosponges. Similar data needs to be collected for the Hexactinellida so as to firmly include this subphylum within the metazoa. Secondly, propagated action potentials are also known from plants and protists (see Mackie, 1970), but until we know the ionic basis of propagation in *Rhabdocalyptus* we cannot compare it with these systems. Since epithelial conduction has evolved independently many times in the metazoa, it in itself is not an indication

of either a primitive or advanced condition. However, now that it is clear hexactinellid sponges are capable of propagating electrical events, by determining the ionic basis of propagation and the structure of the voltage activated ion channels in these sponges we will be able to better understand the evolution of excitability in the metazoa.

REFERENCES

Adams, R.J., Pollard, T.D., 1986. Propulsion of organelles isolated from *Acanthamoeba* along actin filaments by myosin-I. Nature 322:754-756.

Alberts, B., Bray, D., Lewis, J., Raff, M., Roberts, K., Watson, J.D., 1989. Molecular biology of the cell. Garland Publishing, Inc., New York.

Allen, R.D., Metuzals, J., Tasaki, I., Brady, S.T., Gilbert, S.P., 1982. Fast axonal transport in squid giant axon. Science 218:1127-1129.

Allen, R.D., Allen, N.S., Travis, J.L., 1981. Video-enhanced contrast, differential interference contrast (AVEC-DIC) microscopy: A new method capable of analyzing microtubule-related motility in the reticulopodial network of *Allogromia laticollaris*. Cell Motility 1:291-302.

Anastasi, A., Hunt, C., Stebbings, H., 1990. Isolation of microtubule motors from an insect ovarian system: characterization using a novel motility substratum. J. Cell Sci. 96:63-69.

Anderson, P.A.V., 1980. Epithelial conduction: its properties and functions. Progress in Neurobiology 15:161-203.

Atkinson, S.J., Doberstein, S.K., Pollard, T.D., 1992. Moving off the beaten track. Current Biology 2:326-328.

Auzouz, S., Domart-Coulon, I., Doumenc, D., 1993. Gill cell cultures of the butterfish clam *Ruditapes decussatus*. J. Mar. Biotechnol. 1:79-81.

Bagby, R.M., 1972. Formation and differentiation of the upper pinacoderm in reaggregation masses of the sponge *Microciona prolifera* (Ellis and Solander). J. Exp. Zool. 180:217-244.

Bailey, G.B., Day, D.B., McCoomer, N.E., 1992. *Entamoeba* motility: dynamics of cytoplasmic streaming, locomotion and translocation of surface-bound particles, and organization of the actin cytoskeleton in *Entamoeba invadens*. J. Protozoology 39:267-272.

Bearer, E.L., DeGiorgis, J.A., Bodner, R.A., Kao, A.W., Reese, T.S., 1993. Evidence for myosin motors on organelles in squid axoplasm. Proc. Natl. Acad. Sci. USA 90:11252-11256.

Bergquist, P.R., 1978. Sponges. Hutchinson and Co., London.

Bidder, G.P., 1929. Sponges. Encylopaedia Britannica 14th edn:254-261.

Bond, C., 1992. Continuous cell movements rearrange anatomical structures in intact sponges. J. Exp. Zool. 263:284-302.

Bond, C., Harris, A.K., 1988. Locomotion of sponges and its physical mechanism. J. Exp. Zool. 246:271-284.

Borojevic, R., Levi, C., 1964. Etude au microscope électronique des cellules de l'éponge *Ophlitaspongia seriata* (Grant) au cours de la réorganisation après dissociation. Z. Zellforsch. Mikrosk. Anat. 64:708-725.

Boury-Esnault, N., De Vos, L., 1988. *Caulophacus cyanae*, n. sp., une éponge hexactinellide des sources hydrothermales. Biogéographie du genre *Caulophacus* Schulze, 1887. Oceanologica acta 8:51-60.

Boury-Esnault, N., Vacelet, J., 1994. Preliminary studies on the organization and development of a hexactinellid sponge from a Mediterranean cave, *Oopsacas minuta*. *In*: Sponges in Time and Space, van Soest, R.W.M., van Kempen, T.M.G., Braekman, J. (eds.), AA Balkema, Rotterdam, pp. 407-416.

Bowser, S.S., Rieder, C.L., 1985. Evidence that cell surface motility in *Allogromia* is mediated by cytoplasmic microtubules. Can. J. Biochem. Cell Biol. 63:608-620.

Bowser, S.S., Travis, J.L., Bieder, C.L., 1988. Microtubules associate with actin-containing filaments at discrete sites along the ventral surface of *Allogromia* reticulopods. J. Cell Sci. 89:297-307.

Boyd, I., 1981. The spicule jungle of *Rhabdocalyptus dawsoni*: a unique microhabitat, B.Sc. thesis, University of Victoria, Victoria, B.C.

Bradley, M.O., 1973. Microfilaments and cytoplasmic streaming: inhibition of streaming with cytochalasin. J. Cell Sci. 89:297-307.

Brady, S.T., 1985. A novel brain ATPase with properties expected for the fast axonal transport motor. Nature 317:73-75.

Brady, S.T., Lasek, R.J., Allen, R.D., 1985. Video microscopy of fast axonal transport in extruded axoplasm: a new model for study of molecular mechanisms. Cell Motility 5:81-101.

Brady, S.T., Lasek, R.J., Allen, R.D., Yin, H.L., Stossel, T.P., 1984. Gelsolin inhibition of fast axonal transport indicates a requirement for actin microfilaments. Nature 310:56-58.

Bray, D., 1992. Cell Movements. Garland Publishing Inc., New York.

Brien, P., 1937. La réorganisation de l'éponge après dissociation par filtration et phénomènes d'involution chez *Ephydatia fluviatilis*. Archives de Biologie 48:185-268.

Brondstead, H.V., 1953. The ability to differentiate and the size of regenerated cells after repeated regeneration in *Spongilla lacustris*. Q. J. Micr. Sci. 94:177-184.

Burlando, B., Gaino, E., Marchisio, P.C., 1984. Actin and tubulin in dissociated sponge cells. Evidence for peculiar actin-containing microextensions. Eur. J. Cell Biol. 35:317-321.

Buscema, M., De Sutter, D., Van de Vyver, G., 1980. Ultrastructural study of differentiation processes during aggregation of purified sponge archaeocytes. Wilhelm Roux's Archives 188:45-53.

Clark, T.G., Rosenbaum, J.L., 1982. Pigment translocation in detergent-permeabilized melanophores of *Fundulus heteroclitus*. Proc. Natl. Acad. Sci. USA 79:4655-4659.

Conrad, J., Diehl-Seifert, B., Zahn, R.K., Uhlenbruck, G., Zimmermann, E., Müller, W.E.G., 1982. Fibronectin is apparently not involved in species-specific reaggregation of cells from the marine sponge *Geodia cydonium*. J. Cell Biochem 19:395-404.

Coombe, D.R., Jakobsen, K.B., Parish, C.R., 1987. A role for sulfated polysaccharide recognition in sponge cell aggregation. Exptl. Cell Res. 170:381-401.

Curtis, A.S.G., 1962. Pattern and mechanism in the reaggregation of sponges. Nature 196:245-248.

Day, R.M., Lenhoff, H.M., 1981. Hydra mesoglea: a model for investigating epithelial cell-basement membrane interactions. Science 211:291-294.

Dayton, P.K., 1979. Observations of growth, dispersal and population dynamics of some sponges in McMurdo Sound, Antarctica. Colloques internationaux du C.N.R.S. Biologie des spongiares, 291:271-282.

Droz, B., Rambourg, A., Koenig, H.L., 1975. The smooth endoplasmic reticulum: structure and role in the renewal of axonal membrane and synaptic vesicles by fast axonal transport. Brain Res. 93:1-13.

Earnshaw, W.C., 1995. Nuclear changes in apoptosis. Curr. Op. Cell Biol. 7:337-343.

Euteneuer, U., Haimo, L.T., Schliwa, M., 1989. Microtubule bundles of *Reticulomyxa* networks are of uniform polarity. Eur. J. Cell Biol. 49:373-376.

Euteneuer, U., Koonce, M.P., Pfister, K.K., Schliwa, M., 1988. An ATPase with properties expected for the organelle motor of the giant amoeba, *Reticulomyxa*. Nature 332:176-178.

Evans, C.W., Bergquist, P.R., 1974. Initial cell contact in sponge aggregates. J. Microscopie 21:185-188.

Forman, D.S., Brown, K.J., Livengood, D.R., 1983. Fast axonal transport in permeabilized lobster giant axons is inhibited by vanadate. J. Neurosci. 3:1279-1288.

Fraser, C.M., 1932. A comparison of the marine fauna of the Nanaimo region with that of the San Juan Archipelago. Trans. Roy. Soc. Canada 26:49-70.

Frey, S., Marsh, M., Gunther, S., Pelchen-Matthews, A., Stephens, P., Ortlepp, S., Stegmann, T., 1995. Temperature dependence of cell-cell fusion induced by the envelope glycoprotein of Human Immunodeficiency Virus Type I. J. Virology 69:1462-1472.

Fukui, Y., Lynch, T.J., Brzeska, H., Korn, E.D., 1989. Myosin I is located at the leading edges of locomoting *Dictyostelium* amoebae. Nature 341:328-331.

Gaino, E., Magnino, G., Burlando, B., Sara, M., 1993. Morphological responses of dissociated sponge cells to different organic substrata. Tissue and Cell 25:333-341.

Gaino, E., Burlando, B., Sabatini, M., Buffa, P., 1985a. Cytoskeleton and morphology of dissociated sponge cells. A whole-mount and scanning electron microscopic study. Eur. J. Cell Biol. 39:328-332.

Gaino, E., Zunino, L., Burlando, B., Sara, M., 1985b. The locomotion of dissociated sponge cells: a cell-by-cell, time-lapse film analysis. Cell Motility 5:463-474.

Garrone, R., Lethias, C., Escaig, J., 1980. Freeze-fracture study of sponge cell membranes and extracellular matrix. Preliminary results. Biol. Cellulaire 38:71-74.

Gerrodette, T., Flechsig, A.O., 1979. Sediment-induced reduction in the pumping rate of the tropical sponge Verongia lacunosa. Mar. Biol. 55:103-110.

Goldberg, D.J., Harris, D.A., Lubit, B.W., Schwartz, J.H., 1980. Analysis of the mechanism of fast axonal transport by intracellular injection of potential inhibitory macromolecules: evidence for a possible role of actin filaments. Proc. Natl. Acad. Sci. USA 772:7448-7452.

Goldstein, L.S.B., 1991. The kinesin superfamily: tails of functional redundancy. Trends in Cell Biology 1:93-98.

Golz, R., Hauser, H., 1994. Spatially separated classes of microtubule bridges in the reticulopodial network of *Allogromia*. Evidence for a dynein-like ATPase in the filopodial cytoskeleton. Europ. J. Protistol. 30:221-226.

Grölig, F., Williamson, R.E., Parke, J., Miller, C., Anderton, B.H., 1988. Myosin and Ca^{2+}-sensitive streaming in the alga *Chara*: detection of two polypeptides reacting with a monoclonal anti-myosin and their localization in the streaming endoplasm. Eur. J. Cell Biol. 47:22-31.

Haimo, L.T., Thaler, C.D., 1994. Regulation of organelle transport: lessons from color change in fish. BioEssays 16:727-733.

Harris, P., Shaw, G., 1984. Intermediate filaments, microtubules and microfilaments in epidermis of sea urchin tube foot. Cell Tissue Res. 236:27-33.

Harrison, F.W., 1972. The nature and role of the basal pinacoderm of *Corvomeyenia carolinensis* Harrison (Porifera: Spongillidae). Hydrobiologia 39:495-508.

Hasegawa, T., Takahashi, S., Hayashi, H., Hatano, S., 1980. Fragmin: a calcium ion sensitive regulatory factor on the formation of actin filaments. Biochemistry 19:2677-2683.

Hay, E.D., 1981. Cell biology of the extracellular matrix. Plenum Press, New York.

Hille, B., 1984. Ion channels., .

Hirokawa, N., 1982. Cross-linker system between neurofilaments, microtubules, and membranous organelles in frog axons revealed by the quick-freeze, deep-etching method. J. Cell Biol. 94:129-142.

Hirokawa, N., Sato-Yoshitake, R., Kobayashi, N., Pfister, K.K., Bloom, G.S., Brady, S.T., 1991. Kinesin associates with anterogradely transported membranous organelles in vivo. J. Cell Biol. 114:295-302.

Humphreys, T., 1963. Chemical dissolution and in vitro reconstitution of sponge cell adhesions. I. Isolation and functional demonstration of the components involved. Dev. Biol. 8:27-47.

Hyman, L.H., 1940. The Invertebrates. McGraw-Hill, New York.

Ijima, I., 1904. Studies on the Hexactinellida. Contribution IV. (Rossellidae). J. Coll. Sci. imp. Univ. Tokyo 28:13-307.

Ijima, I., 1901. Studies on the Hexactinellida. Contribution I (Euplectellidae). J. Coll.

Sci. imp. Univ. Tokyo 15:1-299.

Imsieke, G., 1994. Ingestion and digestion of *Chlamydomonas reinhardtii* (Volvocales) by the freshwater sponge *Spongilla lacustris* (Spongillidae). *In*: Sponges in Time and Space, van Soest, R.W.M., van Kempen, T.M.G., Braekman, J.-C. (eds.), A.A. Balkema, Rotterdam, pp. 371-376.

Ingold, A.L., Cohn, S.A., Scholey, J.M., 1988. Inhibition of kinesin-driven microtubule motility by monoclonal antibodies to kinesin heavy chains. J. Cell Biol. 107:2657-2667.

Jablonsky, P.P., Hagan, R.P., Grölig, F., Williamson, R.E., 1990. Immunolocalization of Hara calmodulin and the reversibility of cytoplasmic streaming by calcium. *In*: Calcium in plant growth and development, Leonard, R.T., Hepler, P.K. (eds.),,, .

Janson, L.W., Taylor, D.L., 1993. In vitro models of tail contraction and cytoplasmic streaming in amoeboid cells. J. Cell Biol. 123:345-356.

Joshi, H.C., 1993. Gamma tubulin: the hub of cellular microtubule assemblies. BioEssays 15:637-643.

Kachar, B., Reese, T.S., 1988. The mechanism of cytoplasmic streaming in characean algal cells: sliding of endoplasmic reticulum along actin filaments. J. Cell Biol. 106:1545-1552.

Kachar, B., Albanesi, J.P., Fujisaki, H., Korn, E.D., 1987. Extensive purification from *Acanthamoeba castellanii* of a microtubule-dependent translocator with microtubule-activated magnesium ATPase activity. J. Biol. Chem. 262:16180-16185.

Karnaky, K.J., Garretson, L.T., O'Neil, R.G., 1992. Video-enhanced microscopy of organelle movement in an intact epithelium. J. of Morphology 213:21-31.

Kashina, A.S., Baskin, R.J., Cole, D.G., Wedaman, K.P., Saxton, W.M., Scholey, J.M., 1996. A bipolar kinesin. Nature 379:270-272.

Kilian, E.F., 1952. Wasserströmung und Nahrungsaufnahme beim Süssvasserschwamm *Ephydatia fluviatilis*. Anschr. f. vergleich. Physiology 34:407-447.

Killisch, H., Beug, H., Wiche, G., Steffen, W., 1995. Characterization of cytoplasmic dynein in differentiating chicken erythroblasts. Eur. J. Cell Biol. Supplement:191a.

Kirfel, D., Stockem, W., 1995. Microtubule motor proteins of both the kinesin and the cytoplasmic dynein families are present in pinacocytes of fresh water sponges. Eur. J. Cell Biol. Supplement:197a.

Kohno, T., Shimmen, T., 1988. Accelerated sliding of pollen tube organelles along Characeae actin bundles regulated by calcium. J. Cell Biol. 106:1539-1543.

Komnick, H., Stockem, W., Wohlfarth-Botterman, K.E., 1973. Cell motility: mechanisms in protoplasmic streaming and amoeboid movement. Int. Rev. Cytol. 34:169-253.

Koonce, M.P., Schliwa, M., 1986. Reactivation of organelle movements along the cytoskeletal framework of a giant freshwater amoeba. J. Cell Biol. 103:605-612.

Koonce, M.P., Euteneuer, U., McDonald, K.L., Menzel, D., Schliwa, M., 1986. Cytoskeletal architecture and motility in a giant freshwater amoeba, *Reticulomyxa*. Cell Motil. Cytoskeleton 6:521-533.

Korotkova, G.P., 1963. On the types of restoration processes in sponges. Acta biol. Hung. 13:389-406.

Kube-Granderath, E., Schliwa, M., 1995. Gamma tubulin of *Reticulomyxa filosa*: amino acid sequence and expression in bacteria. Eur. J. Cell Biol. Supplement:199a.

Kuroda, K., 1990. Cytoplasmic streaming in plant cells. Int. Rev. Cytol. 121:267-307.

Kuznetsov, S.A., Gelfand, V.I., 1986. Bovine brain kinesin is a microtubule-activated ATPase. Proc. Natl. Acad. Sci. USA 183:8530-8534.

Kuznetsov, S.A., Rivera, D.T., Weiss, D.G., Langford, G.M., 1993. Activation and stabilization of actin-dependent organelle motility by calmodulin. Mol. Biol. Cell 4:275a.

Kuznetsov, S.A., Langford, G.M., Weiss, D.G., 1992. Actin-dependent organelle movement in squid axoplasm. Nature 356:722-725.

La Barbara, Vogel, S., 1976. An inexpensive thermistor flowmeter for aquatic biology. Limnol. Oceanogr. 71:750-756.

Labat-Robert, J., Robert, L., Auger, C., Lethias, C., Garrone, R., 1981. Fibronectin-like protein in Porifera: its role in cell aggregation. Proc. Natl. Acad. Sci. USA 78:6261-6265.

Lancelle, S.A., Cresti, M., Hepler, P.K., 1987. Ultrastructure of the cytoskeleton in freeze-substituted pollen tubes of *Nicotiana alata*. Protoplasma 140:141-150.

Langenbruch, P., Jones, W.C., 1989. A new type of central cell in the choanocyte chambers of *Pellina fistulosa* (Porifera, Demospongiae). Zoomorphology 109:11-14.

Laurent, T.C., Fraser, J.R., 1992. Hyaluronan. The FASEB journal 6:2397-2404.

Lawn, I.D., Mackie, G.O., Silver, G., 1981. Conduction system in a sponge. Science 211:1169-1171.

Lees-Miller, J.P., Helfman, D.M., Schroer, T.A., 1992. A vertebrate actin-related protein is a component of a multisubunit complex involved in microtubule-based vesicle motility. Nature 359:244-246.

Leys, S.P., 1995. Cytoskeletal architecture and organelle transport in giant syncytia formed by fusion of hexactinellid sponge tissues. Biol. Bull. 188:241-254.

Leys, S.P., Mackie, G.O., 1994. Cytoplasmic streaming in the hexactinellid sponge *Rhabdocalyptus dawsoni* (Lambe 1873). *In*: Sponges in Time and Space, van Soest, R.W.M., van Kempen, T.M.G., Braekman, J. (eds.), AA Balkema, Rotterdam, pp. 417-423.

Lillie, S.H., Brown, S.S., 1992. Suppression of a myosin defect by a kinesin-related gene. Nature 356:358-361.

Lippincott-Schwartz, J., Cole, N.B., Marrota, A., Conrad, P.A., Bloom, G.S., 1995. Kinesin is the motor for microtubule-mediated golgi-to-ER membrane traffic. J. Cell Biol. 128:293-306.

Loewenstein, W.R., 1967. On the genesis of cellular communication. Dev. Biol. 15:503-520.

Mackie, G.O., 1984. Introduction to the diploblastic level. *In*: Biology of the integument, Bereiter-Hahn, J., Matoltsy, A.G., Richards, K.S. (eds.), Springer-Verlag, Berlin, pp. 43-46.

Mackie, G.O., 1981. Plugged syncytial interconnections in hexactinellid sponges. J. Cell Biol. 91:103a.

Mackie, G.O., 1979. Is there a conduction system in sponges. Colloques int. Cent. natn. Res. Scient. Biologie des spongiares, 291:145-151.

Mackie, G.O., 1970. Neuroid conduction and the evolution of conducting tissues. Quart. Rev. Biol. 45:319-332.

Mackie, G.O., 1965. Conduction in the nerve-free epithelia of siphonophores. Amer. Zool. 5:439-453.

Mackie, G.O., Meech, R.W., 1985. Separate sodium and calcium spikes in the same

axon. Nature 313:791-793.

Mackie, G.O., Singla, C.L., 1987. Impulse propagation and contraction in the tunic of a compound ascidian. Biol. Bull. 173:188-204.

Mackie, G.O., Singla, C.L., 1983a. Coordination of compound ascidians by epithelial conduction in the colonial blood vessels. Biol. Bull. 165:209-220.

Mackie, G.O., Singla, C.L., 1983b. Studies on hexactinellid sponges. I Histology of *Rhabdocalyptus dawsoni* (Lambe, 1873). Phil. Trans. R. Soc. Lond. B 301:365-400.

Mackie, G.O., Lawn, I.D., Pavans de Ceccatty, M., 1983. Studies on hexactinellid sponges. II. Excitability, conduction and coordination of responses in *Rhabdocalyptus dawsoni* (Lambe 1873). Phil. Trans. R. Soc. Lond. B 301:401-418.

Mackie, G.O., Paul, D.H., Singla, C.M., Sleigh, M.A., Williams, D.E., 1974. Branchial innervation and ciliary control in the ascidian *Corella*. Proc. R. soc. Lond. B 187:1-35.

Marliave, J.B., 1992. Environmental Monitoring through natural history research. Can. Tech. Rep. Fish Aquat. Sci. 1879:199-209.

McClay, D.R., 1971. An autoradiographic analysis of the species specificity during sponge cell reaggregation. Biol. Bull. 141:319-330.

Menzel, D., 1994. Dynamics and pharmacological perturbations of the endoplasmic reticulum in the unicellular green alga *Acetabularia*. Eur. J. Cell Biol. 64:113-119.

Menzel, D., 1987. The cytoskeleton of the giant green alga *Caulerpa* visualized by immunocytochemistry. Protoplasma 139:71-76.

Menzel, D., Elsner-Menzel, C., 1989. Actin-based chloroplast rearrangements in the cortex of the giant coenocytic alga *Caulerpa*. Protoplasma 150:1-8.

Miller, D.D., Callaham, D.A., Gross, D.J., Hepler, P.K., 1992. Free calcium gradient in growing pollen tubes of *Lilium*. J. Cell Sci. 101:7-12.

Misevic, F.N., Burger, M.M., 1993. Carbohydrate-carbohydrate interactions of a novel acidic glycan can mediate sponge cell adhesion. J. Biol. Chem. 268:4922-4929.

Mita, M., Ueta, N., Nagahama, Y., 1988. Effect of gonad-stimulating substance on cyclic AMP production and 1-methyladenine secretion in starfish follicle cells. *In*: Invertebrate and Fish Tissue Culture, Kuroda, Y., Kurstak, E., Maramorosch, K. (eds.), Springer-Verlag, Berlin, pp. 68-71.

Mitchell, D.R., Warner, F.D., 1981. Binding of dynein 21 S ATPase to microtubules. Effects of ionic conditions and substrate analogs. J. Biol. Chem. 256:12535-12544.

Moscona, A.A., 1968. Cell aggregation: properties of specific cell-ligands and their role in the formation of multicellular systems. Dev. Biol. 18:250-277.

Moss, A.G., Tamm, S.L., 1987. A calcium regenerative potential controlling ciliary reversal is propagated along the length of the ctenophore comb plates. Proc. Natl. Acad. Sci. USA 84:6476-6480.

Müller, W.E.G., 1982. Cell membranes in sponges. Int. Rev. Cytol. 77:126-181.

Müller, W.E.G., Diehl-Seifert, B., Gramzow, M., Friese, U., Renneisen, K., Schroder, H.C., 1988. Interaction between extracellular adhesion proteins and extracellular matrix in reaggregation of dissociated sponge cells. Int. Rev. Cytol. 111:211-229.

Naganuma, T., Degnan, B.M., Horikoshi, K., Morse, D.E., 1994. Myogenesis in primary cell cultures from larvae of the abalone, *Haliotis rufescens*. Mol. Mar. Biol. Biotechnol. 3:131-140.

Nedergaard, M., 1994. Direct signaling from astrocytes to neurons in cultures of mammalian brain cells. Science 263:1768-1771.

Noble, P.B., Peterson, S.C., 1972. A two-dimensional random-walk analysis of aggregating sponge cells prior to cell contact. Exptl. Cell Res. 75:288-290.

Nobling, R., Reiss, H.-D., 1987. Quantitative analysis of calcium gradients and activity in growing pollen tubes of *Lilium longiflorum*. Protoplasma 139:20-24.

Nothnagel, E.A., Webb, W.W., 1982. Hydrodynamic models of viscous coupling between motile myosin and endoplasm in characean algae. J. Cell Biol. 94:444-454.

Ogihara, S., 1982. Calcium and ATP regulation of the oscillatory torsional movement in a triton model of *Physarum* plasmodial strands. Exptl. Cell Res. 138:377-384.

Okada, Y., 1928. On the development of a hexactinellid sponge, *Farrea sollasii*. J. Fac. Sci. imp. Univ. Tokyo 4:1-29.

Parish, C.R., Jakobsen, K.B., Coombe, D.R., Bacic, A., 1991. Isolation and characterization of cell adhesion molecules from the marine sponge *Ophlitaspongia tenuis*. Biochimica et Biophysica Acta 1073:56-64.

Patel, N., de Feo, G., Mancillas, J.R., 1991. UNC-116 encodes *C. elegans* kinesin. Neuroscience 17:58a.

Pavans de Ceccatty, M., 1989. L'éponges, à l'aube des communications cellulaires. Science 142:64-72.

Pavans de Ceccatty, M., 1982. In vitro aggregation of syncytia and cells of a hexactinellida sponge. Dev. Comp. Immunol. 6:15-22.

Pavans de Ceccatty, M., 1962. Système nerveux et intégration chez les spongiaires. Ann. Des Sc. Nat., Zool. 12:127-137.

Pavans de Ceccatty, M., 1959. Les structures cellulaires de type nerveux chez *Hippospongia communis* LMK. Ann. Des Sc. Nat., Zool. 12:105-112.

Pavans de Ceccatty, M., Mackie, G., 1982. Genèse et évolution des interconnexions syncytiales et cellulaires chez une Éponge Hexactinellide en cours de réagrégation après dissociation *in vitro*. C.R. Acad. Sc. Paris, t.294:939-944.

Perez, T., 1996. La rétention de particules par une éponge hexactinellide, *Oopsacas minuta* (Leucopsacasidae): le rôle du réticulum. C. R. Acad. Sci. Paris, Sciences de la vie 319:385-391.

Luby-Phelps, K.J., Porter, K.R., 1982. The control of pigment migration in isolated erythrophores of *Holocentrotus ascensionus* (Osbeck) I. Energy requirements. Cell 21:13-28.

Pomponi, S.A., Willoughby, R., 1994. Sponge cell culture for production of bioactive metabolites. *In*: Sponges in Time and Space, van Soest, R.W.M., van Kempen, T.M.G., Braekman, J. (eds.), AA Balkema, Rotterdam, pp. 395-400.

Przysiezniak, J., Spencer, A.N., 1989. Primary culture of identified neurones from a cnidarian. J. Exp. Biol. 142:97-113.

Putnam-Evans, C., Harmon, A.C., Palevitz, B.A., Fechheimer, M., Cormier, M.J., 1989. Calcium-dependent protein kinase is localized with F-actin in plant cells. Cell Motil. Cytoskeleton 12:12-22.

Reed, C., Greenberg, M.J., Pierce, S.K., 1976. The effects of the cytochalasins on sponge cell reaggregation: new insights through the scanning electron microscope. *In*: Aspects of sponge biology, Harrison, F.W., Cowden, R.R. (eds.), Academic Press, Inc., New York, pp. 153-169.

Reid, R.E.H., 1963. Hexactinellida or Hyalospongea. J. Paleontology 37:232-243.

Reiswig, H.M., 1991. New perspectives on the hexactinellid genus *Dactylocalyx* Stuchbury. *In*: Fossil and recent sponges, Reitner, J., Keupp, H. (eds.), Springer-

Verlag, Berlin, pp. 7-20.

Reiswig, H.M., 1990. In situ feeding in two shallow-water Hexactinellid sponges. *In*: New perspectives in sponge biology, Rutzler, K. (eds.), Smithsonian Institution Press, Washington, D.C., pp. 504-510.

Reiswig, H.M., 1979a. Histology of hexactinellida (Porifera). Colloques int. Cent. natn. Rech. scient. 291:173-180.

Reiswig, H.M., 1979b. Hymedesmia. Can. J. Zool. Meeting Abstracts:84a.

Reiswig, H.M., 1971. In Situ pumping activities of tropical demospongiae. Mar. Biol. 9:38-50.

Reiswig, H.M., Mackie, G.O., 1983. Studies on hexactinellid sponges III. The taxonomic status of Hexactinellida within the Porifera. Phil. Trans. R. Soc. Lond. B 301:419-428.

Reiswig, H.M., Mehl, D., 1994. Reevaluation of *Chonelasma* (Euretidae) and *Leptophragmella* (Craticulariidae) (Hexactinellida). *In*: Sponges in Time and Space, van Soest, R.W.M., van Kempen, T.M.G., Braekman, J.-C. (eds.), A.A. Balkema, Rotterdam, pp. 151-165.

Reiswig, H.M., Mehl, D., 1991. Tissue organization of *Farrea occa* (Porifera, Hexactinellida). Zoomorphology 110:301-311.

Ridgeway, E.B., Durham, A.C.H., 1976. Oscillations of calcium ion concentrations in *Physarum polycephalum*. J. Cell Biol. 69:223-226.

Rinkevich, B., Rabinowitz, C., 1993. In vitro culture of blood cells from the colonial protochrodate *Botryllus Schlosseri*. In Vitro Cell. Dev. Biol. 29A:79-85.

Rubaschkin, W., Besuglaja, W., 1932. Symplasten, Syncytien, Zellen im Bindegewebe. Z. Zellforsch. Mikr. Anat. 14:440-464.

Sachs, J., 1892. Physiologische Notizen. Flora 75:1-3.

Salomon, D., Barthel, D., 1990. External choanosome morphology of the hexactinellid sponge *Aulorosella vanhoeffeni* Schulze and Kirkpatrick 1910. Senckenbergiana marit. 21:87-99.

Sawin, K.E., Mitchison, T.J., Wordeman, L.G., 1992. Evidence for kinesin-related proteins in the mitotic apparatus using peptide antibodies. J. Cell Sci. 101:303-313.

Schmid, V., Bally, A., 1988. Species specificity in cell-substrate interactions in medusae. Dev. Biol. 129:573-581.

Schmid, V., Bally, A., Beck, K., Haller, M., Schlage, W.K., Weber, C., 1991. The extracellular matrix (mesoglea) of hydrozoan jellyfish and its ability to support cell adhesion and spreading. Hydrobiologia 216/217:3-10.

Schmidt, J.A., Eckert, R., 1976. Calcium couples flagellar reversal to photostimulation in *Chlamydomonas reinhardtii*. Nature 262:713-715.

Schulze, F.E., 1899. Zur Histologie der Hexactinelliden. Sber.dt. Akad. Wiss. 14:198-209.

Schulze, F.E., 1887. Report on Hexactinellida. Challenger Report 21:1-513.

Schulze, F.E., 1880. On the structure and arrangement of the soft parts in *Euplectella aspergillum*. Royal Society of Edinburgh Transactions 29:661-673.

Shimizu, K., Yoshizato, K., 1993. Involvement of collagen synthesis in tissue reconstitution by dissociated sponge cells. Develop. Growth and Differ. 35:293-300.

Shimizu, T., Kimura, I., 1974. Effects of N-ethylmaleimide on dynein adenosin-triphosphatase activity and its recombining ability with outer fibres. J. Biochem 76:1001-1008.

Shimizu, T., Toyoshima, Y.Y., Vale, R.D., 1993. Use of ATP analogs in motor assays. Methods in Cell Biology 39:167-177.

Shimmen, T., 1988. Characean actin bundles as a tool for studying actomyosin based motility. Bot. Mag. 101:533-544.

Shimmen, T., Tazawa, M., 1985. Mechanism of inhibition of cytoplasmic streaming by Myrmicacin (B-Hydroxydecanoic acid) in *Chara* and *Spirogyra*. Protoplasma 127:93-100.

Shimmen, T., Tazawa, M., 1982. Reconstitution of cytoplasmic streaming in Characeae. Protoplasma 113:127-131.

Shimmen, T., Xu, Y.-L., Kohno, T., 1990. Inhibition of cytoplasmic streaming by sulfate in characean cells. Protoplasma 158:39-44.

Simmons, R.M., Finer, J.T., 1993. Glasperlenspiel II. Current Biology 3:309-311.

Simpson, T.L., 1984. The cell-biology of sponges. Springer Verlag, New York.

Stearns, M.E., 1984. Cytomatrix in chromatophores. J. Cell Biol. 99:144s-151s.

Stearns, M.E., Ochs, R.L., 1982. A functional in vitro model for studies of intracellular motility in digitonin-permeabilized erythrophores. J. Cell Biol. 94:727-739.

Steinberg, G., Schliwa, M., 1995. The *Neurospora* organelle motor: a distant relative of conventional kinesin with unconventional properties. Mol. Biol. Cell 6:1605-1618.

Stossel, T.P., 1993. On the crawling of animal cells. Science 260:1086-1094.

Studnicka, F.K., 1934. The symplastic state of the tissues of the animal body. Biological Reviews and Biological Proceedings of the Cambridge Philosophical Society. 9:263-298.

Swanson, J.A., 1993. Pure thoughts with impure proteins; permeabilized cell models of organelle motility. BioEssays 15:715-722.

Takagi, S., Nagai, R., 1986. Intracellular Ca^{2+} concentration and cytoplasmic streaming in *Vallisneria* mesophyll cells. Plant Cell Physiol. 27:953-959.

Taylor, D.L., Condeelis, J.S., 1979. Cytoplasmic structure and contractility in amoeboid cells. Int. Rev. Cytol. 56:57-143.

Taylor, D.L., Fechheimer, M., 1982. Cytoplasmic structure and contractility: the solation-contraction coupling hypothesis. Phil. Trans. Roy. Soc. Lond. 299:185-197.

Teragawa.C.K., 1986. Sponge dermal membrane morphology: histology of cell-mediated particle transport during skeletal growth. J. Morph. 190:335-347.

Terasaki, M., Bo Chen, L., Fujiwara, K., 1986. Microtubules and the endoplasmic reticulum are highly interdependent structures. J. Cell Biol. 103:1557-1568.

Thaler, C.D., Haimo, L.T., 1992. Control of organelle transport in melanophores: regulation of calcium and cAMP levels. Cell Motil. Cytoskeleton 22:175-184.

Tiezzi, A., Moscatelli, A., Cai, G., Bartalesi, A., Cresti, M., 1992. An immunoreactive homolog of mammalian kinesin in *Nicotiana tabacum* pollen tubes. Cell Motil. Cytoskeleton 21:132-137.

Tominaga, Y., Wayne, R., Tung, H.Y.L., Tazawa, M., 1987. Phosphorylation-dephosphorylation is involved in Ca^{2+}-controlled cytoplasmic streaming of characean cells. Protoplasma 136:161-169.

Tominaga, Y., Shimmen, T., Tazawa, M., 1983. Control of cytoplasmic streaming by extracellular Ca^{2+} in permeabilized *Nitella* cells. Protoplasma 116:75-77.

Toyoshima, I., Yu, H., Steuer, E.R., Sheetz, M.P., 1992. Kinectin, a major kinesin-binding protein on ER. J. Cell Biol. 118:1121-1131.

Travis, J.L., Allen, R.D., 1981. Studies on the motility of the foraminifera I. Ultrastructure of the reticulopodial network of *Allogromia laticollaris* (Arnold). J. Cell Biol. 90:211-221.

Travis, J.L., Bowser, S.S., 1990. Microtubule-membrane interactions in vivo: direct observation of plasma membrane deformation mediated by actively bending cytoplasmic microtubules. Protoplasma 154:184-189.

Ueda, T., Götz von Olenhusen, K., 1978. Replacement of endoplasm with artificial media in plasmodial strands of *Physarum polycephalum*. Exptl. Cell Res. 116:55-62.

Ueda, T., Nakagaki, T., Yamada, T., 1990. Dynamic organization of ATP and birefringent fibrils during free locomotion and galvanotaxis in the plasmodium of *Physarum polycephalum*. J. Cell Biol. 110:1097.

Vale, R.D., Hotani, H., 1988. Formation of membrane networks in vitro by kinesin-driven microtubule movement. J. Cell Biol. 107:2233-2241.

Vale, R.D., Reese, T.S., Sheetz, M.P., 1985a. Identification of a novel force-generating protein, kinesin, involved in microtubule-based motility. Cell 42:39-50.

Vale, R.D., Schnapp, B.J., Mitchison, T., Sheetz, M.P., 1985b. Different axoplasmic proteins generate movement in opposite directions along microtubules in vitro. Cell 43:623-632.

von Dassow, G., Schubiger, G., 1994. How an actin network might cause fountain streaming and nuclear migration in the syncytial *Drosophila* embryo. J. Cell Biol. 127:1637-1653.

Wachtmann, D., Stockem, W., 1992. Microtubule- and microfilament-based dynamic activities of the endoplasmic reticulum and the cell surface in epithelial cells of *Spongilla lacustris* (Porifera, Spongillidae). Zoomorphology 112:117-124.

Wachtmann, D., Stockem, W., Weissenfels, N., 1990. Cytoskeletal organization and cell organelle transport in basal epithelial cells of the freshwater sponge *Spongilla lacustris*. Cell Tissue Res. 261:145-154.

Wakelam, M.J.O., 1988. Myoblast fusion - A mechanistic analysis. *In*: Current topics

in membranes and transport, Bronner, F., Düzgünes, N. (eds.), Academic Press, London, pp. 88-107.

Walker, R.A., Sheetz, M.P., 1993. Cytoplasmic microtubule-associated motors. Annu. Rev. Biochem. 62:429-451.

Wasteneys, G.O., Williamson, R.E., 1991. Endoplasmic microtubules and nucleus-associated actin rings in *Nitella* internodal cells. Protoplasma 162:86-98.

Weiss, P., Hiscoe, H.B., 1948. Experiments on the mechanism of nerve growth. J. Exp. Zool. 107:315-396.

Weissenfels, N., 1992. The filtration apparatus for food collection in freshwater sponges (Porifera, Spongillidae). Zoomorphology 112:51-55.

Weissenfels, N., 1980. Bau und Funktion des Süsswasserschwamms *Ephydatia fluviatilis* L. (Porifera). VII. Die Porocyten. Zoomorphologie 95:27-40.

Weissenfels, N., Wachtmann, D., Stockem, W., 1990. The role of microtubules for the movement of mitochondria in pinacocytes of fresh-water sponges (Spongillidae, Porifera). Eur. J. Cell Biol. 52:310-314.

Williamson, R.E., 1980. Actin in motile and other processes in plant cells. Can. J. Bot. 58:766-772.

Williamson, R.E., 1975. Cytoplasmic streaming in *Chara*: a cell model activated by ATP and inhibited by cytochalasin B. J. Cell Sci. 17:655-668.

Wilson, H.V., 1907. On some phenomena of coalescence and regeneration in sponges. J. Exp. Zool. 5:245-258.

Wyeth, R.C., Leys, S.P., Mackie, G.O., 1996. Use of sandwich cultures for the study of feeding in the hexactinellid sponge *Rhabdocalyptus dawsoni* (Lambe, 1892). Acta Zool. 77:227-232.

Yanagimachi, R., 1988. Sperm-Egg Fusion. *In*: Current Topics in Membranes and Transport, Bronner, F., Düzgünes, N. (eds.), Academic Press, Inc., London, pp. 4-35.

Yonemura, S., Pollard, R.D., 1992. The localization of myosin I and myosin II in *Acanthamoeba* by fluorescence microscopy. J. Cell Sci. 102:629-642.

Yu, W., Centonze, V.E., Ahmad, F.J., Baas, P.W., 1993. Microtubule nucleation and release from the neuronal centrosome. J. Cell Biol. 122:349-359.

APPENDICES

Appendix 1: Permeabilization experiment results from Chapter 3. (Buffers 1-5 are defined below.)

Original buffer	pH	Detergent	Additions	Observations	Reactivation and result with 1mM ATP
1	7.5		Human serum albumin	No effect on streaming or membranes for 20 min.	
		0.04% Saponin		Streaming stopped by thinning out gradually, but the membrane didn't appear to lyse	no reactivation with 1 and 2 mM ATP. Addition of ASW after ATP caused contraction of preparation.
2	6.9	0.15% Brij 58	none	Rapid lysis, some strands of cytoplasm remained	no movement
	6.4	"	none	Tissue withdrew and blebbed	none
	6.9	0.15% Nonidet	none	Strips membrane, tissue pulled away from substrate; tracks remained visible	no movement, remaining tissue pealed away.
		"	3mM vanadate	Strips membrane and stops movement	more difficult to wash tissue away
		"	none	Stips membrane, tissue pulls away from substrate	no movement, remaining tissue pealed away.
		"	100% PHEM	destroyed tissue	none
	6.4	"	50% PHEM in SW	Membrane peals back, no tracks left	none
		4mM Chaps	none	Gently stops movment	none
		8mM Chaps	none	Harsher solubilization	none
3	6.9	0.15% Nonidet	1 mM vanadate, 5%hexylene glycol	Lysed membrane	none
			none	as above	none
		0.15% Brij 58	none	Tissue withdrew and blebbed	none
		glycerol	none	Tissue remaine as when live but surface membrane lysed in 10-15s	caused blebbing of tissue

(Continued on next page)

Appendix 1 (Cont'd): Permeabilization experiments

Original buffer	pH	Detergent	Additions	Observations	Reactivation and result with 1mM ATP
4	7.0	0.1% TX-100	none	Streaming stops slowly, membrane peals away but tracks remained visible with DIC	none
		"	1mM vanadate	Streaming stops and membrane and tissue withdrew from substrate	preparation tore, no reactivation
		0.15% Brij 58	none	Lysed membrane, tissue tore	none
5	6.9	0.15% Brij 58	none	Lysed tissue without tearing. Streaming very slow to stop	unclear whether lysed. Still some organelle movement
		0.3% Brij 58	50% PHEM	Apparent lysis- organelles stop moving, see strands of tissue (poss. MT bundles), no pealing of membrane	none
	7.4	0.15% Brij 58	none	Some blebbing of tissue, unclear whether membrane is lysed	none
	8.0	"	none	Same as above	none
	7.0	"	50% PHEM	Some pealing of tissue away from substrate; organelle movement is slow to stop	none
	6.9	0.15% Brij 58	100% PHEM,	Same as pH 7.4	none
		"	50% PHEM, 5% hexylene glycol	lysis	possible slight reactivation
		"	50% PHEM, 5% HG, 1mM vanadate	lysed and tore membrane	none
		0.15% TX100	50%hexylene glycol, 1mM Vanadate	tissue pealed away from substrate	none
		0.02% Saponin	as above	membrane burst, tore and vesiculated	none

Buffers: (1) "Electrode solution": KCl (400mM), $MgCl_2$ (2mM), $CaCl_2$ (1mM), $NaCl_2$ (50mM) HEPES(10mM), EGTA (11mM), NMG (58mM), HCl (28mM), pH7.5, (2) "Reticulomyxa solution": 5% hexylene glycol, sodium orthovanadate (1mM), 0.15% Brij 58, 50% PHEM, Pipes (30mM), Hepes (12.5 mM), EGTA (4 mM), $MgCl_2$ (1 mM), pH 7.0, (3) PEM: Pipes (50mM), EGTA (1mM), $MgCl_2$ (0.5 mM) pH 6.9

(4) PEG-GTX: 4% Polyethylene glycol MW 600, 10% glycerol, Pipes (10 mM), EGTA (5 mM), KOH (10 mM), KCl (27mM), 0.15% TX-100, pH 7.0, (5) PHEM: Pipes (50mM), Hepes (25mM), EGTA (10 mM), $MgCl_2$ (2 mM), pH 6.9

IMAGE EVALUATION
TEST TARGET (QA-3)

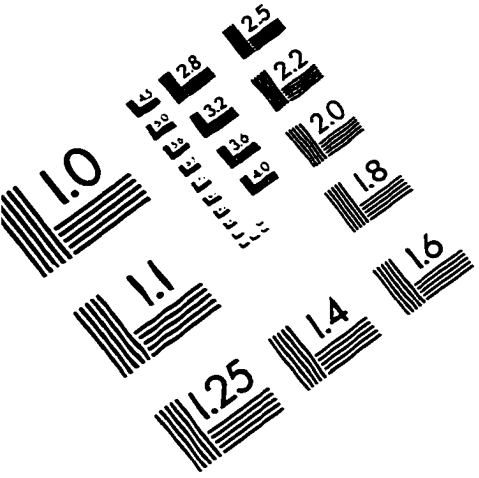

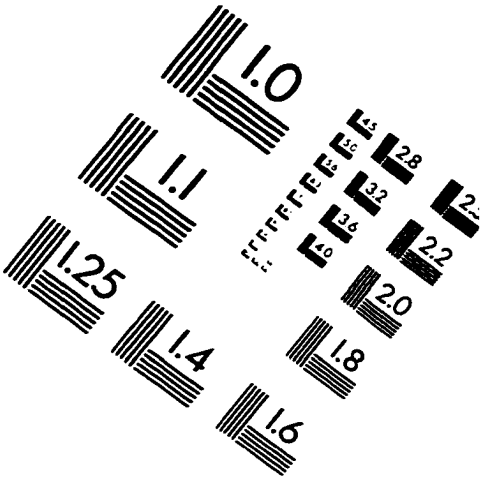

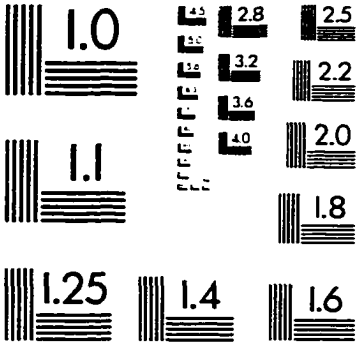

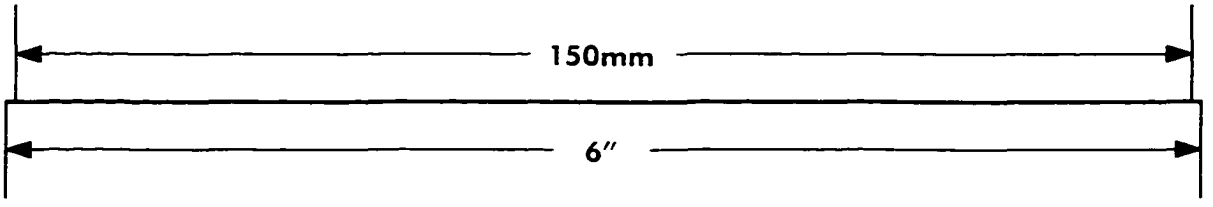

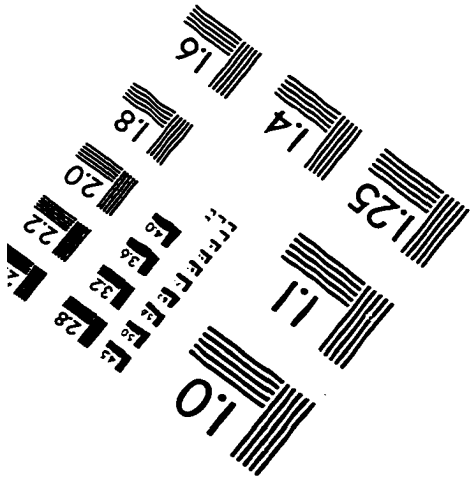

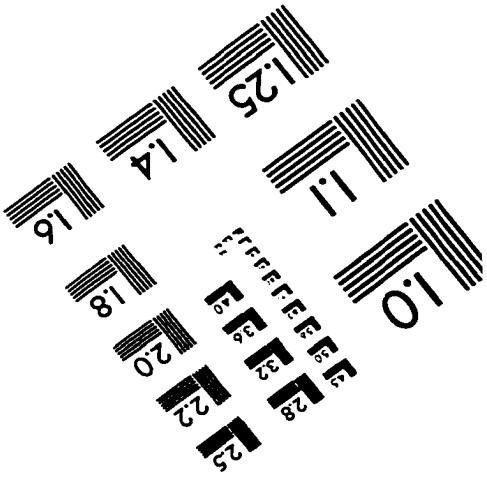

APPLIED IMAGE, Inc
1653 East Main Street
Rochester, NY 14609 USA
Phone: 716/482-0300
Fax: 716/288-5989